

2015

Vascular smooth muscle: a target for treatment of aging-induced aortic stiffness

<https://hdl.handle.net/2144/13678>

"Downloaded from OpenBU. Boston University's institutional repository."

BOSTON UNIVERSITY
COLLEGE OF ENGINEERING

Dissertation

**VASCULAR SMOOTH MUSCLE:
A TARGET FOR TREATMENT OF AGING-INDUCED AORTIC STIFFNESS**

by

YUAN ZHAO GAO

B.S., Johns Hopkins University, 2006
M.S., Mount Sinai School of Medicine of New York University, 2010

Submitted in partial fulfillment of the
requirements for the degree of
Doctor of Philosophy

2015

© 2015 by
YUAN ZHAO GAO
All rights reserved

Approved by

First Reader



Kathleen G. Morgan, Ph.D.
Professor and Chair of Health Sciences

Second Reader



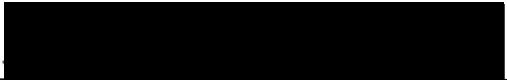
Bela Suki, Ph.D.
Professor of Biomedical Engineering

Third Reader



Michael L. Smith, Ph.D.
Associate Professor of Biomedical Engineering

Fourth Reader



Dimitrije Stamenovic, Ph.D.
Associate Professor of Biomedical Engineering

Fifth Reader



Tyrone M. Porter, Ph.D.
Associate Professor of Biomedical Engineering
Associate Professor of Mechanical Engineering

**VASCULAR SMOOTH MUSCLE:
A TARGET FOR TREATMENT OF AGING-INDUCED AORTIC STIFFNESS**

YUAN ZHAO GAO

Boston University College of Engineering, 2015

Major Professor: Kathleen G. Morgan, Ph.D., Professor and Chair of Health Sciences

ABSTRACT

Cardiovascular disease is the leading cause of human death worldwide. Currently, the prevalence of cardiovascular disease and health care costs associated with its onset continue to increase in both developed and developing societies. Concordant with the need to improve preventative measures is the imperative to develop more effective and efficient remedies for incident cardiovascular pathologies. Increased aortic stiffness with aging has recently emerged as an early, independent, and consistent physiological predictor of cardiovascular disease and represents an attractive target for possible therapeutic options. The success of any biomedical strategy in this regard is incumbent upon comprehension of biological processes and mechanical properties attributable to constituent components within the aortic wall.

This dissertation tested the hypothesis that aging-induced changes to smooth muscle maintenance of biomechanical homeostasis within the aorta lead to undesirable increases in stiffness, correlative with increased risk of negative cardiovascular outcomes. Conventionally, mechanical studies and models have identified extracellular matrix as the primary determinant of changes in stiffness, but new research presented here shows that this may not be true. In viable *ex vivo* preparations of aortic tissue, roughly half of the

maximal elastic modulus results from alpha-agonist activation of smooth muscle cells. Investigation of the biochemical interactions that characterize this effect revealed a link between aging and decreased expression of Src, a kinase involved in numerous signaling pathways governing cellular growth and survival, as well as defective regulation of focal adhesions between the smooth muscle cells and extracellular matrix.

These findings were integrated into a model of aortic contractility and stiffness that establishes an aging-impaired regulatory complex comprising focal adhesions and non-muscle actin cytoskeleton in vascular smooth muscle cells. A better understanding of the mechanisms underlying this model may motivate the design of potential therapeutics, deliverable to previously overlooked target sites within aortic smooth muscle, and ultimately novel treatments for aging-induced cardiovascular disease.

Table of Contents

Abstract.....	iv
List of Tables	xi
List of Figures.....	xii
List of Abbreviations	xv
Chapter 1: Introduction and Background.....	1
1.1 Purpose.....	1
1.2 Aortic Stiffness as an Emergent Focus of Cardiovascular Research	1
1.2.1 Cardiovascular Disease.....	1
1.2.2 Pulse Wave Velocity: The Clinical Standard for Aortic Stiffness.....	2
1.3 The Importance of <i>Ex Vivo</i> Material Stiffness	4
1.3.1 Biomechanical Limitations of Pulse Wave Velocity	4
1.3.2 Functional Versus Material Stiffness.....	5
1.3.3 Building a Contextual Bridge	6
1.4 Aortic Vascular Tissue.....	7
1.4.1 General Wall Structure	7
1.4.2 Smooth Muscle Cells	9
1.4.3 Focal Adhesions.....	12
1.4.4 Extracellular Matrix	16
1.5 Targeting Aging-Induced Increases in Aortic Stiffness.....	17
1.5.1 Changes with Aging in Aortic Structure and Function.....	17
1.5.2 The Case for Studying Vascular Smooth Muscle.....	20

Chapter 2: Materials and Methods	22
2.1 Disclosure.....	22
2.2 Ethical Approval	22
2.3 Mouse Models of Aortic Stiffness	22
2.4 Aortic Tissue Sampling.....	24
2.4.1 Preparation of Tissue	24
2.4.2 Measurements of Aortic Geometry.....	24
2.5 Evaluation of Aortic Tissue Stiffness <i>Ex Vivo</i>	25
2.5.1 Uniaxial Stretching Apparatus and Normalization of Force Measurements	25
2.5.2 Quasi-Static Stress-Strain Curves.....	27
2.5.3 High-Frequency Low-Amplitude Sinusoidal Perturbations	28
2.5.4 Confirmation of Vascular Smooth Muscle Viability	30
2.6 Biochemical Analysis.....	31
2.7 Cell-Permeable Decoy Peptides.....	31
2.7.1 Design and Synthesis	31
2.7.2 Loading Solutions.....	32
2.7.3 Tissue Loading and Unloading.....	34
2.8 Reagents	37
2.9 Statistics	37
Chapter 3: Aging Impairs Smooth Muscle Mediated Regulation of Aortic Stiffness	38
3.1 Disclosure.....	38
3.2 Summary	38
3.3 Introduction	39

3.4	Results	40
3.4.1	Physiologic optimal length in mouse aorta does not change with age	40
3.4.2	Baseline aortic wall tension increases with aging at optimal length but stiffness decreases.....	43
3.4.3	<i>Ex vivo</i> baseline stiffness does not increase in hypertensive mouse models of high-fat-diet and angiotensin II	45
3.4.4	Baseline stiffness increases in Sirtuin-1 knockout mice with angiotensin II pretreatment.....	46
3.4.5	Increased passive aortic stiffness with aging occurs only beyond physiologic strain levels	50
3.4.6	Warming aortic tissue from cooled state produces opposite effects on stress versus stiffness.....	52
3.4.7	Vascular smooth muscle cells account for up to half of maximal total aortic stiffness	53
3.4.8	Tyrosine phosphorylation of focal adhesion proteins is impaired with aging due to decreased Src expression	57
3.4.9	Aging impairs action of a Src small molecule inhibitor on aortic stress and stiffness	59
3.4.10	Aging-induced impairment of Src-mediated regulation of active stiffness in mouse aorta begins between 14–24 months of age	60
3.5	Discussion	62
3.5.1	Additive model of aortic stress and stiffness consists of separable components that highlight major contributions from vascular smooth muscle cells.....	62
3.5.2	Baseline aortic stiffness establishes important mechanistic links between vascular smooth muscle cells and extracellular matrix proteins	64
3.5.3	Impaired regulation of shock absorber function by focal adhesions and non-muscle cytoskeleton is a source of increased aortic stiffness with aging.....	67

Chapter 4: Cell-Permeable Decoy Peptides Target Focal Adhesion and Cytoskeletal Regulation of Aortic Stiffness	73
4.1 Summary	73
4.2 Introduction	74
4.3 Results	78
4.3.1 Talin-vinculin binding site cell-permeable peptide inhibits active aortic stiffness in young and old mice	78
4.3.2 Neuronal Wiskott-Aldrich syndrome protein cell-permeable peptide inhibits active aortic stiffness in young mice	80
4.4 Discussion	82
4.4.1 TLN-VBS inhibition of active stiffness in old mice demonstrates therapeutic potential and motivates further investigation of focal adhesion shock absorption	82
4.4.2 Future studies are required for confirmation of N-WASP-CA efficacy and further pharmacological considerations.....	84
Chapter 5: Assessment of Applied Biomechanical Methods in Evaluation of <i>Ex Vivo</i> Aortic Stiffness	86
5.1 Summary	86
5.2 Quantitative Modeling of Vascular Smooth Muscle Contributions to Total Aortic Stiffness.....	86
5.2.1 Concurrence with Presented Discoveries.....	86
5.2.2 Vascular Smooth Muscle Cells as Protective Dampers in a Modified Maxwell Model of Total Aortic Stiffness.....	87
5.2.3 Vascular Smooth Muscle Recruitment of Collagen.....	88
5.2.4 Model Applicability to Aortic Stiffness.....	89
5.3 Methodological Advantages in Reductionism and Physiological Relevance of High-Frequency Low-Amplitude Stiffness Measurements.....	91
5.4 Motivating Factors for Future Improvements in Measurements of <i>Ex Vivo</i> Aortic Geometry	97

5.4.1	Initial Length.....	97
5.4.2	Axial Strain and Axial Shortening.....	98
5.4.3	Wall Thickness.....	99
5.4.4	Cross-Sectional Area and True Circumferential Strain	100
5.5	Interpretation of <i>Ex Vivo</i> Results for <i>In Vivo</i> Predictions	104
Chapter 6: Conclusions		110
Bibliography		113
Curriculum Vitae		129

List of Tables

Chapter 2: Materials and Methods

Cell-permeable decoy peptide (CPP) sequences and stocks	33
---	----

List of Figures

Chapter 1: Introduction and Background

1.1. Idealized architecture of a healthy human artery	8
1.2. The smooth muscle cell model of cytoskeleton	10
1.3. Regulation of smooth muscle cell contractility	15
1.4. Interrelationships between vessel composition, structure, elasticity, geometry, impedance to blood flow, and cardiac work	18

Chapter 2: Materials and Methods

2.1. Representative age ranges for mature life history stages in C57BL/6J mice	23
2.2. Fluorescence microscopy of a young mouse aortic wall cross-section	26
2.3. <i>Ex vivo</i> steady-state stiffness methods	29
2.4. Apparatus for peptide loading protocol with aortic tissue	36

Chapter 3: Aging Impairs Smooth Muscle Mediated Regulation of Aortic Stiffness

3.1. Physiologic optimal length in young and old mouse aorta	42
3.2. At optimal length, baseline aortic wall tension increases with aging, but stiffness decreases	44
3.3. Baseline stiffness does not increase with high-fat diet or angiotensin II pretreatment	47

3.4. Sirtuin-1 knockout mice have increased baseline stiffness as measured <i>ex vivo</i> and <i>in vivo</i> with angiotensin II pretreatment	49
3.5. Passive aortic stiffness via mechanical stress-strain increases with aging only beyond physiologic strain range	51
3.6. Warming aortic tissue from cooled state produces opposite effects on stress versus stiffness	54
3.7. VSMCs contribute significantly to aortic stress and stiffness at optimal length via HFLA method	56
3.8. Agonist-induced, PP2-sensitive focal adhesion signaling is impaired in old aortas	58
3.9. Agonist-induced increases in aortic stress and stiffness with Src kinase inhibitor pretreatment are higher with aging	61
3.10. Src-mediated regulation of active aortic stress and stiffness is likely defective by 24 months of age in C57BL/6J mice	63
3.11. Additive model of stress and stiffness consists of separable components	65
3.12. Shock absorption via Src-mediated focal adhesion/non-muscle cytoskeleton regulation is defective in old aortas	68
3.13. Contractile activation of venous smooth muscle alters engagement of the cell-matrix adhesion via cortical actin switch and facilitates ERK activation via Src	71

Chapter 4: Cell-Permeable Decoy Peptides Target Focal Adhesion and Cytoskeletal

Regulation of Aortic Stiffness

4.1. Talin domain map	76
4.2. Conceptual diagram of cell-permeable decoy peptide mechanism targeting focal adhesion structural proteins	77
4.3. Talin-vinculin binding site CPP inhibits active aortic stress and stiffness in young and old mice	79
4.4. Neuronal Wiskott-Aldrich syndrome protein CPP inhibits active stiffness in young mice	81

Chapter 5: Assessment of Applied Biomechanical Methods in Evaluation of *Ex Vivo*

Aortic Stiffness

5.1. Modified Maxwell model for total wall stress in the brachial artery	90
5.2. HFLA stretch <i>ex vivo</i> induces stress softening and indicates possible protective effect from vascular smooth muscle	94
5.3. HFLA stiffness measurements minimize viscoelastic response from aortic tissue	95
5.4. Deriving a correction factor for true circumferential strain in uniaxial stretch of aortic tissue	101
5.5. Frequency dependence of the magnitude of normalized dynamic elastic modulus during control and active states in dogs	107

List of Abbreviations

AGE	Advanced Glycation End-Product
AHX	1-Aminohexanoic Acid
Ang II	Angiotensin II
ANOVA	Analysis of Variance
CaD	Caldesmon
CPP	Cell-Permeable Peptide
CVD	Cardiovascular Disease
CytoD	Cytochalasin D
c-Src	Proto-Oncogene Tyrosine-Protein Kinase Src
dVSMC	Differentiated Contractile Vascular Smooth Muscle Cell
E	Young's Modulus (Material Stiffness)
E_p	Peterson's Modulus (Functional Stiffness)
ECM	Extracellular Matrix
ERK	Extracellular Signal-Regulated Kinase
FA	Focal Adhesion
FAK	Focal Adhesion Kinase
FITC	Fluorescein Isothiocyanate
HFHS	High-Fat/High-Sucrose Diet
HFLA	High-Frequency Low-Amplitude Sinusoidal Strain
IP	Immunoprecipitation

KCl	Potassium Chloride
kDa	Kilodaltons
kPa	Kilopascals
L-NAME	L-NG-Nitroarginine Methyl Ester
MLCK	Myosin Light-Chain Kinase
MMP	Matrix Metalloproteinase
MT	Magnetic-Microneedle Technology
ND	Normal Diet
NMC	Non-Muscle Cytoskeleton
NO	Nitric Oxide
NOS	Nitric Oxide Synthase
N-WASP	Neuronal Wiskott-Aldrich Syndrome Protein
PDMS	Polydimethylsiloxane
PE	Phenylephrine (Alpha-Adrenergic Agonist)
PLA	Proximity Ligation Assay
PSS	Physiological Salt Solution
pTyr	Phosphotyrosine
PWV	Pulse Wave Velocity
SEM	Standard Error of the Mean
SIRT1	Sirtuin 1
SMC	Smooth Muscle Cell
SMKO	Smooth Muscle Knockout

TAT	Transactivator of Transcription
TGF- β	Transforming Growth Factor- β
TLN-VBS	Talin-Vinculin-Binding-Site
t-d	Temperature-Dependent
VSM	Vascular Smooth Muscle
VSMC	Vascular Smooth Muscle Cell
-X	Inactive/Scrambled-Sequence

Chapter 1: Introduction and Background

1.1 Purpose

Aortic stiffness is an early and independent biomarker of aging-induced cardiovascular disease. This dissertation introduces new biological knowledge regarding the underlying mechanisms regulating aortic stiffness attributable to vascular smooth muscle cells within the vessel wall, as well as how these mechanisms change with aging. The findings are presented in a biomechanical context, relative to the contributions of other wall components, in order to highlight the importance of vascular smooth muscle as a site of biochemical changes correlated with increased stiffness. These observations motivated the subsequent investigation of potential therapeutics targeting the cellular processes that modulate aortic stiffness.

1.2 Aortic Stiffness as an Emergent Focus of Cardiovascular Research

1.2.1 Cardiovascular Disease

Cardiovascular disease (CVD), a designation for the spectrum of dysfunction and disorders that affect the heart and blood vessels, is the leading cause of death worldwide and becoming increasingly prevalent in underdeveloped and developing countries (Mendis et al. 2011). Mortality rates have decreased in highly-developed countries, but it has been shown that currently available preventative measures are less effective in adults than in young people (McGill Jr. et al. 2008). Risk factors are myriad and include age, chronic conditions, family history, diet, and lifestyle. Statistical accounts and projections

of incidence, death, and health care costs are stark. Presently, CVD is responsible for more than one out of every three deaths in the United States. This figure may increase to ~44% between 2014 and 2030, while more than doubling the direct medical costs over this timespan, before accounting for additional indirect costs due to lost productivity (Mozaffarian et al. 2015). Thus, this pervasive public health issue presents an imperative to improve preventative care for CVD.

1.2.2 Pulse Wave Velocity: The Clinical Standard for Aortic Stiffness

In recent years, arterial stiffness has entered the spotlight as a specific and independent risk factor that may wield potent prognosticative power. Arterial stiffness is known to precede conditions associated with CVD such as hypertension and atherosclerosis, which are subsequently linked to causes of mortality such as heart failure, stroke, and kidney disease (Dustan et al. 1996, Guerin et al. 2001, Kaess et al. 2012, Ross 1999, Ross 1993). Consequently, arterial stiffness is gaining traction as a critically important concept in combating the human and societal costs of CVD.

In broad terms, arterial stiffness is the resistance of arteries to deformation in response to an applied force. **Pulse wave velocity (PWV)** is a non-invasive measurement of hemodynamic properties that is readily obtainable *in vivo* and highly reproducible (Wilkinson et al. 1998). Mathematically, it represents the velocity of a pulse resulting from systolic ejection of blood from the left ventricle, characterized by the ratio of distance ΔL between two measuring sites of a pulse wave to the time delay Δt between observations of the wave at each site, or $\Delta L/\Delta t$. Classically, PWV is interpretable as an

approximation of arterial stiffness by its relation to the **elastic modulus** of a blood vessel as described by the Moens-Korteweg equation (Korteweg 1878):

$$PWV = \sqrt{Eh/2\rho a} \quad \text{Equation 1}$$

where E is the Young's modulus or material stiffness, h and a are the thickness and radius of the vessel wall respectively, and ρ is blood density. Most commonly, PWV is measured via ultrasound between the carotid and femoral arteries (Mitchell 2009).

Large arteries are better determinants of age-related cardiovascular risk, given that they are compositionally different from peripheral arteries and change much more drastically with aging (Greenwald 2007, Trachet et al. 2015). The value of PWV as a representation of **aortic stiffness** and an early, independent, and reproducible biomarker of CVD is well-documented and thematically recurrent in medical and scientific literature. Increased PWV has been observed in a broad spectrum of individuals ranging from aged individuals with no other apparent disease (Mattace-Raso et al. 2006, Willum-Hansen et al. 2006) to those with disorders such as hypertension (Laurent et al. 2001), diabetes mellitus (Cruickshank et al. 2002), emphysema (McAllister et al. 2007), and end-stage renal failure (Blacher et al. 1999). Elevated PWV in the large vessels leads to increased transmission of high pressures to small vessels downstream and is thought to cause remodeling of the microcirculation and subsequent adverse effects on end organ function. Recently, increases in PWV have been shown both to precede and be augmented by hypertension (Weisbrod et al. 2013). Collectively, these studies in humans

indicate that increased aortic PWV is prognostic, and may be causative, of cardiovascular disease and mortality (Ben-Shlomo et al. 2013, Laurent and Boutouyrie 2007, Mitchell et al. 2007).

Other indirect, non-invasive measurements of arterial stiffness, such as augmentation index (AIx), focus on the analysis of pressure waves emanating from the heart during pulsation and how they relate to heart rate and mean arterial pressure (Wilkinson et al. 2000). While viable, these methods do not necessarily offer a simpler, more accurate, or more useful representation of stiffness (Vyas et al. 2007). Currently, PWV remains the clinical “gold standard” in this regard.

1.3 The Importance of *Ex Vivo* Material Stiffness

1.3.1 Biomechanical Limitations of Pulse Wave Velocity

Given the ease with which it can be obtained, PWV is a useful estimate of aortic stiffness. Unfortunately, it may also be an oversimplification of actual vessel mechanics which are much more complex. The applicability of the Moens-Korteweg relation between PWV and the mathematical definition of aortic stiffness is dependent on the assumption that the wall is isotropic and homogeneous and undergoes small isovolumetric changes in response to pulse pressure wave propagation. It has been shown in previous studies that this assumption does not hold (Clark and Glagov 1985, Gosling and Budge 2003). Furthermore, PWV is also sensitive to changes in heart rate and blood pressure (Mitchell et al. 1997). Therefore, this equation is inaccurate beyond conditions of specific pressures and wall geometry.

1.3.2 Functional Versus Material Stiffness

In standard terminology derived from past studies, there are two common definitions of stiffness as measured from the response of vessels to specific applied pressures *ex vivo*. **Functional stiffness**, also known alternatively as the **pressure-strain elastic modulus (E_p)** or Peterson's modulus, refers to the ratio of the change in pressure to the change in strain, which itself is a normalized, dimensionless measurement of the change in vessel diameter relative to its value at some reference, such as systole or diastole. **Material stiffness**, also known as **Young's modulus (E)**—equivalent to the elastic modulus in the Moens-Korteweg equation—is functional stiffness normalized across the thickness of the arterial wall. Young's modulus is the most independent representation of the intrinsic property of a material to resist deformation when a force is applied to it (Gamble et al. 1994, Greenwald 2007, O'Rourke 1990).

It is more accurate to categorize PWV as representative of functional stiffness. Functional stiffness is derived from material stiffness, but the opposite is not true. This is a subtle difference rarely appreciated in the literature. Frequently, the type of stiffness presented in studies is not explicitly clarified as either material or functional stiffness. Precise evaluation of arterial wall thickness is also difficult, which may account for why Young's modulus is not as thoroughly pervasive in reports of stiffness throughout the literature as it should be. Again, different terms used in reference to biomechanical properties of aorta may present significant difficulties, compounded by the prevalence of terms reciprocal to stiffness such as "compliance" and "distensibility," which are sometimes used interchangeably among studies in the context of independence from

vessel geometry. Even when attempting to normalize for geometry, one must tread with caution. Dimensional calculations based upon cross-sectional area, blood vessel diameter, or blood volume may all be equally valid but also mutually unintelligible without proper definitional context. The most concise discussion of this complicated canvas is provided by Bank and Kaiser, who cite conflicting results attributable to imprecise terminology and additionally summarize their own study showing that changes to PWV in brachial arteries, in response to smooth muscle relaxation, are not necessarily predictive of *any* corresponding change in material stiffness (Bank and Kaiser 1998).

1.3.3 Building a Contextual Bridge

Assessment of aortic stiffness exists on multiple scale levels. Macroscale techniques such as PWV relate to the hemodynamics of pulsatile blood flow; they are applicable in a clinical setting and more easily interpretable. Inversely, microscale techniques are difficult to employ non-invasively, but better elucidate the mechanisms causative of changes in the physical properties of blood vessels (Kohn et al. 2015). Despite the advantages in accessibility to defining aortic stiffness by way of a representative measurement such as PWV, there is a need for improvement in the contextualization of the biological activity underlying the dynamics of stiffness. While PWV is an easily demonstrable and a clinically valuable measure of functional stiffness, there is also a strong impetus to evaluate material stiffness directly to explain how different components of the aortic wall, a highly complex and layered network of interconnected cellular and extracellular elements, contribute to altered or defective

mechanisms in disease models. This is most conveniently and commonly done *ex vivo* by subjecting aortic tissue to mechanical stretch.

Therefore, one primary objective of this dissertation is to establish a logical connection between *ex vivo* material stiffness measurements and observable regulatory effects of stiffness by constituent components of the aortic wall. Naturally, the ability to do so rests upon a comprehensive biological understanding of these components.

1.4 Aortic Vascular Tissue

1.4.1 General Wall Structure

The aortic wall is a stratified composite of smooth muscle cells (SMCs) and extracellular matrix, as well as connective components such as cadherins and integrins linking them; each layer is different in its specific proportionality of these constituents. Moving outward through the vessel surrounding the arterial lumen, the major layers of the arterial wall are the intima, the media, and the adventitia. The intima includes endothelial cells that are in direct contact with blood flow. Elastin, organized into a three-dimensional lamellar network that contains collagen bundles between layers, is prevalent in the media, which also contains most of the SMCs (Matsumoto and Nagayama 2011, Wagenseil and Mecham 2009). Outside the external elastic lamina lies the adventitia, where fibroblasts produce most of the aortic wall's collagen (Wagenseil and Mecham 2009). A schematic of the aortic wall appears in **Figure 1.1**.

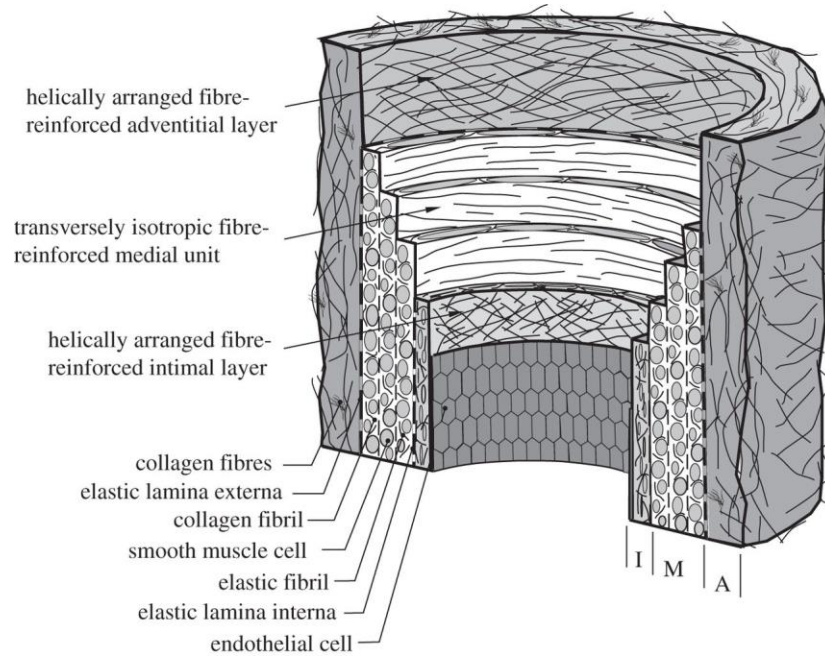


Figure 1.1. Idealized architecture of a healthy human artery (Tsamis et al. 2013). Arterial structure consists of an inner layer (intima, I), middle layer (media, M), and outer layer (adventitia, A). The intima is composed mainly of a single layer of endothelial cells. The media contains smooth muscle cells, a network of elastin and collagen fibrils, and elastin lamellae. The adventitia is primarily composed of thick bundles of collagen fibers.

1.4.2 Smooth Muscle Cells

Vascular smooth muscle cells (VSMCs) are involved in contractile and synthetic processes and are capable of exhibiting different phenotypes corresponding to these functions. By altering the diameter of the arterial lumen during contraction and relaxation, contractile VSMCs, which make up the majority of vasculature, maintain homeostatic blood pressure. Synthetic VSMCs facilitate long-term adaptive measures via synthesis of ECM components and instigation of cell proliferation and migration during vessel remodeling due to injury or other environmental perturbations. There are marked differences between contractile and synthetic SMCs. Contractile SMCs are spindle-shaped and relatively non-motile, while synthetic SMCs are shorter, possess high numbers of organelles involved in protein synthesis, and exhibit migratory behavior (Rensen et al. 2007). Consistent with these categorizations is the fact that when cultured, VSMCs change in phenotype from contractile to synthetic (Campbell and Campbell 1995).

The structure of VSMCs is a lattice consisting of the non-muscle cytoskeleton and a contractile apparatus (see **Figure 1.2**). The cytoskeleton has as its major components intermediate filaments, accounting for shape maintenance, and actin filaments, which interact with cytoplasmic dense bodies. Traditionally, the primary link from the SMC cytoskeleton to the contractile apparatus is in the form of these dense bodies, which contain α -actinin and bind to oppositely polarized actin filaments of the contractile apparatus (Draeger et al. 1990, Small and Gimona 1998).

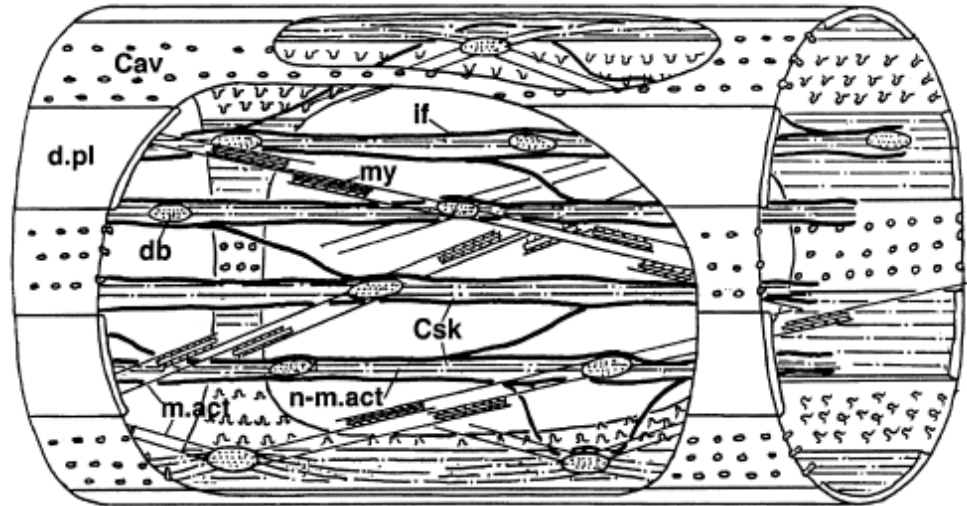


Figure 1.2. The smooth muscle cell model of cytoskeleton (Csk). Shown are the non-muscle actin filaments (n-m. act) that interact with dense bodies (db), muscle actin filaments (m. act) and myosin (my) of the contractile apparatus, intermediate filaments (If), and dense plaques or cortical focal adhesions (dpl) (Small and Gimona 1998).

As in all muscle and some non-muscle cells, the actomyosin cross bridge cycle is the fundamental mechanism of contractility in SMCs. Myosin filaments activated by contractile stimuli are able to “row” along actin filaments through ATPase activity and generate tension, shortening the cell as a result. Increases in intracellular calcium levels activate myosin light-chain kinase (MLCK), which regulates the cross bridge cycle via phosphorylation (Ogut and Brozovich 2003, Uehata et al. 1997).

Studies have shown that actin polymerization is also a predicate for smooth muscle contraction; the contraction of SMCs is associated with a transition in a small proportion of total actin in the cell from globular, or monomeric, to filamentous, and inhibition of actin polymerization results in a decrease in contractility (Cipolla and Osol 2002, Flavahan et al. 2005, Kim et al. 2010, Srinivasan et al. 2008, Zhang et al. 2005). This same inhibition, however, has been found not to have an effect on either intracellular calcium levels or myosin light-chain phosphorylation (Gunst and Zhang 2008, Shaw et al. 2003). While actin filaments constitute up to 20% of all protein content, only a subset collectively known as contractile actin is involved in interacting with myosin. Actin-binding proteins, such as caldesmon, serve as regulators of the accessibility of actin to myosin. These proteins are themselves regulated by upstream signaling molecules such as extracellular signal-regulated kinases (ERK1/2) (Kim et al. 2008, Yamin and Morgan 2012). Thus, myosin activity and actin availability are two major factors that affect cell contractility. A third potential influence on contractility in VSMCs is actin cytoskeletal remodeling, confirmed in recent studies by our group (Kim et al. 2010, Saphirstein et al. 2015).

Actin filaments also interact with longitudinal arrays on the membrane skeletons of SMCs known as dense plaques or focal adhesions, sites of mechanotransduction (Gerthoffer and Gunst 2001, Li et al. 2009, Small and Gimona 1998).

1.4.3 Focal Adhesions

Mechanotransduction, the process by which biochemical responses manifest from mechanical signals, is mediated in vasculature by virtually all major components in the vessel walls, including cytoskeletal structures and transmembrane receptors in the VSMCs, ECM components such as elastin and collagen, cell-cell adhesions, and cell-matrix adhesions (Ingber 2006, Ingber 2003).

Focal adhesions (FAs) are macromolecular complexes that belong to the latter category. They physically connect the cytoskeleton to ECM, generally via heterodimeric integrins, and also serve as sites of transmission for both regulatory signals and mechanical activity, capable of recognizing both physical and chemical stimuli in the cellular environment (Geiger et al. 2009). More than 150 proteins have been reported to have an association with FAs; organization and interaction among these proteins allows for diversity in structure and function (Zaidel-Bar et al. 2007, Zamir and Geiger 2001). Focal adhesion activity is traceable as part of a growth and maturation cycle in the form of a positive feedback loop, dependent upon the development of tension to grow, and prone to rapid dissociation upon relaxation (Wolfenson et al. 2009).

FAs enable two-way mechanical signaling, either from external forces (outside-in) or internal tension generated from actomyosin contraction (inside-out). Recent studies

have shown that actomyosin-generated forces modulate molecular kinetics of FAs (Wolfenson et al. 2011). More generally, FA size, quantity, and organization can be controlled by cell shape through changes in cell contractility. On the other hand, while ECM binding is necessary for FA formation, ECM by itself is insufficient for the promotion of FA assembly, although external forces are still capable of inducing FA development (Chen et al. 2003, Galbraith et al. 2002). In concert with studies that demonstrate an ability of cell shape to regulate contractile force, these findings show that regulation of FA assembly obeys an inside-out mechanism (Chen et al. 2003, Tan et al. 2002, Wang et al. 2002). This may have further implications regarding an intrinsic link between VSMCs and FAs in their contributions to arterial stiffness.

While FA integrins are not catalytic—any signaling caused by interactions with ECM must be transduced into cells through integrin-associated proteins (Hynes 2002, Juliano 2002, Schwartz 2001)—tyrosine phosphorylation of cytoskeletal and signaling proteins is one of many intracellular signaling events that result from integrin clustering. Focal adhesion kinase (FAK) is a tyrosine kinase that is localized to integrin clusters. FAK is recruited by the focal adhesion targeting region, a C-terminal domain with binding sites for integrin-associated proteins such as talin and paxillin (Rembold et al. 2007). These proteins may regulate arterial contraction based on previous research demonstrating this effect in airway smooth muscle (Schlaepfer et al. 2004, Wang et al. 1996).

The activated catalytic domain of FAK auto-phosphorylates Y397, facilitating the binding of Src-family kinases to the motif surrounding Y397. This formation of a FAK-

Src complex increases Src kinase activity, which in turn mediates additional phosphorylation of FAK within an activation loop of its kinase domain, located at Y576-Y577, as well as C-terminal domain residues Y861 and Y925. The net result is maximal FAK-associated activity and multiple intracellular signaling cascades, including the promotion of adaptor proteins such as paxillin, cytoskeletal proteins such as α -actinin, and GTPases such as Ras and Rho, the latter of which is a family of cellular molecular switches that regulate the formation and disassembly of actin-based cytoskeletal structures (Izaguirre et al. 2001, Kuo et al. 2011, Martinez-Lemus et al. 2009, Mitra et al. 2005, Schlaepfer et al. 1999). Therefore, the FAK-Src complex is a target of interest in ascertaining the role that focal adhesion growth and regulation may play in arterial stiffening.

There have not been many studies conducted upon FAs associated with non-migrating contractile SMCs, which account for the vast majority of what is observed *in vivo* in the vasculature. Given their importance as a conduit between the VSMCs and ECM of the arterial wall, FAs must be taken into account in the development of any comprehensive model of wall mechanics. A schematic summary of VSMC-mediated regulatory pathways of aortic stiffness related to FAs is shown in **Figure 1.3**.

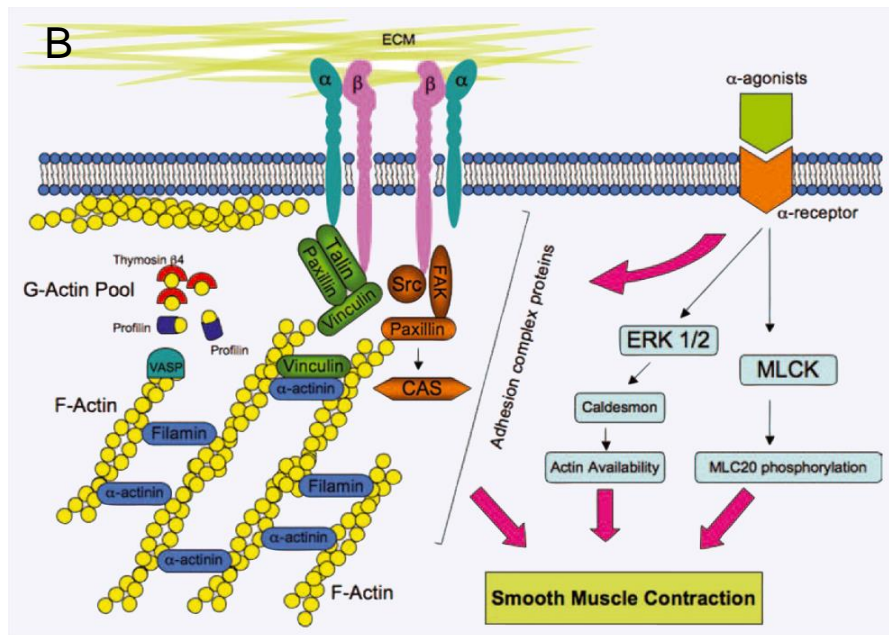
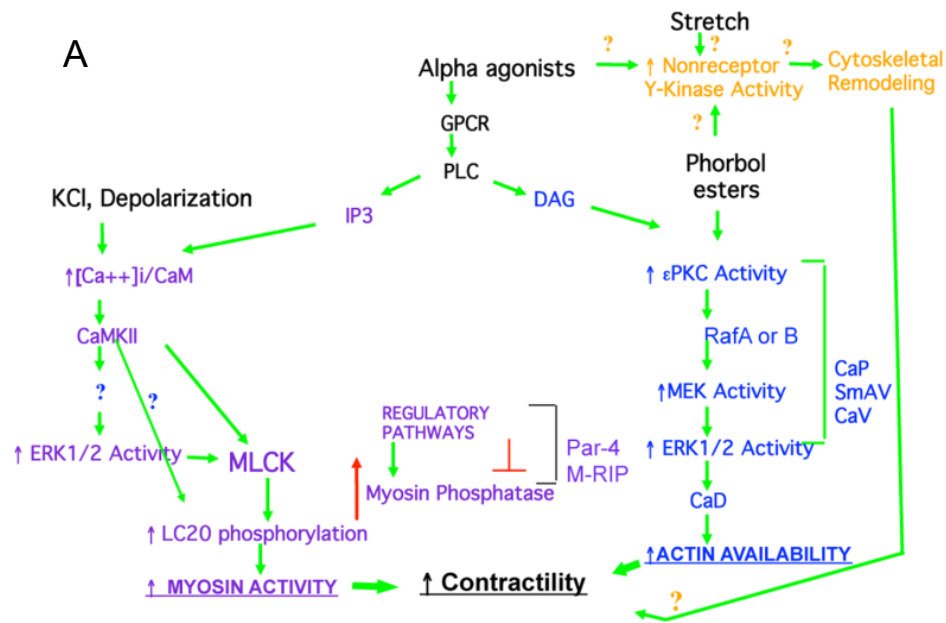


Figure 1.3. Regulation of smooth muscle contractility (Kim et al. 2008). (A) Demonstrated and putative signaling pathways that regulate myosin activity, actin availability, and cytoskeletal remodeling all contribute to contractility in vascular smooth muscle. (B) Focal adhesion complex linker (green) and signaling (orange) proteins promote cytoskeletal remodeling in response to mechanical and/or contractile stimuli.

1.4.4 Extracellular Matrix

In healthy arteries, the tunica media is the most mechanically significant layer of the wall. A helical, lamellar helical network of elastin fibers in the media, approximately circumferential in orientation, transfers stress throughout the wall (Holzapfel et al. 2000). Wavy Type I collagen fibers define a clear plane of separation between successive layers of this elastin network (Clark and Glagov 1985). These collagen bundles are of indefinite arrangement at low stress. Only with an increase in pressure and stretch does the collagen also align itself circumferentially (Dobrin 1978, Roach and Burton 1957, Wolinsky and Glagov 1964). Therefore, at low pressures, the load is taken on almost entirely by elastin, while the gradually unfolding collagen fibers bear increasingly more tension as the vessel continues to be stretched. It is well-documented that arterial stiffness is non-linear; at high pressures, it becomes much more difficult to distend the vessel, owing to the increase in stiffness in the form of collagen recruitment. This behavior is critical for protection against aneurysms and rupture (Shadwick 1999). Recent studies indicate that the adventitial layer, in which ECM material is predominantly collagen, may also bear a significant contribution to stiffness (Greenwald 2007, Schulze-Bauer et al. 2002, Xie et al. 1995). This framework buoys a long-held notion among biomechanical researchers that tissue stiffness can be largely attributed to ECM (Wagenseil and Mecham 2009).

1.5 Targeting Aging-Induced Increases in Aortic Stiffness

1.5.1 Changes with Aging in Aortic Structure and Function

As of 2015, it is estimated that more than 85 million people in the United States have at least one type of CVD; more than half of these (43–44 million) are at least 60 years of age. As a correlative factor with increased aortic stiffness and subsequently higher risk of CVD, senescence is the ideal context in which to develop potential therapeutics.

Many physical and biochemical changes occur within the aortic wall with aging. In broad terms, these have ramifications on blood flow, pressure, and burden on the heart (Lakatta 2003). As illustrated in **Figure 1.4**, resulting positive feedback that leads to further remodeling culminate in functional changes at the cellular level that may play a role in further aortic stiffening (Greenwald 2007). Therefore, any attempt to canonize a model of increased aortic stiffness with aging—and related conditions such as hypertension and atherosclerosis—must incorporate a comprehensive understanding of these effects on structure and function in different wall components. Otherwise, clinical treatments that aim to reduce aortic stiffness may be poorly directed and lacking in specificity.

Changes with aging in aortic ECM are perhaps the most readily observable. There is general agreement that, with aging, the ratio of collagen to elastin in wall tissue increases, and that both the density and integrity of the fatigued and progressively disorganized elastin lamellae decrease, although the absolute amounts of both matrix proteins decrease (Cattell et al. 1996, Greenwald 2007). Underlying causes of these

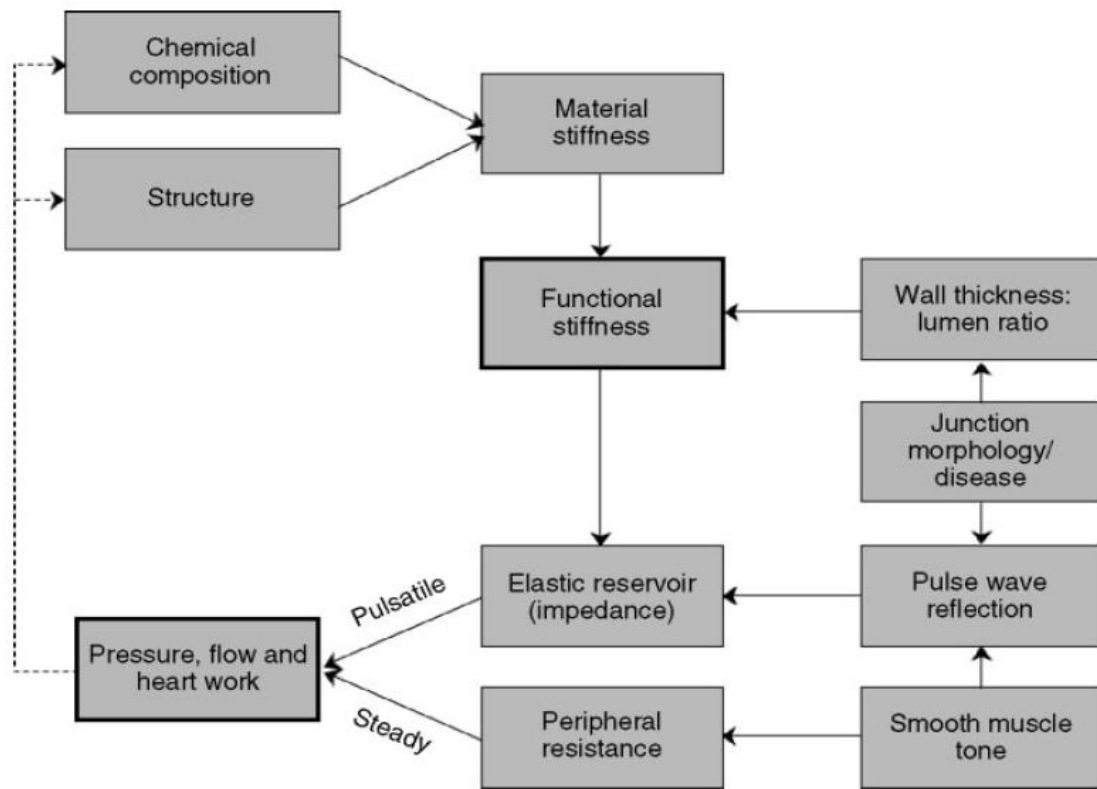


Figure 1.4. Interrelationships between vessel composition, structure, elasticity, geometry, impedance to blood flow, and cardiac work (Greenwald 2007). An increased burden on the major conduits of the circulatory system results in an increase in vessel stiffness that propagates to peripheral vasculature, which in turn triggers further stiffness increases in a positive feedback mechanism.

changes in the ECM include cross-linking of collagen and possibly also elastin, induced by accumulation of advanced glycation end-products (AGEs) resulting from slow and chemically irreversible rearrangements produced by glycation and oxidizing reactions within protein molecules. This translates to an increase in aortic material stiffness (Aronson 2003, Konova et al. 2004, Winlove et al. 1996).

Meanwhile, VSMCs are capable of switching their phenotype from contractile to synthetic with aging, causing fundamental changes in cellular function. As the SMCs migrate and proliferate, the intima thickens and the aorta undergoes increases in lumen diameter and wall thickness (Avolio et al. 2011, Glagov et al. 1993, Intengan and Schiffrin 2000). The cells themselves are also stiffer (Qiu et al. 2010). These effects give rise to defects in the mechanotransductive processes of VSMCs, which are commonly observed in a wide range of diseases (Ingber 2006, Ingber 2003).

Finally, the endothelium has also become increasingly visible in this regard, as it is responsible for widespread effects on cellular and extracellular processes throughout the aortic wall and especially those linked to VSM function. Nitric oxide (NO) produced by endothelial cells induces vasodilation and relaxation in VSM (Russell and Watts 2000). NO bioavailability is reduced with aging, which attenuates this benefit, increasing the stiffness of VSM as a result. This downstream effect may characterize yet another powerful positive feedback loop where the increased stiffness leads to further reduction of NO (Avolio et al. 2011, Cannon III 1998).

1.5.2 The Case for Studying Vascular Smooth Muscle

While all major biological components of the aortic wall play integral roles in the upkeep of normal cardiovascular function, it is clear from a brief outline of aging-induced effects on the aorta that vascular smooth muscle represents a common thread involved in all major structural and functional changes that deserves to be the focus of ongoing investigation.

The biological mechanisms underlying the contributions of vascular smooth muscle cells to the determination and regulation of aortic stiffness, and the effects of aging on these mechanisms, are not well understood. While numerous classical and recent studies of vascular mechanics attribute the majority of vessel wall stiffness largely to the ECM (Berry et al. 1975, Fleenor et al. 2010, Fleenor et al. 2012, Greenwald 2007, Wagenseil and Mecham 2009, Wolinsky and Glagov 1964), which is prominently featured in quantitative models (Holzapfel and Ogden 2010, Humphrey and Holzapfel 2011, Valentin et al. 2011, Wagenseil and Mecham 2012, Zulliger and Stergiopoulos 2007), there are also those that indicate that vascular smooth muscle activation produces non-negligible increases in stiffness (Bank et al. 1996, Barra et al. 1993, Gao et al. 2014).

The analysis of biomechanics in vascular smooth muscle can provide a quantitative description of hemodynamic phenomena such as blood flow and pulsatile wave propagation (Murphy 1988). Understanding changes to the mechanical properties of blood vessels is vital to assembling a broader grasp of how aging and other forms of disease affect cardiovascular physiology. By employing a quantitative approach to parse contributions to aortic stiffness from constituent components of the aortic wall, one may

identify the corresponding biological mechanisms that most significantly determine and regulate aortic stiffness and study how they change with aging. A rigorous regimen of *ex vivo* biomechanical and biochemical analyses to probe and understand these mechanisms in vascular smooth muscle may facilitate the design of potential therapeutics deliverable to previously overlooked targeting sites, leading to novel treatments for the onset and progression of cardiovascular disease with aging.

Chapter 2: Materials and Methods

2.1 Disclosure

Text and figures in the following sections in this chapter were modified from (Gao et al. 2014): 2.2, 2.4.1, 2.4.2, 2.5.1, 2.5.2, 2.5.3, 2.5.4, and 2.6.

2.2 Ethical Approval

All procedures were performed in accordance with protocols approved by the Boston University Institutional Animal Care and Use Committee (Permit Number: A3316-01). Animals (C57BL/6J mice) were maintained according to guidelines in the NIH Guide for the Care and Use of Laboratory Animals. Acquisition and usage of animals were in compliance with federal, state, and local laws. Euthanasia with isoflurane inhalation preceded expedient removal of tissue.

2.3 Mouse Models of Aortic Stiffness

Most of the research outlined here is based upon aorta samples from the C57BL/6, or Black 6, mouse model. Vasculature in rodent models such as Black 6 do not resemble humans as closely as that in ferrets, for example (Cavagna et al. 2000). Nevertheless, Black 6 offers distinct advantages due to its widely and robustly understood physiology and genetics, as well as its accessibility. Compiled through extensive studies, the aging curve in **Figure 2.1** provides age equivalency between C57BL/6J mice and humans, enabling proper contextualization of vascular aging studies performed in these animals

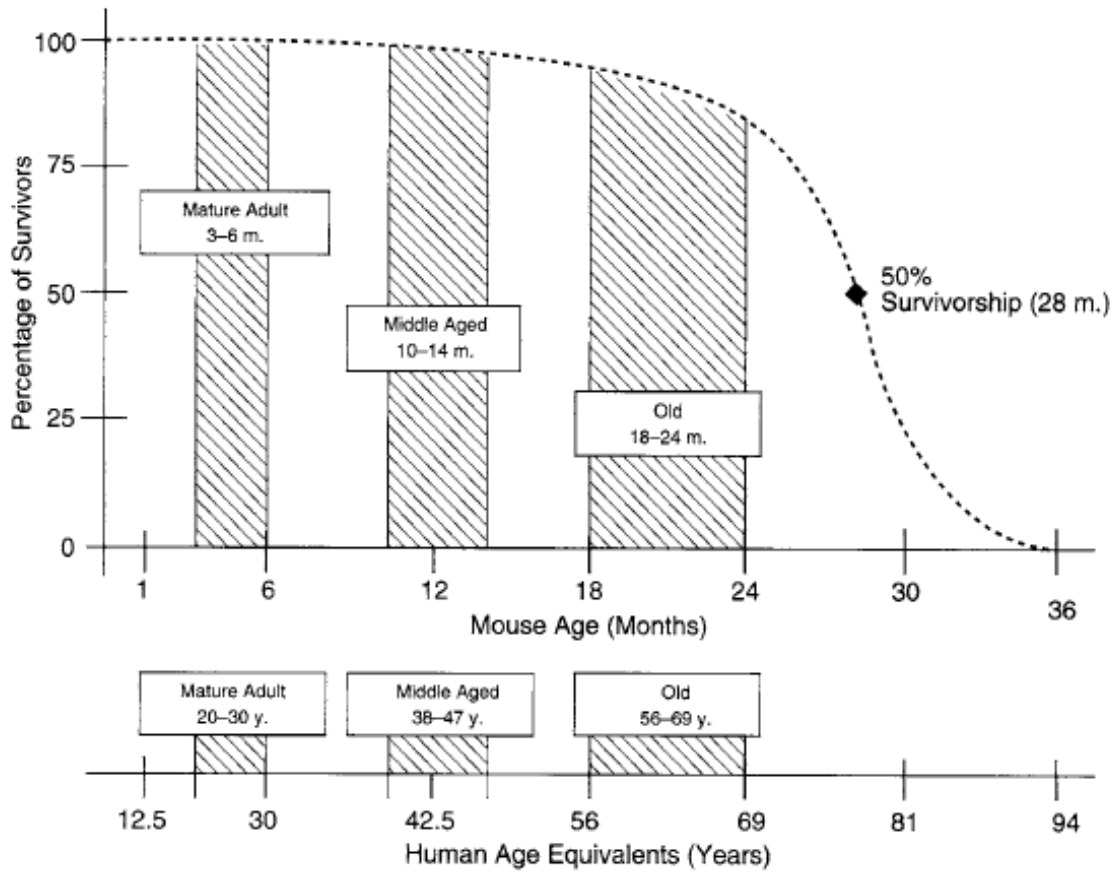


Figure 2.1. Representative age ranges for mature life history stages in C57BL/6J mice. Comparative development rates between mice and humans are as follows: 150 times faster between birth and 1 month, 45 times faster between 1–6 months, 25 times faster at > 6 months (Flurkey et al. 2007).

Aortas were excised from euthanized male C57BL/6J mice according to protocols approved by the Institutional Care and Use Committee (IACUC) of Boston University. Studies were performed on “young” and “old” mouse populations at 3 and 29 months of age respectively, with variability of ± 1 month. Animals were provided by Jackson Labs, with support from the National Institute of Aging.

2.4 Aortic Tissue Sampling

2.4.1 Preparation of Tissue

Harvested aortas were immediately placed in a physiological salt solution (Krebs PSS: 120 mM NaCl, 5.9 mM KCl, 11.5 mM dextrose, 25 mM NaHCO₃, 1.2 mM NaH₂PO₄, 1.2 mM MgCl₂, 2.5 mM CaCl₂; pH = 7.4) equilibrated with 95%-5% O₂-CO₂. Loose perivascular fat was removed from aortic samples. Segments of 4–5 mm in axial length (unloaded) were isolated from the proximal end of the descending thoracic aorta. There was no significant difference in axial length from cut segments with age.

2.4.2 Measurements of Aortic Geometry

Axial length and outer diameter of samples were measured under a light microscope (4x) during aortic dissection of unloaded segments in PSS. Small rings adjacent to both ends (proximal and distal) of the thoracic aorta ring to be studied were incubated for 30 minutes in nuclear stain (NucBlue from Life Technologies). After the incubation period, individual rings were imaged with fluorescence microscopy (20x) for auto-fluorescence of medial elastin fibers and the NucBlue stain via NIS-Elements

software (Nikon Instruments); **Figure 2.2** features an image of a sample ring. For each ring, 15–20 measurements were taken and averaged to obtain a single value for the medial thickness. These measurements of both proximal and distal thoracic aortic rings were then averaged to obtain a single representative unloaded wall thickness measurement for the thoracic aorta segment to be studied.

2.5 Evaluation of Aortic Tissue Stiffness *Ex Vivo*

2.5.1 Uniaxial Stretching Apparatus and Normalization of Force Measurements

Thoracic aorta segments were suspended in an organ bath (volume: 60 mL), submerged in oxygenated Krebs PSS warmed to 37°C by a thermostat-controlled water bath and circulation system to maintain viability and threaded with triangular wire clasps. This allows the segments to be stretched uniaxially in a way that simulates circumferential distension. Results from all of Chapter 4, as well as Chapter 3.4.5, were obtained using wire of 0.01 inches in diameter. All other results were obtained using wire of 0.005 inches in diameter.

Stretch was monitored by the Model 300C Dual-Mode Lever Arm System by Aurora Scientific, Inc. (Aurora Scientific, Ontario, Canada) and performed by using an electronic input to the lever arm motor via a function generator. Chart software (AD Instruments) was used for data acquisition from the system. The extent of stretch performed to obtain a steady-state force response, known as the operating length and specific to each sample, was established as circumferential strain ϵ , a percentage of outer aortic diameter of that sample in the unloaded state.

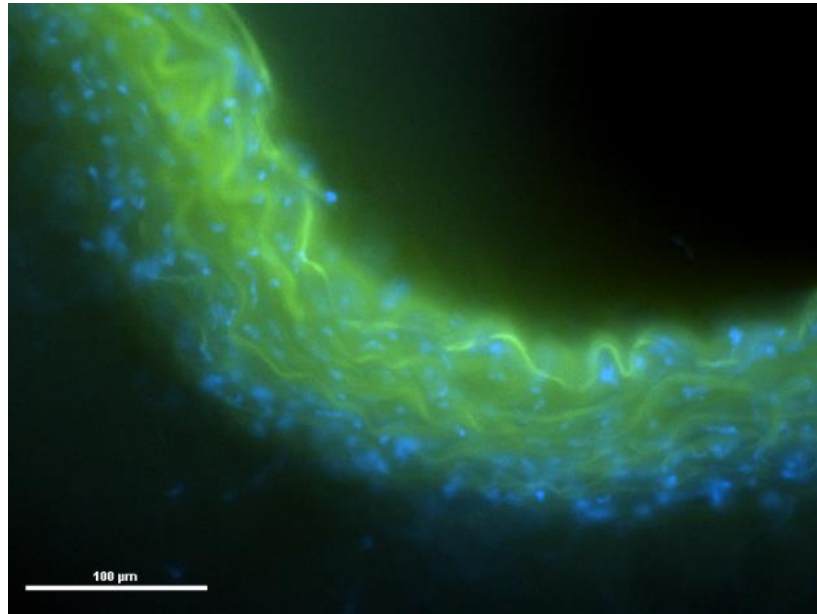


Figure 2.2. Fluorescence microscopy of a young mouse aortic wall cross-section. Wall thickness of an aortic sample is measured from fluorescence of medial elastin fibers (green) and nuclear stain for smooth muscle cells (blue).

The lever arm also served as a force transducer, allowing for measurements of a steady-state force F , the equilibrated response after stretching to the operating length. Dividing force by the axial length l of the tissue normalizes it to wall tension. Circumferential stress σ was obtained by normalizing F to cross-sectional area A of unloaded tissue: $\sigma = F/A$ and $A = 2hl$, where h is the wall thickness and l is the axial length.

2.5.2 Quasi-Static Stress-Strain Curves

Using the same stretching apparatus, stress-strain curves were obtained from force responses to slow, high-amplitude ramp stretches applied from the unloaded state, or slack length. The strain rate applied to aortic samples was 20% per second, up to either a maximum of 400% or the point of tissue yield and rupture. The force response corresponding to the loading curve was normalized to stress. Stiffness values for specific strains were obtained by plotting stress against strain and calculating the local slope, i.e., the elastic modulus, around specific strain levels. Tissues were maintained in calcium-free PSS (120 mM NaCl, 5.9 mM KCl, 11.5 mM dextrose, 25 mM NaHCO₃, 1.2 mM NaH₂PO₄, 1.2 mM MgCl₂, 2 mM EGTA; pH = 7.4) to isolate passive mechanical properties of the aortic wall attributable to extracellular matrix and minimize contributions from vascular smooth muscle cells.

2.5.3 High-Frequency Low-Amplitude Sinusoidal Perturbations

Ex vivo aortic stiffness is defined in this study as the material stiffness of aortic tissue, equivalent to the elastic modulus derived from directly measurable circumferential force responses to small-length oscillations (Kawai and Brandt 1980). High-frequency (40 Hz), low-amplitude (+1% of slack diameter superimposed upon optimal length) sinusoidal strain (HFLA) was applied persistently to obtain a time course of force-response data. Based on previous studies and confirmed experimentally here, these parameters resulted in negligible phase lag of the force response or breakage of actomyosin cross bridges in the tissue (Brozovich and Morgan 1989). Solution changes were conducted without disturbance to the ongoing movement of the lever arm or the force trace as monitored via software.

As shown in **Figure 2.3**, oscillatory sinusoidal input produced a force response from which the change in stress is calculated as the amplitude of the force output waveform (ΔF) normalized to cross-sectional area A . Stiffness is defined as this change in stress divided by the change in strain (1%, ΔL) imposed atop the strain of the operating length (L). This strain was applied to equilibrated tissue at least 30 minutes after stretch to L . Effectively, the HFLA protocol produces a local stress-strain relationship in the neighborhood of the operating length L ; the stiffness is the elastic modulus as calculated from this response.

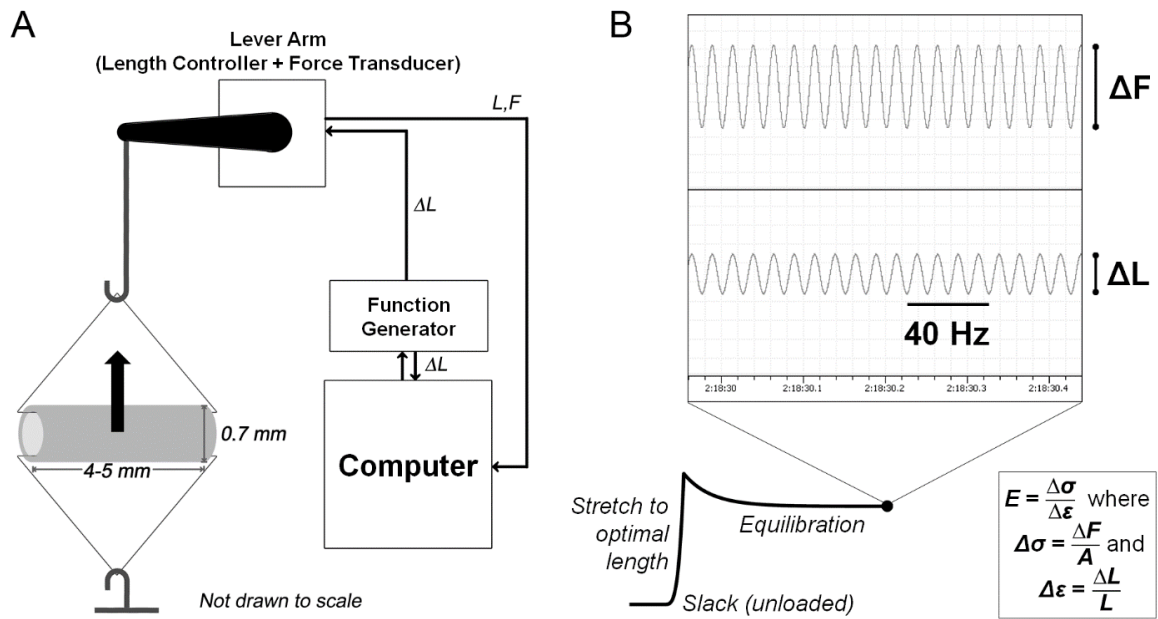


Figure 2.3. Ex vivo steady-state stiffness methods. (A) Schematic of lever arm for stiffness measurements; steady-state force response measured from stretching the tissue sample (shown here with typical unloaded *ex vivo* geometry) is that which is experienced in the circumferential direction at the center of the axial cross-section (arrow). **(B)** Representative force trace with sample inset of electronic recordings for high-frequency low-amplitude (HFLA) oscillatory stretch; sinusoidal length input (ΔL) and force output (ΔF) were used to calculate stiffness at optimal length L . Stiffness E is the ratio of change in stress ($\Delta\sigma$, equivalent to ΔF normalized to cross-sectional area A), to change in strain experienced by tissue ($\Delta\varepsilon$).

2.5.4 Confirmation of Vascular Smooth Muscle Viability

Prior to all steady-state force measurements made using the lever arm length controller, I used 51mM KCl PSS (75 mM NaCl, 51 mM KCl, 11.5 mM dextrose, 25 mM NaHCO₃, 1.2 mM NaH₂PO₄, 5.35 mM MgCl₂, 2.5 mM CaCl₂; pH = 7.4) to confirm VSMC viability in all aortic samples. This solution depolarizes smooth muscle cells and opens voltage-gated calcium channels, increasing intracellular calcium levels and inducing muscle contraction. A stimulation period of 15 minutes enabled samples to approach contractile steady-state. After confirming VSMC viability, I washed out the KCl with Krebs PSS and allowed samples an equilibration period of 30 minutes to return to an inactivated baseline.

To maximally activate VSMCs in these samples, I then performed a two-step treatment. First, I added 10 μM alpha agonist phenylephrine (PE), which has previously been shown to increase contractility by both actin- and myosin-mediated mechanisms (Yamin and Morgan 2012) maximally at the noted concentration (Russell and Watts 2000). Equilibration occurred 15 minutes after addition of PE. Second, after equilibration, I followed with the addition of 300 μM L-NG-nitroarginine methyl ester (L-NAME), a cell-permeable precursor of nitroarginine that inhibits nitric oxide synthase (NOS) (Barton et al. 1998, Rees et al. 1990). Nitric oxide, a product of the intimal endothelial monolayer in the mouse arterial wall, alters aortic smooth muscle tone and would be expected to alter stiffness. Equilibration was reached 20 minutes after addition of L-NAME.

2.6 Biochemical Analysis

Screening with phosphotyrosine immunoblots as an indicator of focal adhesion signaling in quick-frozen young and old mouse aorta homogenates was performed with the technical help of Cynthia Gallant and Qian Qian Lin. Tissues were quick-frozen in an acetone/dry ice slurry containing 10% trichloroacetic acid (TCA) & 10 mM dithiothreitol (DTT), homogenized and processed at 4°C as described previously by our group (Marganski et al. 2005). The homogenization buffer, designed to preserve native phosphoprotein levels, consisted of 20 mM MOPS, 4% SDS, 10% glycerol, 10 mM DTT, 20 mM β -glycerophosphate, 5.5 μ M leupeptin, 5.5 μ M pepstatin, 20 KIU aprotinin, 2 mM Na_3VO_4 , 1 mM NaF, 100 μ M ZnCl_2 , 20 μ M AEBSF, and 5 mM EGTA. Densitometric analysis of immunoblots was performed using Odyssey Infrared Imaging System (LI-COR Biosciences, Lincoln, NE). Tyrosine phosphorylation densitometry was normalized to that of alpha-tubulin densitometry. Tyrosine phosphorylation was examined after 15 minutes exposure of the vascular tissue to PE. At this time point, VSMC activation has reached steady-state values, corresponding to the maximally effective dosage of 10 μ M (Russell and Watts 2000).

2.7 Cell-Permeable Decoy Peptides

2.7.1 Design and Synthesis

A preliminary investigation of possible synthetic therapeutic treatments for increased aortic stiffness regulated by vascular smooth muscle, as detailed in this thesis, sought to determine the potential of two cell-permeable peptides (CPP) that competitively

inhibit binding sites relevant to regulatory processes for focal adhesion protein-protein interactions as well as actin polymerization within aortic vascular smooth muscle cells. CPP sequences were designed by Robert Saphirstein, former member of the Morgan group at Sargent College and Dr. Paul Leavis of Tufts University with an Applied Biosystems model 433A peptide synthesizer by solid-state peptide synthesis using fluorenylmethoxycarbonyl chemistry (Kim et al. 2008).

Peptides were acetylated at their N-termini and a TAT (transactivator of transcription) protein transduction domain with the 14-amino-acid sequence GSGYGRKKRRQRRR was coupled at the C-termini in order to mediate transfer across the cell membrane (Heitz et al. 2009, Marganski et al. 2005). AHX (1-aminohexanoic acid), a six-carbon bridge molecule, was used to attach fluorescent tags (FITC or rhodamine) enabling visual confirmation of permeation without adverse effects on stability. The C-terminus of the AHX is attached to the first lysine in the TAT sequence, while the fluorophore is attached to the N-terminus. The study presented in this dissertation focuses on two CPPs in active and inactive/scrambled-sequence (-X) forms as presented in the **Table**: TLN-VBS and N-WASP-CA. Mass spectrometry confirmed product purity.

2.7.2 Loading Solutions

From dry powder, loading solutions for CPPs were prepared by dissolution and dilution. For each peptide, experimental loading volumes were obtained via diluting 1 mM stock solutions. Both forms of TLN-VBS were readily soluble in Krebs PSS. To

Stock	Name	Sequence (5'-3')	Label	Mass (Da)
1	TLN-VBS	GRPLLQAAKGLAGAVSELLRSAQPA	FITC	4762
2			Rhodamine	4827
3			None	4116
4	TLN-VBS-X	LLRRSQAALGAAAEVLPQALSGPGK	FITC	4762
5	N-WASP-CA	TSGIVGALMEVMQKRSKAIHSSDED- EDEDDEEDFEDDDEWED	FITC	6907
6	N-WASP-CA-X	DEMLEQEKGDESGIDSGDKDMEEV- DSWEVEDHSETDIADDE	Rhodamine	6957
7			None	6372

Table 1. Cell-permeable decoy peptide (CPP) sequences and stocks. Two CPPs were designed for competitive inhibition of binding sites, resulting in disruption of protein-protein interactions within focal adhesions (TLN-VBS) and processes involved in actin polymerization (N-WASP-CA). These CPPs were used in tissue experiments as inhibitors of increases in aortic stiffness induced by agonist stimulation of vascular smooth muscle. The inactive scrambled forms (-X) of these CPPs were also synthesized to serve as a negative control in these tissue stiffness experiments. Several peptide stocks were labeled with one of two fluorescent labels (FITC or rhodamine) as denoted; corresponding total molecular masses in Daltons are tabulated.

dissolve N-WASP-CA, calcium- and magnesium-free Hanks buffered salt solution: 137 mM NaCl, 5.4 mM KCl, 0.42 mM NaH₂PO₄ • H₂O, 0.44 mM KH₂PO₄, 4.17 mM NaHCO₃, 10 mM HEPES, 5.55 mM dextrose; pH = 7.4) was used as the solvent, with additional volumes of 1 N NaOH and HCl required to complete dissolution and maintain the physiological pH of 7.4. Corresponding to the **Table**, proportional volume ratios were: 89.5% Hanks, 5.5% NaOH, 5% HCl for Stock 5; and 94.5% Hanks, 3% NaOH, 2.5% HCl for Stocks 6 and 7. Starting with this 1 mM stock solution for each experiment, dilution into additional salt solution was performed to obtain 600 μL of loading volume with the desired concentrations of peptide: 100 or 250 μM in Krebs (TLN-VBS) or Hanks (N-WASP-CA).

2.7.3 Tissue Loading and Unloading

Immersing an aortic tissue sample in loading solution is essentially a pre-treatment procedure; in other words, it must be done before stimulation of the vascular smooth muscle. In order to conserve peptide stock, loading was not done in the 60 mL organ bath. Instead, one-hundredth of the volume (600 μL) was prepared for use, as detailed in the previous section, into the “loading tray,” an apparatus consisting of a 900-μL well (1.5 cm x 1.5 cm x 0.4 cm) cut into a disk of polydimethylsiloxane (PDMS) gel, glued to a double stack of small weigh boats. This loading tray was designed and built with the assistance of Robert Saphirstein.

After dissection of an aortic ring segment, I threaded it with a single triangular wire clasp parallel to a piece of straight wire, then transferred the tissue to the loading

tray containing the loading solution. Using small surgical pins, I manually stretched the tissue to the physiologic strain level corresponding to 80% of the tissue's unloaded outer diameter by pulling the triangular clasp and wire apart to the precise length as measured with a light microscope. The tray was then moved to sit atop the organ bath, which was filled with distilled water and heated to 37°C with the circulation system. The dimensions of the weigh boat enable its depth to be submerged within the heated water while lying balanced atop the organ bath, allowing the liquid in the organ bath to transfer heat to the contents of the tray. Finally, the loading solution was bubbled gently with the appropriate gas: 95%-5% O₂-CO₂ for Krebs and O₂ for Hanks. Therefore, the peptide is able to permeate the vascular smooth muscle cells under the "physiologic" conditions established as if the tissue had been mounted inside the organ bath itself. The entire apparatus is shown in **Figure 2.4**.

I employed a loading period of 30 minutes, after which the apparatus was dismantled, and the tissue unmounted from the wires and returned into the dissection dish. This completed the peptide loading phase. The regular procedure of mounting the tissue onto the standard uniaxial stretching apparatus followed, with the additional step of delaying the initial stretch to optimal length by an additional 30 minutes after mounting, in order to allow the tissue to recover from the loading procedure and regain its original unloaded dimensions.

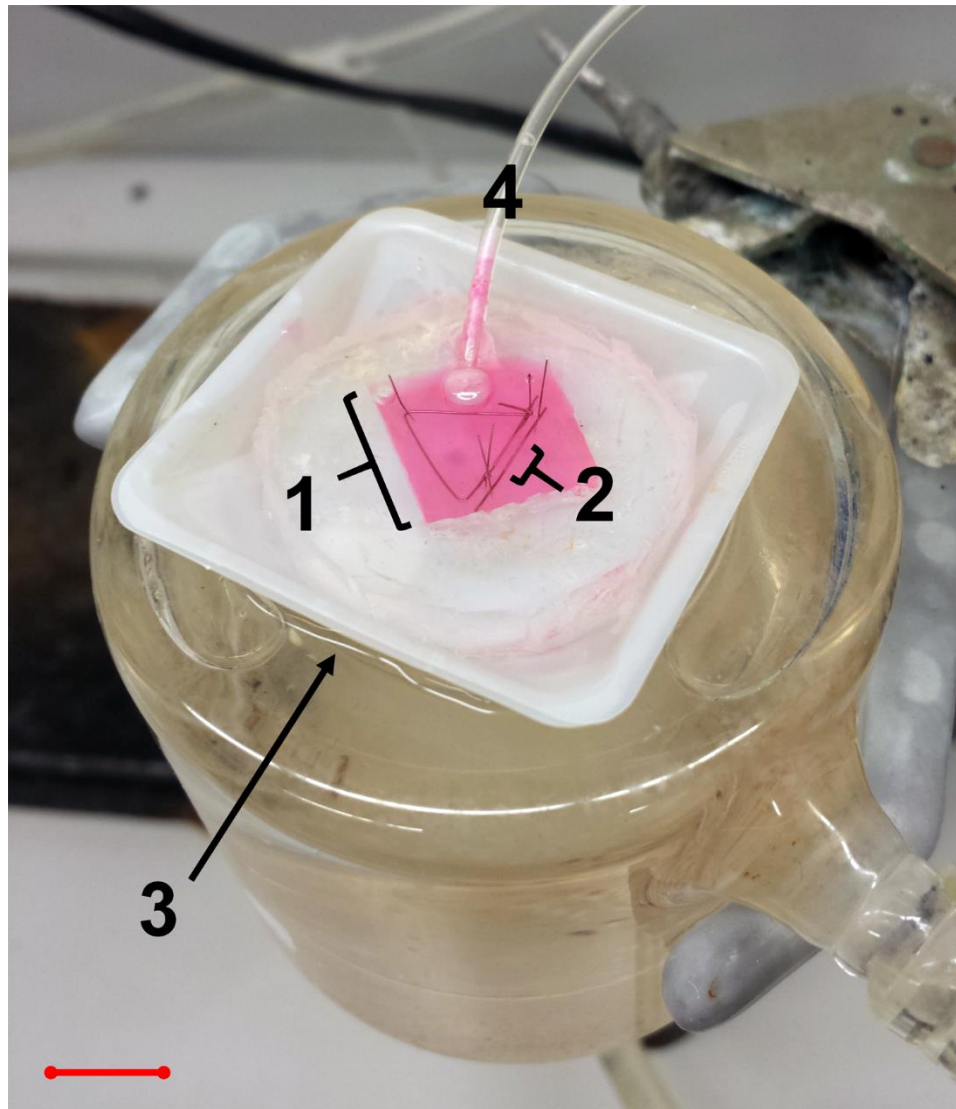


Figure 2.4. Apparatus for peptide loading protocol with aortic tissue. (1) A small volume of peptide loading solution (here tagged with rhodamine) is pipetted into a 900- μ L well (1.5 cm x 1.5 cm x 0.4 cm) cut into a disk of polydimethylsiloxane gel that is glued to a double stack of weigh boats. (2) Aortic tissue sample is manually stretched uniaxially to 80% strain and immersed in the loading solution. (3) The weigh boat rests atop an organ bath filled with water warmed to 37° C to simulate body temperature. (4) Oxygen line is arranged to provide gentle bubbling into the loading solution. Red scale bar: 1 cm.

2.8 Reagents

Agonist phenylephrine (PE) was obtained from Sigma-Aldrich. PP2 (10 mM in solution) was purchased from EMD Biosciences (La Jolla, CA). L-NAME (dry powder) was purchased from Cayman Chemical Company (Ann Arbor, MI). NucBlue live cell stain was purchased from Life Technologies (Eugene, OR). Antibodies used for biochemical analysis were phosphotyrosine (mouse, 1:500) from BD Biosciences (San Jose, CA) and alpha-tubulin (rabbit, 1:50,000) from Abcam (Cambridge, MA).

2.9 Statistics

Results are reported as mean \pm standard error. Unless explicitly stated otherwise in figure legends, single statistical comparisons were made with two-tailed Student's t-tests, while analysis of variances (ANOVA) and Sidak's post-hoc test were used for all instances of multiple comparisons. Significance tests were performed in GraphPad Prism and significance was defined at levels of $p < 0.05$, 0.01 , and 0.001 .

Chapter 3: Aging Impairs Smooth Muscle Mediated Regulation of Aortic Stiffness

3.1 Disclosure

Text and figures in the following sections in this chapter were modified from (Gao et al. 2014): 3.2, 3.3, 3.4.1, 3.4.2, 3.4.5, 3.4.7, 3.4.8, 3.4.9, 3.5.1, 3.5.2, and 3.5.3 up through “Recently, our group has shown that the regulatory role of NMC extends to venous stiffness ...”

3.2 Summary

Increased aortic stiffness is an early and independent biomarker of cardiovascular disease. Here, I tested the hypothesis that vascular smooth muscle cells (VSMCs) contribute significantly to aortic stiffness and investigated the mechanisms involved. The relative contributions of VSMCs, focal adhesions (FAs), and extracellular matrix to stiffness in mouse aorta preparations at optimal length and with confirmed VSMC viability were separated by the use of small molecule inhibitors and activators. Using biomechanical methods designed for minimal perturbation of cellular function, I directly quantified changes with aging in aortic material stiffness. An alpha adrenoceptor agonist, in the presence of L-NAME to remove interference of endothelial nitric oxide, increases stiffness by 90–200% from baseline in both young and old mice. Interestingly, increases are robustly suppressed by the Src kinase inhibitor PP2 in young but not old mice. Phosphotyrosine screening revealed, with aging, a biochemical signature of markedly impaired agonist-induced FA remodeling previously associated with Src signaling.

Protein expression measurements confirmed a decrease in Src expression with aging. Thus, I report here an additive model for the *ex vivo* biomechanical components of the mouse aortic wall in which: 1) VSMCs are a surprisingly large component of aortic stiffness at physiologic lengths and 2) regulation of the VSMC component through FA signaling and hence plasticity is impaired with aging, diminishing the aorta's normal shock absorption function in response to stressors.

3.3 Introduction

Aortic stiffness, a biomechanical property of material and structure, is clinically assessed using *in vivo* observations of pulse wave velocity (PWV). Increased PWV is an early and independent biomarker of cardiovascular disease.

It is far from clear how changes in blood vessel properties contribute to observed increases in PWV. A mathematical relationship between PWV and vessel stiffness has been described by the Moens-Korteweg equation, in which PWV is proportional to the square root of elastic modulus, alternatively known as material stiffness (Greenwald 2007), and also dependent on wall thickness and vessel diameter. However, the Moens-Korteweg equation is predicated on several simplifying and non-physiologic assumptions, including uniformity of vessel composition (Clark and Glagov 1985, Gosling and Budge 2003), as well as dynamic values of vessel geometry that are difficult to quantify *in vivo*. Therefore, in order to understand more comprehensively the relationship between PWV and aortic material stiffness, it is first necessary to determine

ex vivo how changes to material properties of the blood vessel wall and its subcomponents contribute to aging-induced increases in aortic stiffness.

VSMCs may play an important role in effecting and affecting aortic stiffness, although their contributions relative to that of ECM and the effects of aging have not been ascertained. Here, aortic mechanical properties were directly measured to assess aortic stiffness in tissue samples from mice confirmed to contain viable smooth muscle cells. I demonstrated that these properties are separable into quantifiable components distinguished by activation levels of VSMCs and that, unexpectedly, smooth muscle contributes up to half of total material stiffness. These measurements were performed for the first time in old mouse aortas using direct mechanical distension to produce circumferential strain, in contrast to previous biomechanical studies of old aortas utilizing pressurization (Pezet et al. 2008, Philibert et al. 2012). Furthermore, I show that with aging, regulatory pathways related to focal adhesion signaling in the smooth muscle cell are lost, an effect expected to compromise the ability of the proximal aorta of an old mouse to perform its normal function as a hemodynamic shock absorber and maintain appropriate stiffness levels in the presence of *in vivo* challenges.

3.4 Results

3.4.1 Physiologic optimal length in mouse aorta does not change with age

The physiologic range of circumferential stretch ratios experienced by mouse aorta *in vivo* during normal blood flow is between 1.5–1.8 (Wagenseil and Mecham 2012), i.e., a circumferential strain of 50–80%. To select the value within this range most

appropriate for stiffness measurements reflective of physiologic VSMC contributions, I determined the physiologic optimal length of the tissue, the value for which active force production is maximal, both in young and old mouse aortas (Blaustein et al. 2012). This was done via analysis of a length-tension curve, normalized to a stress-strain curve, for induced aortic vascular smooth muscle contractility.

At 20% increments of sustained circumferential strain, up to 200% total strain, the contraction resulting from 15 minutes' steady-state equilibration with 51mM KCl PSS was recorded. After subsequent washout with Krebs PSS and another 30 minutes of equilibration, the tissue was stretched to the next increment of 20% strain. As shown in **Figure 3.1A**, the contractile force production at 80% circumferential strain is not significantly different from maximal force production and is also within the in vivo range of circumferential strain measured by Wagenseil and Mecham. Furthermore, optimal length was determined not to differ between young and old mice. Thus, 80% was used as the operating strain for all subsequent *ex vivo* stiffness measurements.

The induced contractile stress accounted for approximately half of the total aortic stress experienced at the operating strain of 80% and that this proportion is greater in old mice, as shown in **Figure 3.1B**. Therefore, the role of smooth muscle in the makeup of total aortic stress is far from trivial, and when fully stimulated, VSMCs contributes proportionally more with aging. While this was highly encouraging of a more rigorous investigation, I first sought to compare the results of our methodology to those established in the literature, which focuses mostly on passive stiffness characterized by extracellular matrix.

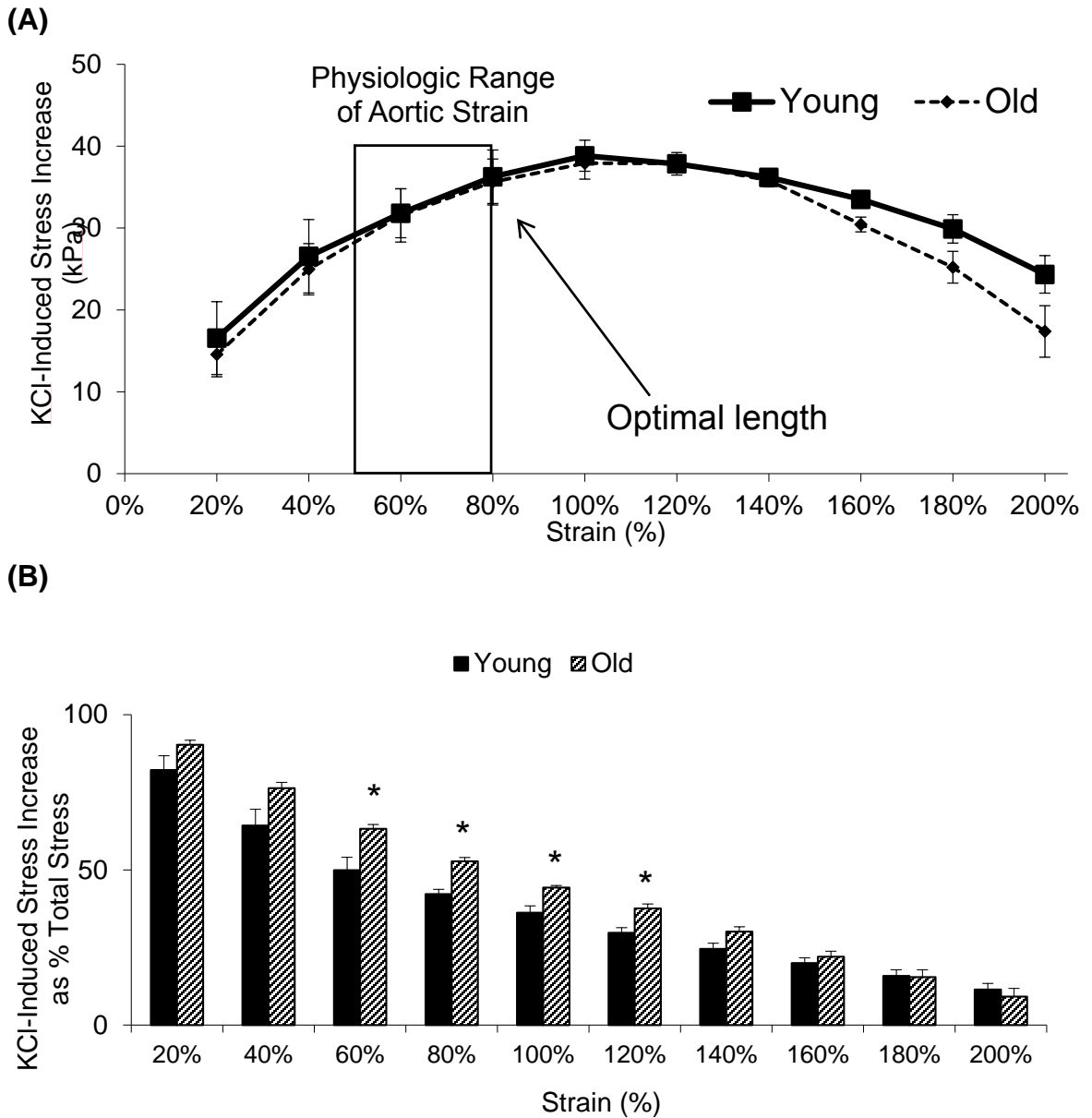


Figure 3.1. Physiologic optimal length in young and old mouse aorta. (A) The strain level at which maximal contractile stress (kPa) occurs within physiologic ranges of aortic strain was determined to be 80% in both young and old mice (n = 3 each). (B) At 80% strain, maximal contractile stress constitutes a greater proportion of total stress (53%) in old aortas compared to that in young aortas (42%); *, p < 0.05.

3.4.2 Baseline aortic wall tension increases with aging at optimal length but stiffness decreases

Measurements from 13 young and 12 old mice demonstrated significant increases in average outer vessel diameter at slack length (young: 755 ± 10 , old: 936 ± 17 μm , $p < 0.001$) and wall thickness (young: 56.9 ± 0.4 , old: 76.9 ± 0.9 μm , $p < 0.001$). Assuming cylindrical geometry of each wall at slack length, inner diameter was inferred also to increase with age and approximated by subtracting twice the thickness from the outer diameter, resulting in means of 641 μm in young versus 782 μm in old.

Baseline force is defined as that experienced by an aortic tissue sample stretched to 80% strain and allowed to equilibrate. The baseline stiffness (elastic modulus) was measured as the resultant ratio of change in stress to change in strain in response to high-frequency low-amplitude (HFLA) changes in length (1% of slack diameter), as a sinusoidal oscillatory stretch superimposed upon optimal length. Changes in strain were minimized to cause essentially negligible perturbation of the tissue.

Observed at steady-state after equilibration at optimal length, baseline force increased significantly with aging (+34%, $p < 0.001$) in response to being stretched to the operating strain of 80% (**Figure 3.2A**). In vivo, wall tension is an important parameter, particularly under hypertensive conditions, as it has been linked to changes in transforming growth factor- β (TGF- β) and NO release from the endothelium (Prado and Rossi 2006). When wall tension (**Figure 3.2B**) is calculated by dividing the measured force by axial length, there is also a significant increase with aging (+32%, $p < 0.001$). However, when normalized by cross-sectional area to calculate stress (**Figure 3.2C**), no

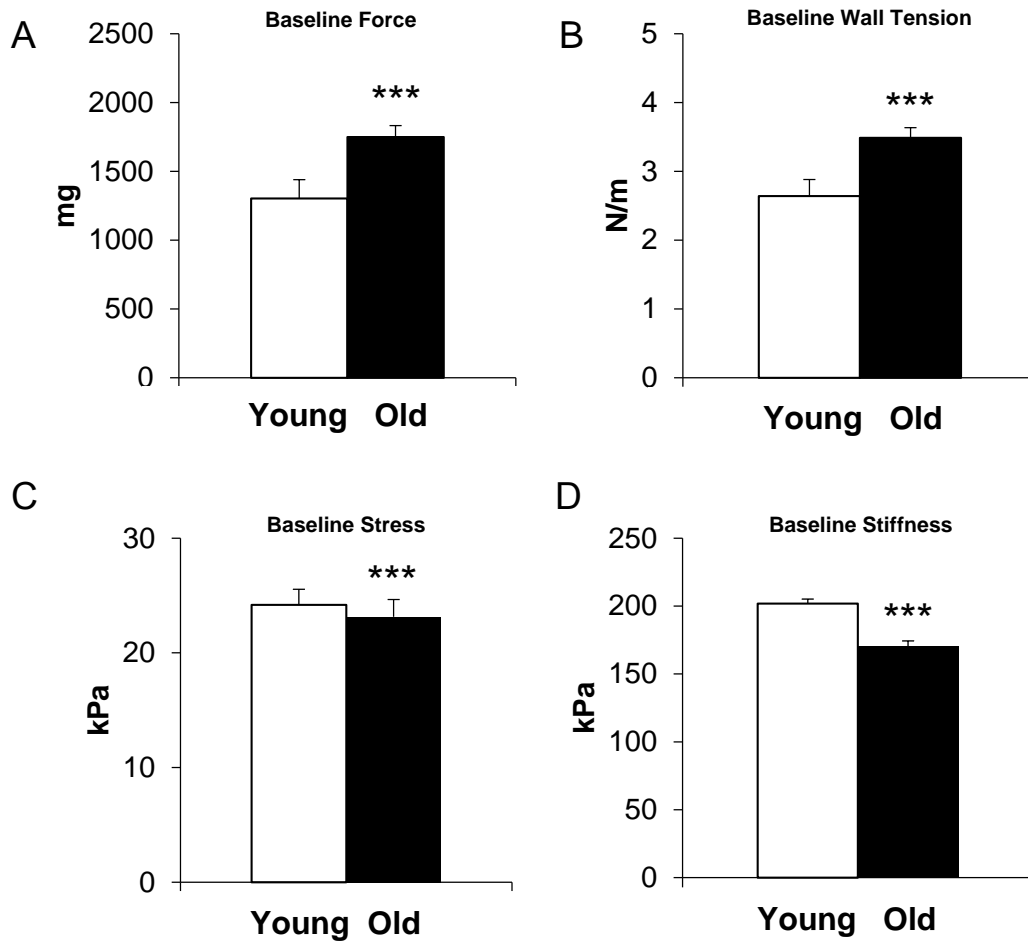


Figure 3.2. At optimal length, baseline aortic wall tension increases with aging, but stiffness decreases. Values are mean \pm SE; ***, $p < 0.001$. (A) Baseline aortic stiffness via stress-strain measurements in the absence of agonist decreases with aging. (B) Baseline steady-state force increases with aging. (C) Wall tension, equivalent to force normalized to axial length, increases with aging. (D) Stress, equivalent to tension normalized to wall thickness, does not change with aging. (E) Baseline aortic stiffness via HFLA measurements in the absence of agonist decreases with aging. $n = 15$ young and 18 old for (A), 13 young and 12 old for (B), (C), (D), (E).

difference is seen, indicating that vessel geometry is the primary effector of increased wall tension.

I performed small HFLA stretches to calculate stiffness and found that the baseline value actually significantly decreased by 16% with aging ($p < 0.001$) as shown in **Figure 3.2D**. This was surprising given previous reports of increased PWV in old mice (Reddy et al. 2003). It is clear that baseline *ex vivo* material stiffness, calculated as elastic modulus, fails to account for aging-induced increases in PWV alone when applied to the Moens-Korteweg equation in conjunction with changes in wall geometry.

3.4.3 *Ex vivo* baseline stiffness does not increase in hypertensive mouse models of high-fat-diet and angiotensin II

Hypertension is closely associated with both aging and increased aortic stiffness. Although it was surprising that *ex vivo* baseline stiffness did not increase with aging, I sought to confirm the hypothesis of higher stiffness expected in diseased mouse models reflective of hypertensive physiology.

For the first part of a collaborative study with the Vascular Biology Section at the Whitaker Cardiovascular Institute of Boston University Medical Center, I collected *ex vivo* stiffness measurements on aortas extracted from male C57BL/6J mice of two different hypertensive model populations. The first population, consisting of ten-month-old (middle-aged) mice that were fed an eight-month high-fat/high-sucrose (HFHS) diet, was also the subject of a published study by the Vascular Biology Section, in which significant physiological changes such as increased pulse wave velocity and mean arterial

pressure, decreased nitric oxide availability, as well as indication of kidney damage, were all observed (Weisbrod et al. 2013). These mice were compared against a set of normal-diet (ND) controls. The second population consisted of eight-week-old male C57BL/6J mice that were infused with a seven-day regimen of subpressor angiotensin II (Ang II), which induces downstream hypertensive effects including hypertrophy of the arterial medial layer and collagen deposition (Fleenor et al. 2010, Wang et al. 2010). These mice were compared against control animals that underwent saline infusion.

I was surprised to find that neither hypertensive model population displayed an increase in baseline stiffness values obtained by HFLA stretch, as shown in **Figure 3.3**. Once again, the anticipated increase in aortic material stiffness through direct biomechanical measurements does not occur *ex vivo*, despite the observation of an increase in PWV.

3.4.4 Baseline stiffness increases in Sirtuin-1 knockout mice with angiotensin II pretreatment

The second part of our collaboration with the Vascular Biology Section at the Whitaker Cardiovascular Institute of Boston University Medical Center shifted the focus from changes predominantly in aortic matrix to those affecting smooth muscle cells, specifically a model for Sirtuin 1 (SIRT1) deficiency in VSMCs. SIRT1 is a deacetylase that acts on important metabolic regulatory transcription factors and an anti-aging gene (Nemoto et al. 2005, Rodgers et al. 2005). The role in vasculature of SIRT1 is not entirely clear, but studies have identified SIRT1 as a homeostatic factor in vasculature

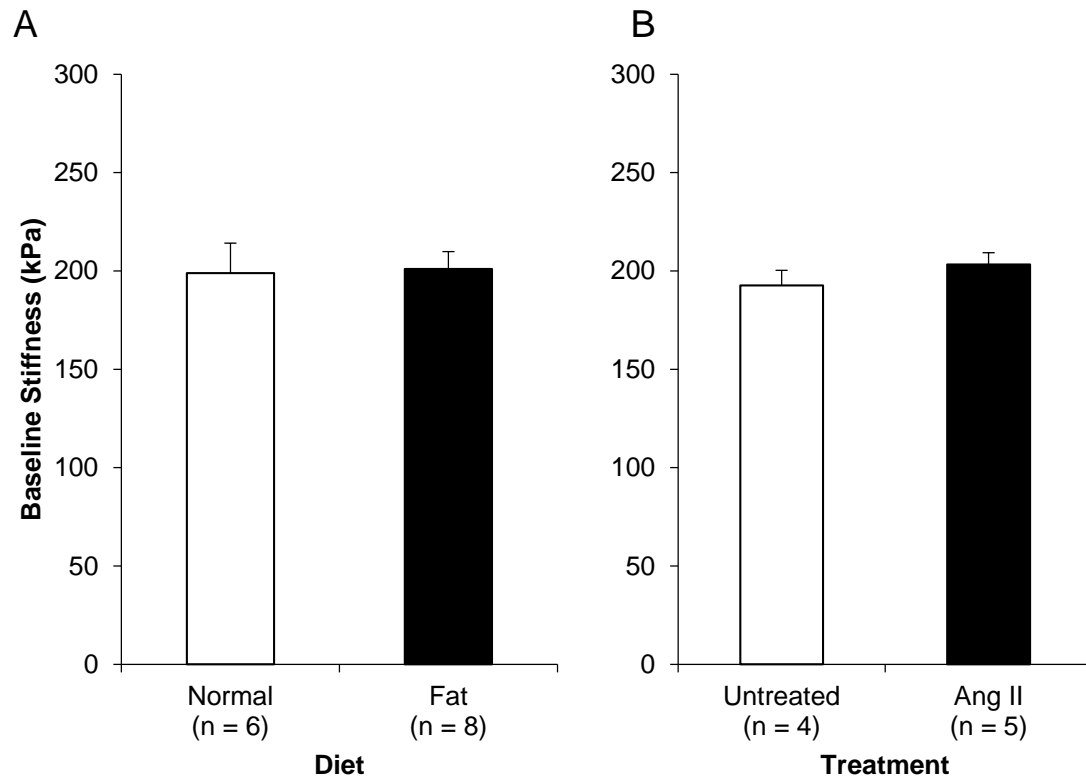


Figure 3.3. Baseline stiffness does not increase with high-fat diet (A) or angiotensin II pretreatment (B). No increase in baseline stiffness was observed in either of two diseased mouse models of hypertension against controls.

and key correlate of anti-oxidant and anti-inflammatory effects in various organ systems (Haigis and Sinclair 2010, Kawai et al. 2011, Yeung et al. 2004, Zhou et al. 2011). In mice, SIRT1 in VSMCs has been shown to shield against atherosclerotic and hypertensive effects by downregulating angiotensin II type 1 receptor expression, attenuating induced vascular remodeling (Gorenne et al. 2013).

I studied aortas from mutant mice bearing a deletion of SIRT1 (smooth muscle knockout, SMKO) that underwent a 5–7 day treatment course with Ang II to observe the biomechanical phenotype resulting from the absence of this protection. Upon applying HFLA stretch to SMKO mice, as well as wild-type controls, both with saline and Ang II infusions, I ascertained baseline stiffness as shown in **Figure 3.4**. The combination of the SIRT1 knockout and Ang II treatment produced a significant increase in baseline stiffness. Additionally, my collaborators found excellent consistency between my *ex vivo* measurements and their *in vivo* pulse wave velocity recordings.

When considering this outcome in the context of other observations made by the collaborators, there emerges a strong motivation to enhance our biomechanical understanding of aortic stiffness as pertaining to VSMCs. In SMKO mice, 70% of the population die of aortic dissection within two weeks after the beginning of treatment. Compared to Ang II wild-type mice, SMKO aortas exhibited significantly less adventitial collagen, but oxidant production in cultured VSMCs increased. Furthermore, aortic medial thickness decreased, with constituent elastin fibers suffering noticeable deformation, in concordance with higher expression of matrix metalloproteinases (MMPs) (Fry et al. 2015). These findings show that VSM SIRT1 is vitally important in

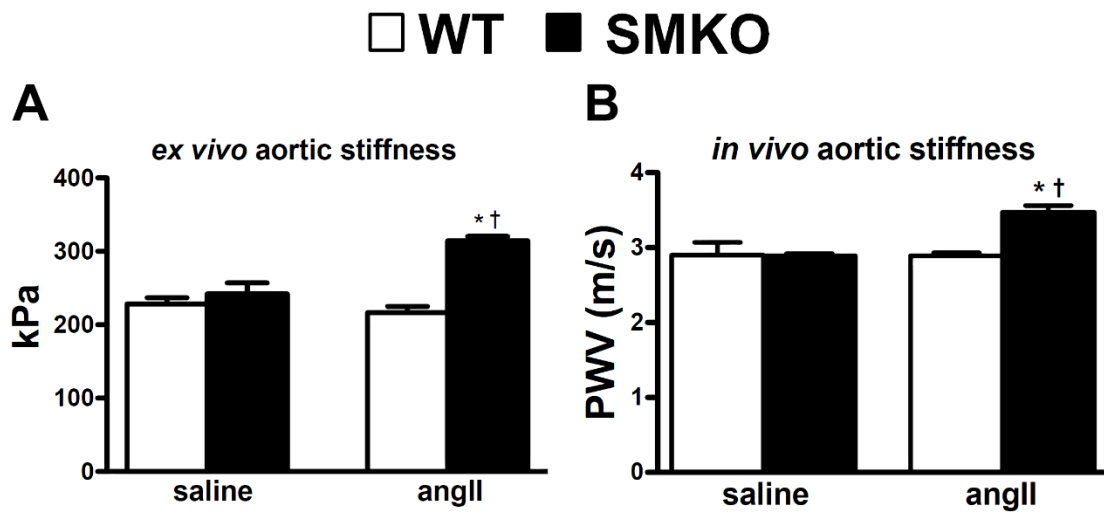


Figure 3.4. Sirtuin-1 knockout mice have increased baseline stiffness as measured *ex vivo* (A) and *in vivo* (B) with angiotensin II pretreatment. *, $p < 0.05$ versus saline; #, $p < 0.05$ versus wild-type, $n = 4-5$ for each population. Modified from (Fry et al. 2015).

maintaining the integrity of the aortic wall in response to hypertrophic agents such as Ang II, and presents critical justification for a more thorough investigation into the role of VSM and its regulatory mechanisms in anchoring aortic structure and function.

3.4.5 Increased passive aortic stiffness with aging occurs only beyond physiologic strain levels

Before turning to study VSM contributions to aortic stiffness, I deemed it necessary to reconcile the apparent discrepancy between our steady-state baseline results and stiffness results from other studies in the literature (Fleenor et al. 2014), I constructed stress-strain curves for young and old mouse aortas by subjecting tissue samples to slow, high-amplitude ramps spanning a range of strains from 0–250%, well beyond physiologic levels and beyond even the upper limit of previously acquired length-tension curves. Additionally, I eliminated any possible contributions from VSM by deactivating them in a calcium-free environment, mimicking the conditions established in similar studies (Fleenor et al. 2012). Passive aortic stiffness values were calculated as the local slopes of the stress-strain curve at 25%-strain intervals, with the exception of replacing the 75% point with 80% in correspondence with optimal length.

As shown in **Figure 3.5**, a significant increase with aging exists in stress and stiffness, beginning at strains of 250% and 200% respectively. Between 100–200% strain, the stress-strain curve for old aorta appears to overtake that of young aorta, which leads to higher stiffness values at higher strains. Thus, these results are compatible with increased passive stiffness attributed to old aortas in previous *ex vivo* studies which

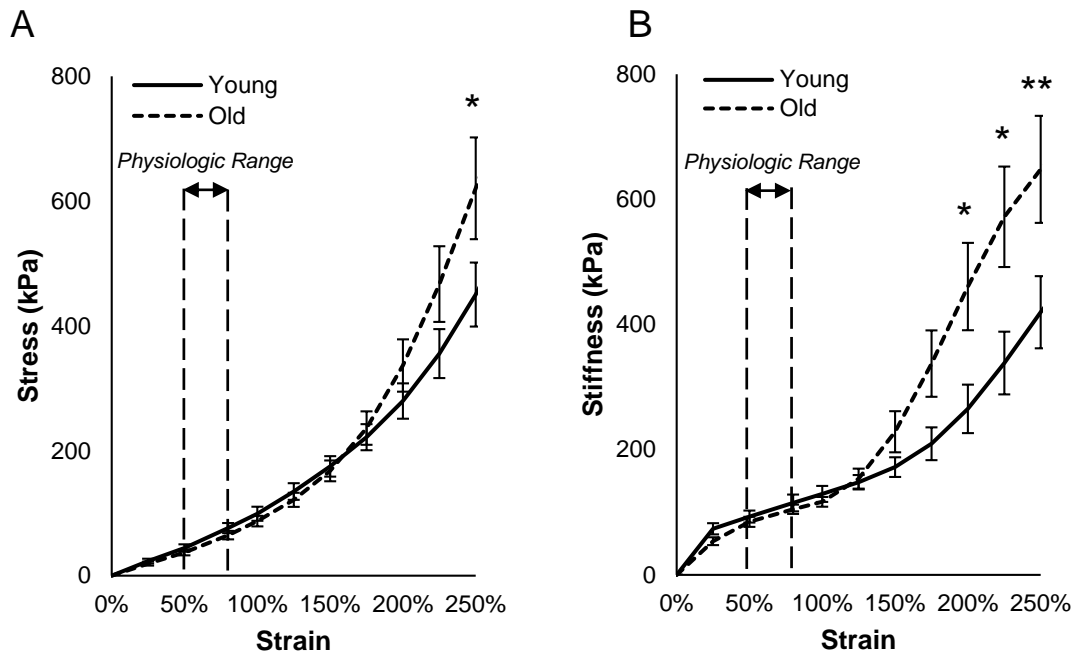


Figure 3.5. Passive aortic stiffness via mechanical stress-strain increases with aging only beyond physiologic strain range. Stress (A) and stiffness (B) plotted against strain for young and old proximal thoracic aortas in calcium-free environment using ramp input from slack to failure. No significant difference is observed at low strains, including the physiologic range of 50–80%. At higher strain levels, when collagen is heavily recruited due to large-amplitude stretching, old aortas are stiffer. $n = 6$ young, 7 old; values are mean \pm SE; */**, $p < 0.05/0.01$.

evaluate stiffness at higher strains (Fleenor et al. 2014, Fleenor et al. 2012, Pezet et al. 2008). Additionally, the stress-strain curve shows a downward trend in baseline stiffness with aging at physiologic strain ranges, qualitatively comparable to stiffness measured via the HFLA protocol.

3.4.6 Warming aortic tissue from cooled state produces opposite effects on stress versus stiffness

Having ascertained the difference in passive stiffness between young and old mice, I sought a better understanding of the distinction between baseline and passive stiffness. Previous studies in ferret aorta have defined a temperature-dependent aspect of VSMC contractility known as intrinsic tone. Cooling equilibrated vascular tissue suppresses the activity and contributions to wall stress and stiffness of VSMCs; this process is reversible upon warming the tissue back to body temperature (Pawlowski and Morgan 1992). From this, it follows that baseline stress and stiffness should comprise, in part, an intrinsic component that is observable by adjusting the environmental temperature of viable aortic tissue samples.

Therefore, in the context of these *ex vivo* studies, I am able to establish the broader notion of a temperature-dependent (t-d) aortic tone as the increase in force observed when viable aortic tissue is warmed from a deactivated state (2°C) to baseline at body temperature, which can be normalized to stress using wall geometry. Similarly, t-d stiffness is the difference between baseline stiffness and the measurement obtained at a cooled (deactivated) state via HFLA stretch. By this definition, t-d stress and stiffness are

not direct measurements. Rather, they are relative changes evaluated between two discrete observations: the deactivated and baseline states. I performed reversible cooling experiments with tissue in smaller sample populations young and old mice, for which increases in both stress and stiffness upon warming were expected from each population.

As shown in **Figure 3.6**, t-d stress is a positive value, while t-d stiffness is negative, a surprising change that was not seen in ferret aorta. In other words, stress increases and stiffness decreases when aortic tissue is warmed to baseline from a cooled state, highlighting a crucial and previously unstudied qualitative distinction between stress and stiffness in mouse aorta.

While these trends were undoubtedly interesting and provoked consideration of subsequent tangents focusing on the composition of stiffness, it was clear that there was little additional information to be gleaned from the baseline in search of a discrete contribution to total stiffness from VSMCs. Therefore, activation of the smooth muscle cells was necessary to advance this objective.

3.4.7 Vascular smooth muscle cells account for up to half of maximal total aortic stiffness

To study the contributions of VSM to aortic stiffness under more typically physiological conditions, I activated VSMCs in young and old aortas with PE, then L-NAME as detailed in Chapter 2.5.4. Steady-state stress and HFLA stiffness values were obtained after each equilibration period. I define the active stress and stiffness as the increases from baseline observed after addition of PE, reflecting the activation of the

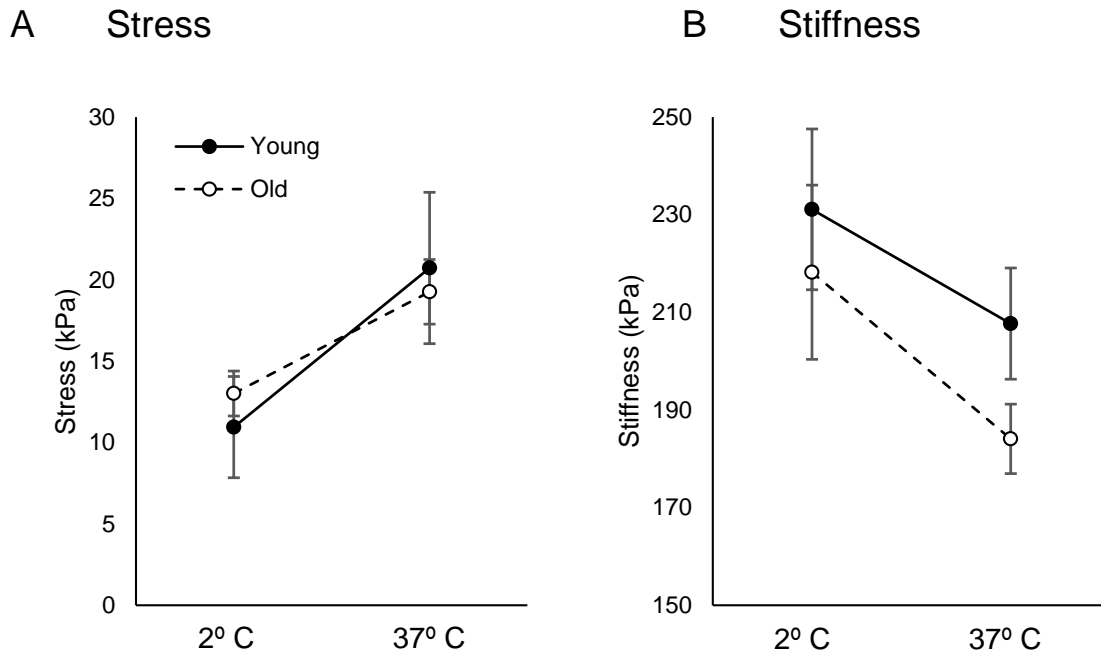


Figure 3.6. Warming aortic tissue from cooled state produces opposite effects on stress versus stiffness. Warming equilibrated aortic tissue at optimal length to deactivate smooth muscle cells induces opposite effects on stress (positive change) (**A**) and stiffness (negative change) (**B**), observable in young and old mice. Temperature-dependent decrease in stiffness is consistent with known properties of collagen. n = 3 young, 4 old; values are mean \pm SE.

smooth muscle cells. Treatment with L-NAME induced no change in baseline stress or baseline stiffness values after 30 minutes ($< 2\%$ change, ns), indicating that the VSMCs must be activated with agonist in order for NOS inhibition to have an effect on stress and stiffness, further supporting the concept that the active component is separable and necessarily dependent upon agonist stimulation. I define maximal active stress and stiffness as the increases from baseline observed after addition of both PE and L-NAME, or in purely quantitative terms, the sum of the active and NO-inhibited components.

No significant difference in the magnitude of the PE effects alone was seen between young and old mice (comparing white bars to corresponding black bars in **Figure 3.7A–B**). After 15 minutes of stimulation with PE, I treated aortas with L-NAME for an additional 20 minutes, with PE still active. Stress and stiffness significantly increased further, as shown in **Figure 3.7A–B** ($p < 0.001$). A smaller increase in stress resultant from NO inhibition was observed with aging as shown in **Figure 3.7A** ($p < 0.001$), reflecting the probable decrease in endothelial NO production with aging, as has previously been reported in other studies (Brandes et al. 2005, Taddei et al. 2001). On the other hand, no such difference in L-NAME-induced stiffness increases were seen (**Figure 3.7B**).

When baseline and maximal active components of aortic stress and stiffness are plotted to display different fractions of the total, as shown in **Figure 3.7C–D**, it becomes evident that activated aortic smooth muscle (the source of maximal active components) accounts for more than half of maximal total stress and approximately half of maximal stiffness.

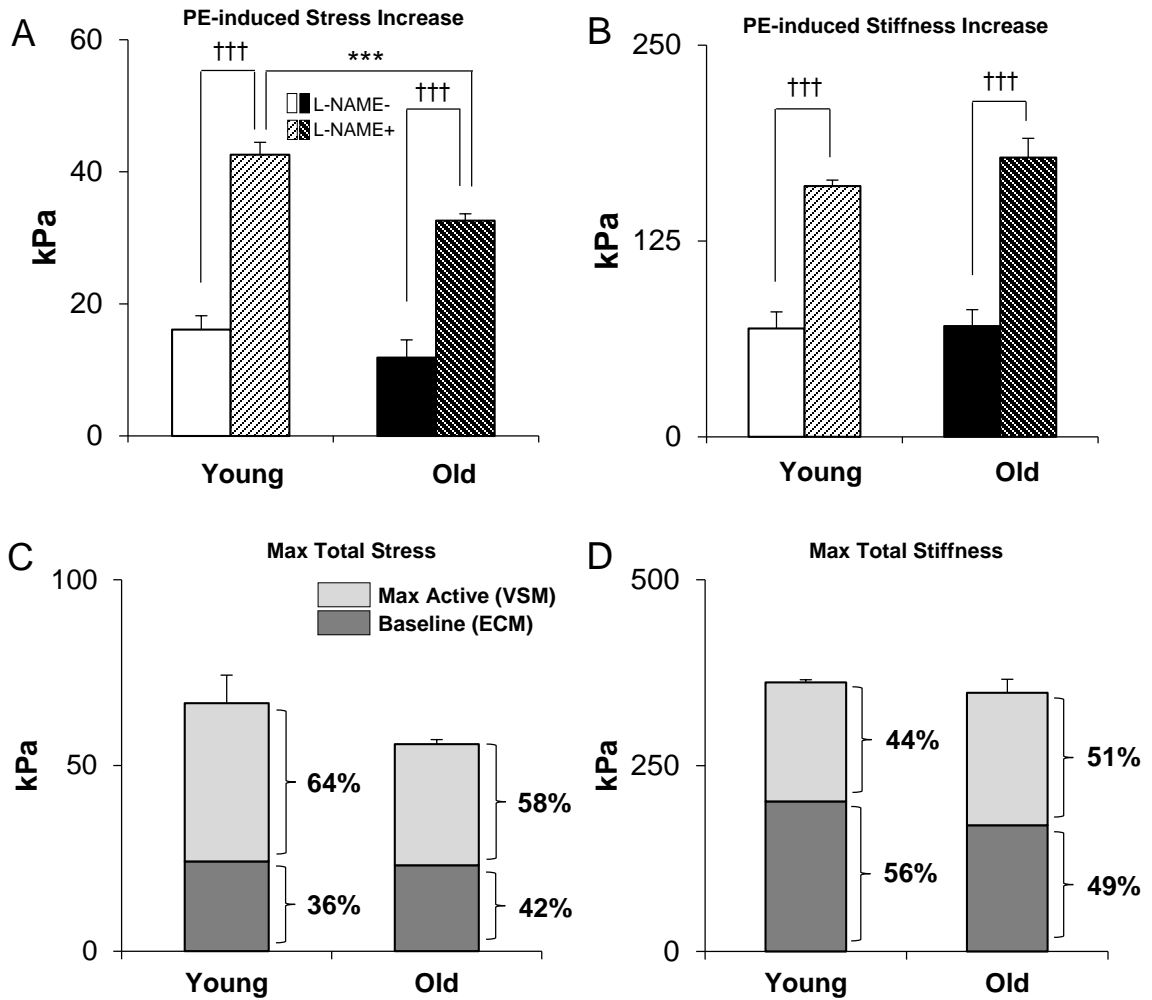


Figure 3.7. VSMCs contribute significantly to aortic stress and stiffness at optimal length via HFLA method. (A, B) Addition of alpha agonist phenylephrine (PE) increases aortic stress and stiffness from baseline values. Further treatment with L-NAME to remove effects of endothelial nitric oxide further augments these increases. $n = 4$ for both young and old; values are mean \pm SEM; † indicates a difference with L-NAME. **(C, D)** Maximally activated vascular smooth muscle accounts for approximately half of maximal total aortic stress and stiffness with aging. Absolute values are mean \pm SEM. ††† indicates $p < 0.001$ with addition of L-NAME.

3.4.8 Tyrosine phosphorylation of focal adhesion proteins is impaired with aging due to decreased Src expression

Increases in aortic stiffness resulting from VSM activity give rise to the question of what molecular mechanisms underlie these contributions. Our group has previously shown that focal adhesions play a key role in regulating aortic stiffness (Saphirstein et al. 2013). The Src kinase inhibitor PP2 suppresses focal adhesion dynamics as measured by tyrosine phosphorylation and endosomal recycling of focal adhesion proteins in aortic smooth muscle (Min et al. 2012, Poythress et al. 2013). This specifically alters cortical stiffness of VSMCs as measured by magnetic-microneedle technology (Saphirstein et al. 2013). In contractile VSMCs, focal adhesion signaling during cell adhesion events is a major source of tyrosine phosphorylation (pTyr) (Romer et al. 2006). The majority of remaining phosphorylation events can be attributed to Ser/Thr phosphorylations (Li et al. 2009).

Phosphotyrosine levels in PE-stimulated young aortas were measured with the assistance of Cynthia Gallant and Qian Qian Lin. Several pTyr bands increased significantly in the presence of the agonist ($p < 0.05$). Past work has identified the tyrosine phosphorylated bands in aorta as containing Cas (130 kDa), FAK (125 kDa), and paxillin (68 kDa) (Min et al. 2012). This increase was readily inhibited in the presence of PP2, an inhibitor of Src kinase (**Figure 3.8A**). In contrast, the agonist produced no significant increase in tyrosine phosphorylation and PP2 produced no statistically significant decrease in phosphorylation in old aortas under the same conditions (**Figure 3.8B**).

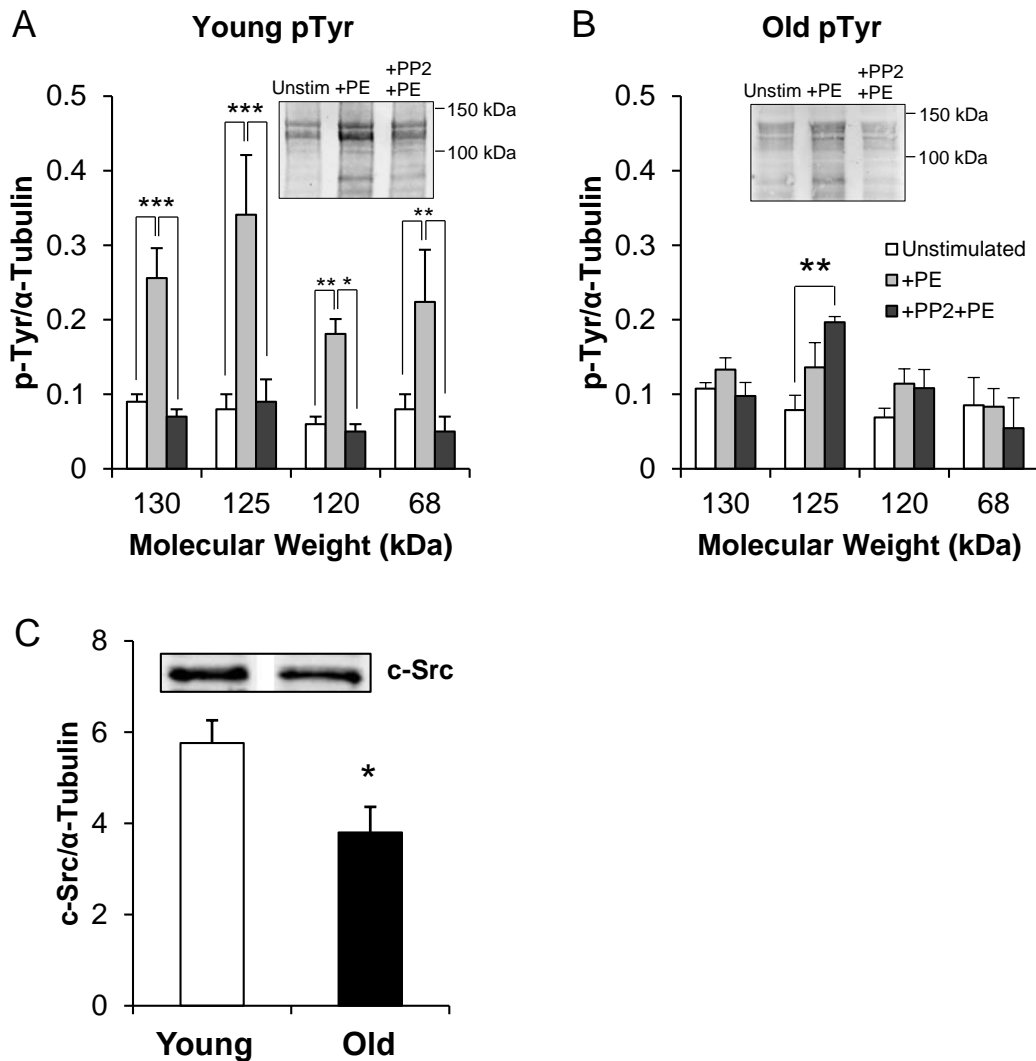


Figure 3.8. Agonist-induced, PP2-sensitive focal adhesion signaling is impaired in old aortas. (A, B) Mean \pm SEM of densitometry for pTyr for young and old mouse aortas with typical blots shown. Typical gel image brightness was adjusted for visual clarity but densitometry was based on raw data. $n = 10$ young unstimulated, 4 young +PE and +PE+PP2, 5 old for each treatment; */**/***, $p < 0.05/0.01/0.001$. **(C)** Densitometry of c-Src immunoblots of young and old aortic homogenates ($n = 3$ each). Typical c-Src blot shown in inset; bands are from the same gel but have been digitally moved adjacent to each other. $n = 3$ young, 3 old; *, $p < 0.05$.

To investigate further the ineffectiveness of Src inhibition in old aortas, I worked with Cynthia Gallant to assay directly expression levels of c-Src by immunoblot analysis. Densitometry of c-Src immunoblots of aortic homogenates, as shown in **Figure 3.8C**, revealed a significant decrease in c-Src levels in aged aortas compared to young aortas, thus at least in part providing an explanation for the impaired regulation of FA signaling in the aortas from old mice. Since tubulin was used in these studies for normalization, the possibility arose that tubulin levels could differ with aging. To test for this, tubulin levels were quantified in young and old mouse aortas, normalized to another “housekeeping” protein, GAPDH, and no significant difference was detectable (young: 0.646 ± 0.149 , old: 0.509 ± 0.122 , $n = 12$ each, $p = 0.48$).

3.4.9 Aging impairs action of a Src small molecule inhibitor on aortic stress and stiffness

Since I have previously shown that focal adhesion signaling regulates stiffness in young aortas, the biochemical results above predict that the aortas from old mice should have impaired stress and stiffness responses to PP2. Thus, I sought to establish the impact of inhibition of Src and focal adhesion signaling on stress and stiffness in the context of aging. After equilibration at baseline, aortas were treated with PP2 (10 μ M), which induced no significant change in stress or stiffness after 30 minutes of exposure in either young or old aortas ($< 2\%$ change, ns). After this pre-treatment, I activated the samples with PE for 15 minutes.

As previously reported (Saphirstein et al. 2013) and confirmed here, PP2 reduced active stress and stiffness in young aortas, but in marked contrast, the Src inhibitor produced no significant change in the maximal active stress of old aortas (-2%, ns) and a slight decrease in maximal active stiffness (-14%, $p < 0.05$). In comparing young and old samples I found that, in the presence of PP2, maximal active stress (**Figure 3.9A**) and stiffness (**Figure 3.9B**) of old aortas are more than twice those of young aortas. Thus, the *ex vivo* removal of the regulatory mechanism of focal adhesion signaling which normally is able to decrease stiffness in young vessels leads to a high stiffness state in old vessels, reminiscent of the increased PWV measurement in vivo in old vessels (Reddy et al. 2003).

3.4.10 Aging-induced impairment of Src-mediated regulation of active stiffness in mouse aorta begins between 14–24 months of age

As a brief footnote to these findings, our group has recently begun to construct an aging curve to track the deterioration of Src-mediated regulation of active stiffness. In collaboration with Diana Zhang, medical student at Boston University School of Medicine, we repeated PP2 inhibition experiments on a set of young C57BL/6J mice using the same protocol, then followed with mice from two age populations previously not investigated: 14 months and 24 months. These correspond to the upper limits of “middle-aged” and “old” ranges depicted in **Figure 2.1** equivalent to 47 and 69 human years respectively (Flurkey et al. 2007). In this work, I will instead refer to these two groups as “early middle-aged” and “late middle-aged” mice to make the distinction from

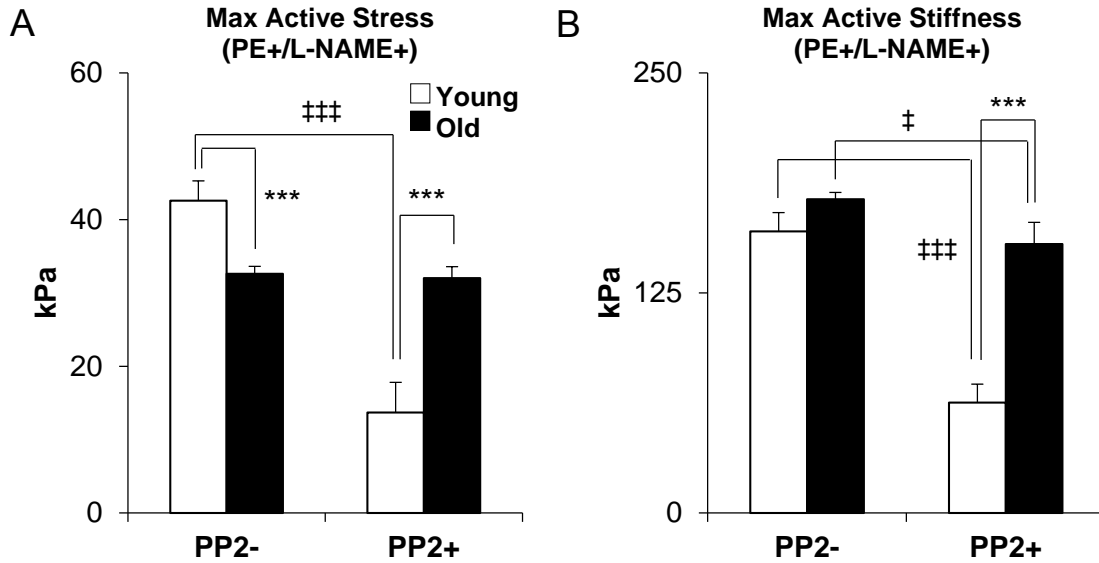


Figure 3.9. Agonist-induced increases in aortic stress and stiffness with Src kinase inhibitor pretreatment are higher with aging. Thoracic aortas pre-treated with 10 μ m PP2 contract and stiffen less in young but not old mice in the presence of maximal activation (PE plus L-NAME). As a result, maximal active stress (**A**) and stiffness (**B**) increase more than twofold with aging under these conditions with HFLA measurements. Also shown for comparison are control maximal active data in the absence of PP2 (PP2-), reproduced from **Figure 3.7A–B**. Absolute values are mean \pm SEM; n = 3 young, 4 old; *** indicates $p < 0.001$ with aging; †/‡/‡‡/‡‡‡ indicates $p < 0.05/0.001$ with addition of PP2.

“old” 29-month mice.

Data as shown in **Figure 3.10** suggest that initial decline in normal VSMC-dependent function of the Src pathway occurs between the early and late middle-aged states. PP2 pretreatment successfully induced knockdown of PE-induced stress and stiffness increases in 3- and 14-month-old mice, but by 24 months of age, Src inhibition was no longer effective. These data provide a framework for further biomechanical and biochemical inquiry.

3.5 Discussion

3.5.1 Additive model of aortic stress and stiffness consists of separable components that highlight major contributions from vascular smooth muscle cells

A major finding of the present study is that the smooth muscle cell is a major source and regulator of vascular stiffness, in contrast with the often assumed dominance of extracellular matrix in effecting changes in wall stiffness with aging (Greenwald 2007). Activated VSM has previously been incorporated into mathematical models of vessel stiffness derived from pressurization studies (Gleason et al. 2008, Rachev and Hayashi 1999). Furthermore, it is known from the literature that in the peripheral vasculature, the level of VSM activation has a dramatic effect on its load-bearing capabilities (Bank et al. 1996).

Here I quantified directly the contributions from VSM activation as percentages of total stiffness in an additive model established from real-time observations of force responses to mechanical uniaxial stretch and subsequent normalization to elastic

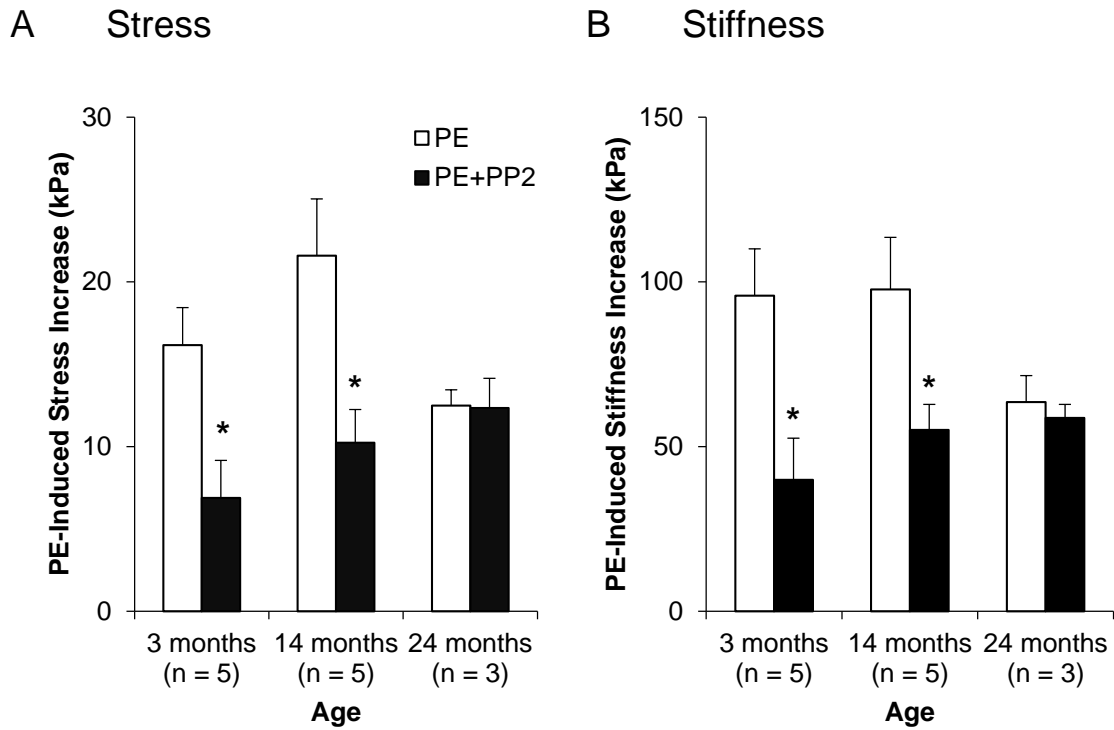


Figure 3.10. Src-mediated regulation of active aortic stress (A) and stiffness (B) is likely defective by 24 months of age in C57BL/6J mice. PP2 effectively inhibits agonist-induced stress and stiffness increases at 3 and 14 but not 24 months of age. n = 5 at 3 months, 4 at 14 months, and 3 at 24 months. *, $p < 0.05$ by Student's t-test.

modulus. The components of the model, defined and separable under our experimental conditions, are presented visually in **Figure 3.11**, incorporating timescales of a typical experimental trace. These findings establish a new perspective in evaluating the relative importance of different biomechanical components in the aortic wall and especially emphasize the large proportion of maximal total stiffness supervised by active VSMCs.

3.5.2 Baseline aortic stiffness establishes important mechanistic links between vascular smooth muscle cells and extracellular matrix proteins

Baseline stiffness is defined here to reflect the biomechanical properties of an *ex vivo* aortic sample without agonist activation of the VSMCs. It is largely characterized by extracellular matrix (ECM), consistent with the lack of change in baseline mechanical properties under either PP2 or L-NAME treatment. Nevertheless, it is important to note the distinction between “baseline” and “passive” in that baseline reflects a non-zero contribution from VSMCs. Our initial hypothesis—that “intrinsic” tone of aorta, defined by Pawlowski et al. as the VSMC component of baseline measurable by reversible cooling, is the sole “temperature-dependent” component of baseline—was disproven by the negative change in stiffness that accompanies the warming of tissue from 2–37° C. The t-d component of baseline characterizes not only VSMCs but also matrix, consistent with known material properties of elastin and collagen. In a previous study of porcine aortic wall, at least 2000 indentations of both media and adventitia revealed a trending decrease in elastic modulus when warming from room temperature (25° C) to body temperature (37° C) (Beenakker et al. 2012). Furthermore, type I collagen has been

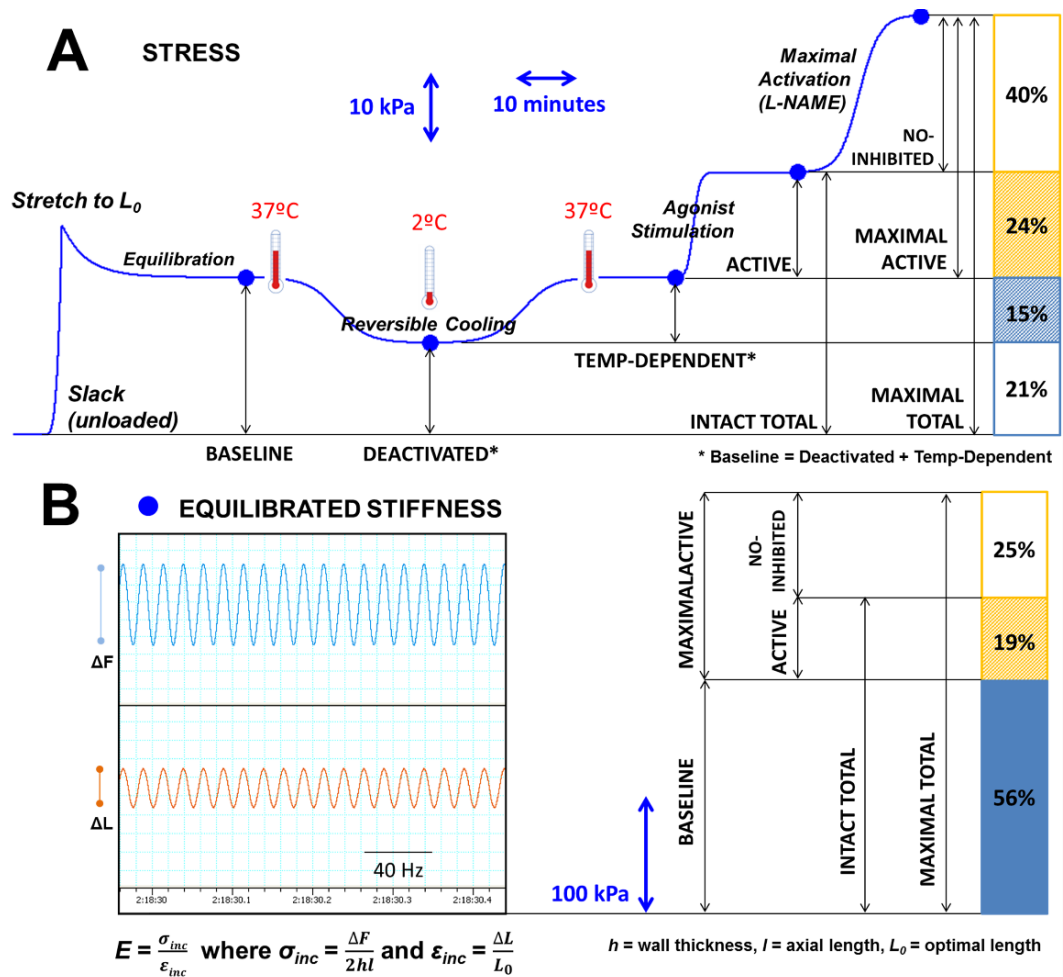


Figure 3.11. Additive model of aortic stress and stiffness consists of separable components. (A) Representative result stress trace for young mouse aorta with scale for time and typical magnitudes of stress showing matrix-dominant **baseline** (blue), separable from **active** and **NO-inhibited** smooth muscle components. **Maximal active**, **intact total**, and **maximal total** stress are obtained by summing combinations of the three basic components. Baseline further comprises **deactivated** and **temperature-dependent** components; the latter is the observable change from the former by warming to body temperature. **(B)** Stiffness measurements were made at marked time points along trace from force responses to high-frequency (40 Hz), low-amplitude oscillations in length. Proportions of analogous stiffness components for young mouse aorta at 37° C shown, with scale for typical magnitudes.

shown to be thermally unstable, likely to enable melting and refolding of helices to provide extra fiber strength and elasticity (Leikina et al. 2002). Therefore, the “deactivated” stress and stiffness of aortic tissue observable in its cooled state reflects passive matrix elements, but not the entirety of those that make up the baseline.

Indeed, the studies conducted on SMKO mice indicate that VSMCs and elastin harbor an especially important codependent link, with elastin regulating VSMC proliferation (Brooke et al. 2003) and SIRT1 playing a critical and potentially necessary role in maintaining structure and preventing dissection (Fry et al. 2015). The chronic and severe disorganization and fragmentation of elastin fibers caused by the SMKO result in “brittleness,” a characterization of the wall observable when equivalent strains on the vessel produce higher stresses, as well as higher baseline stiffness values. This induces a propensity to dissect during blood flow due to the aorta’s inability to accommodate these higher stresses. Recently, others have found that while the medial layer in mouse aorta thickens with aging, resulting in lower cellular density and higher collagen content, the amount of elastin did not change significantly (Wheeler et al. 2015). One interpretation of this finding is that the altered structure of the media weakens formerly stable linkages between VSMCs and elastin due to the interference of collagen.

On the other hand, acute agonist-induced effects are attributed solely to aortic VSMC contributions to stress and stiffness and can be further parsed into those that occur with and without the presence of endothelial nitric oxide production, respectively. Establishing such discrete quantities provides a way to compare the relative importance of different biological constituents of the aortic wall in their contributions to aortic stress

and stiffness. Our results demonstrate that when activated, VSMCs are undeniably significant effectors of both total aortic stress and vascular stiffness and, interestingly, are strongly subjected to persistent regulation by endothelial nitric oxide production.

3.5.3 Impaired regulation of shock absorber function by focal adhesions and non-muscle cytoskeleton is a source of increased aortic stiffness with aging

In old aortas, the inefficacy of PP2 implicates focal adhesions (FAs) as a site of defective cellular signaling with aging. It has previously been shown that Src-dependent aortic focal adhesion signaling and focal adhesion cycling play a critical role in regulating stress and stiffness induced by activation of VSMCs in young mice (Poynthress et al. 2013, Saphirstein et al. 2013). I show here that old mice lose the response to the inhibitory effects of the Src inhibitor PP2 on agonist-induced stress, stiffness, and phosphotyrosine increases.

These results can be framed within the context of total aortic VSMC biomechanics as shown in **Figure 3.12**. The attachment of myosin cross bridges to actin in activated smooth muscle cells is a major component of agonist-induced stress and stiffness increases in VSMCs, while focal adhesions are known to play the important role of linking the contractile filaments, through the non-muscle cytoskeleton (NMC), to the extracellular matrix and the vessel wall via integrins. Alpha agonists as shown here and in past studies of VSM regulate both the contractile filaments and the FAs (Kim et al. 2008, Saphirstein and Morgan 2014). Normal FAs in young aortas provide the capacity to regulate their maturation cycles and their connections to the NMC to accommodate

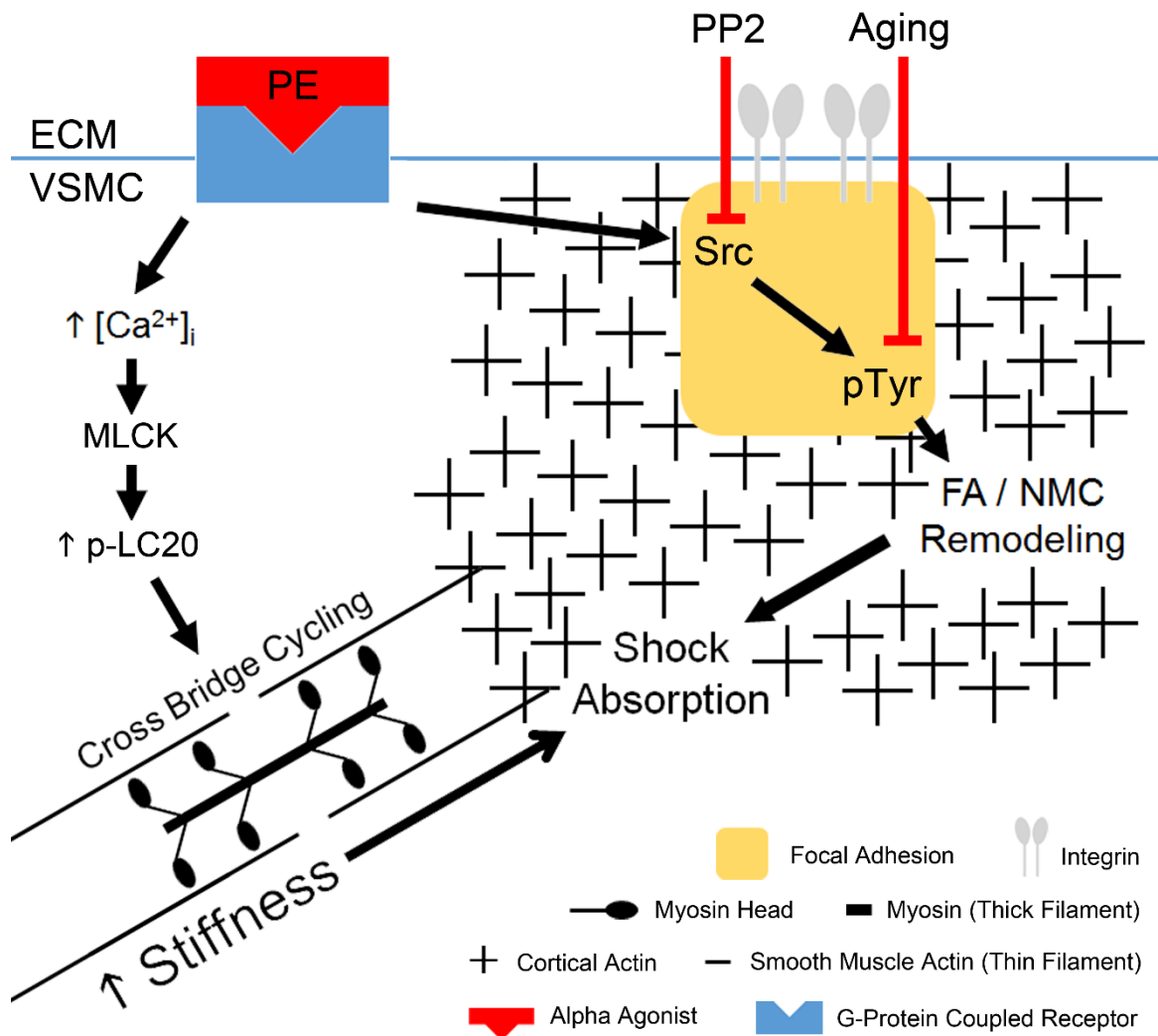


Figure 3.12. Shock absorption via Src-mediated focal adhesion/non-muscle cytoskeleton regulation is defective in old aortas. Model of how changes in stiffness generated by cross bridge attachment and remodeling of focal adhesions and non-muscle cortical cytoskeleton can be regulated by a PP2-sensitive mechanism present in young but not old aortas. Abbreviations: FA: focal adhesion; NMC: non-muscle cytoskeleton; MLCK: myosin light chain kinase.

changes in vessel stress and stiffness and provide, in essence, shock absorption against *in vivo* hemodynamic events. A similar mechanism proposing independent co-activation of cytoskeletal remodeling and cross bridge cycling has been proposed for airway smooth muscle (Gunst and Zhang 2008, Zhang and Gunst 2008). The NMC-FA remodeling regulatory pathway and its consequent potential for shock absorption function is lost in old mice.

Recently, our group has shown that the regulatory role of NMC extends to venous stiffness (Saphirstein et al. 2015). Experiments using ferret portal vein that agonist-induced increases in cortical stiffness in freshly-isolated contractile VSMCs are attenuated by inhibitors of actin polymerization (cytochalasin D; CytoD) but not Src (PP2), although increases in tissue stiffness are inhibited by both. This points to the existence of a cortical actin “switch” that is regulated by an agonist such as PE and promotes transmission of force and stiffness from the contractile machinery inside VSMCs through the FAs to the ECM. Also implied is the existence of at least some regulatory factors of stiffness within the FA-NMC complex that are independent of one component or the other. Unlike with tissue stiffness, FAs do not appear to regulate cortical stiffness directly; PP2 did not reduce PE-induced increases in cortical stiffness, measured with magnetic-microneedle technology (MT), and FA size (approximately 20 μm^2 in area) did not change with PE stimulation (Saphirstein et al. 2015). Furthermore, signaling through the FAK-Src complex was found to affect downstream phosphorylation of caldesmon (CaD) by extracellular-signal-regulated kinase (ERK). CaD is a protein that, when unphosphorylated, binds actin filaments to inhibit actomyosin interactions.

Phosphorylation of CaD by ERK1/2 disinhibits actin, increasing its availability and augmenting cross bridge cycling (Huang and Wang 2006, Lee et al. 2000, Li et al. 2009). We found that PE induces an increase in phospho-ERK levels inhibitable by PP2, reinforcing the importance of Src as a regulator of VSMC signaling pathways that contribute to aortic stiffness (Saphirstein et al. 2015).

As a result, it is necessary to improve the FA-NMC regulatory model to distinguish between FA- and NMC-oriented signaling pathways and connect FA signaling to actomyosin contractility. These conclusions are summarized in **Figure 3.13**, with the caveat that they are valid in ferret portal vein cultured VSMCs and not necessarily non-cultured VSMCs in mouse aorta. In particular, we have yet to ascertain thoroughly the differences between aorta and portal vein with respect to effects of PP2. Given that PP2 inhibits tissue stiffness in aorta and does not inhibit cortical stiffness in portal vein, a clarifying study on whether PP2 does inhibit aortic cortical stiffness using MT is warranted. If it does not, then additional factors that affect focal adhesion dynamics at the tissue level must be considered. Nevertheless, this expanded model putatively elaborates upon the preliminary mechanistic account of aortic shock absorption that I provided in my aging study.

Any aging-impaired protective mechanism fulfilled by vascular smooth muscle cells are more likely to be native in the aorta rather than the peripheral vasculature, given the relative lack of increase in peripheral pulse wave velocity with aging (Mitchell 2008). In aorta, focal adhesions are coupled with the role of the non-muscle cytoskeleton to link smooth muscle cell cross bridge activity to extracellular components of the aortic wall.

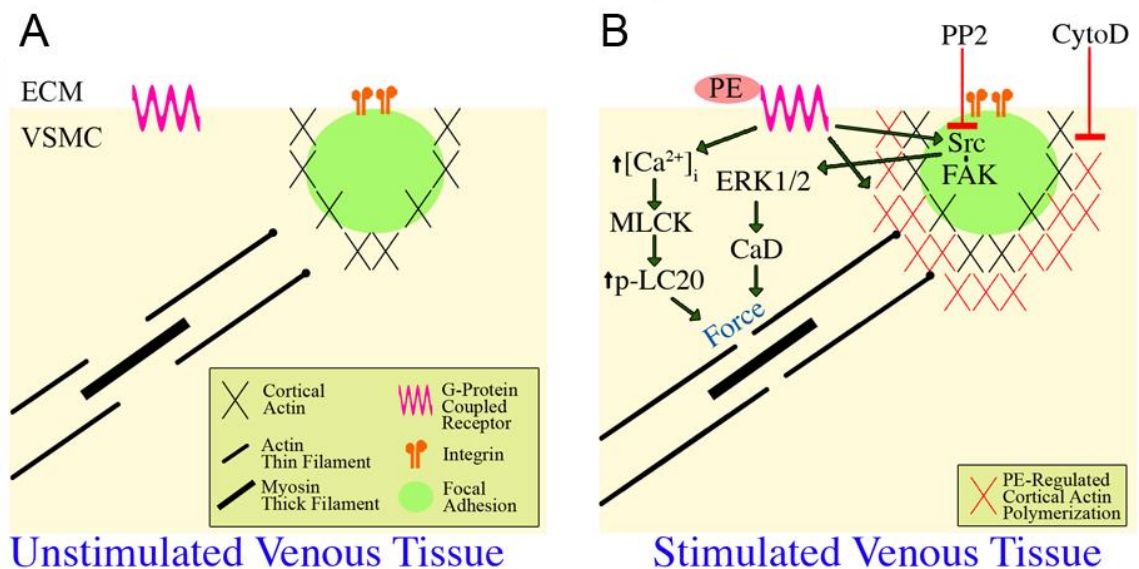


Figure 3.13. Contractile activation of venous smooth muscle alters engagement of the cell-matrix adhesion via cortical actin switch and facilitates ERK activation via Src (Saphirstein et al. 2015). (A) Diagrammatic view of unstimulated cell shows that the non-muscle cortical actin cytoskeleton linked to the focal adhesions is disengaged from a population of the contractile filaments. (B) Agonist (phenylephrine; PE) activation activates two important signaling pathways: first, the promotion of Src, resulting in the facilitation of downstream signaling to extracellular-signal-regulated kinases (ERKs) and caldesmon (CaD) phosphorylation, which lead to contractility and stiffening due to cross bridge attachment; and second, an increase in cortical non-muscle actin polymerization to increase the engagement (the “actin switch”) of the non-muscle cortical cytoskeleton with the contractile filaments. These pathways are inhibited by PP2 and CytoD respectively, which act correspondingly on Src and actin polymerization.

The adhesion-cytoskeleton complex acts as an adaptive shock absorber that readily accommodates increases in material stiffness with smooth muscle activation. Focal adhesion regulation of actomyosin contractility is likely defective with aging, resulting in the reduced capacity for this complex to attenuate aortic stiffening, correlative with other structural and functional changes in the vascular smooth muscle cells, as well as extracellular matrix proteins. Therefore, the focal adhesions and non-muscle cytoskeleton of vascular smooth muscle cells represent potential therapeutic targets in the context of preventing or reversing increases in aortic stiffness. The reasons are four-fold: first, the smooth muscle cell is a major contributor to and regulator of stiffness at physiologic lengths, as shown here; second, agonist activation of smooth muscle promotes changes in non-muscle cytoskeleton in response to increased contractility; third, a Src small molecule inhibitor is sufficient to counteract stiffness increases at the tissue level through focal adhesion remodeling and downstream effects on signaling; and fourth, this capacity is diminished with aging. Greater understanding of these mechanisms may facilitate future biomedical developments to reverse this aging-induced deficiency.

Chapter 4: Cell-Permeable Decoy Peptides Target Focal Adhesion and Cytoskeletal Regulation of Aortic Stiffness

4.1 Summary

Having revealed critical regulatory factors of aortic stiffness in vascular smooth muscle that are impaired with aging, I proceeded to explore synthetic therapeutic options designed to compensate for these defects. In past studies, members of our group have used novel constructs and techniques to probe vascular smooth muscle cell activity, deliverable via attachment to molecules known as cell-permeable decoy peptides, which are able to penetrate the cell membrane. Here, I used two previously developed peptides with the potential to act upon active (smooth muscle mediated) aortic stiffness concordant with the biologically mechanistic model developed from my aging study: one inhibits focal adhesion protein-protein interactions, possibly restoring the normal function of the smooth muscle shock absorber; while the other inhibits actin polymerization, a key process governing the dynamics of the non-muscle cytoskeleton in smooth muscle cells. I evaluated these two peptides by performing *ex vivo* stiffness experiments on young and old aortas to observe their effects on active stiffness. The decoy peptide targeting focal adhesions proved to be effective in both young and old aortas, supporting our biological model and presenting strong, if possibly non-specific, therapeutic potential meriting further investigation, while the peptide targeting actin polymerization showed promise in young aortas but requires additional experiments to resolve its consequence with aging.

4.2 Introduction

Cell-permeable peptides (CPPs), alternatively known as cell-penetrating peptides or transduction peptides (Joliot and Prochiantz 2004), describe a class of peptide molecules that can translocate through cellular membranes and act as delivery vectors into the cytoplasm and nucleus by tethering normally impermeable cargoes, ranging in size from DNA fragments and nanoparticles to larger proteins (Heitz et al. 2009, Joliot and Prochiantz 2004). Two important characteristics broadly define all known CPPs: they are amphipathic and positively charged at physiologic pH, (Zorko and Lagnel 2005). The TAT (transactivator of transcription) peptide of human immunodeficiency virus 1 (HIV-1) is among the most diverse and widely used among all CPP candidates (Gupta et al. 2005, Heitz et al. 2009, Zorko and Lagnel 2005). Our group has shown that TAT is usable as a delivery mechanism for actin monomers into VSMCs to monitor polymerization (Kim et al. 2010). In light of these previous findings, as well as the recognition from my aging study of focal adhesions and non-muscle cytoskeleton as components of a protective mechanism enacted by VSMCs upon the aortic wall, I used two CPPs previously developed by Robert Saphirstein of our group, TLN-VBS and N-WASP-CA, as candidates of interest for inquiry into potential synthetic regulators of increased aortic stiffness resulting from activation of VSMCs.

Previously, Saphirstein designed a TAT-decoy peptide construct, TLN-VBS, which targets and disrupts FA protein-protein interactions by competitively inhibiting a binding site for vinculin on talin. Vinculin is a structural component of focal adhesions that undergoes conformational changes from closed to open when activated and interacts

directly with talin and actin (Ziegler et al. 2006). Talin links transmembrane integrin to actin and, when bound to vinculin, crosslinks with additional actin to reinforce focal adhesions (Mierke 2009). Talin has 11 binding sites for vinculin (Critchley 2009), as shown in **Figure 4.1**, three of which were selected for synthesis of CPPs designed to compete with talin for vinculin and inhibit focal adhesion reinforcement. **Figure 4.2** features a schematic for this mechanism of action. From the three, I selected the one that had demonstrated localized uptake under fluorescent microscopy in cultured cells, as well as a lower ratio of cell attachment on an adhesion assay (Saphirstein 2013). This suggested reduced focal adhesion development under this treatment and motivated its usage in stiffness experiments.

The second peptide candidate designed by Saphirstein targets actin polymerization and branching within the non-muscle cytoskeleton (Saphirstein 2013). The Arp2/3 protein complex, regulated by neuronal Wiskott-Aldrich Syndrome protein (N-WASP), forms branched actin networks and has been shown to regulate contractility in airway smooth muscle (Gunst and Zhang 2008, Zhang et al. 2005). While it has not previously been used in studies of intact vascular smooth muscle, N-WASP-CA—the peptide used in this study, consisting of the domain in full-length N-WASP that binds Arp2/3 (Gunst and Zhang 2008)—has previously been used by our group to demonstrate blockage of agonist-induced actin polymerization in cultured cells (Kim et al. 2008).

Using these CPPs as drug analogs, I conducted *ex vivo* stiffness experiments to assess the effect of TLN-VBS on the active components of stress and stiffness as I previously defined in the additive model detailed in Chapter 3.5.1.

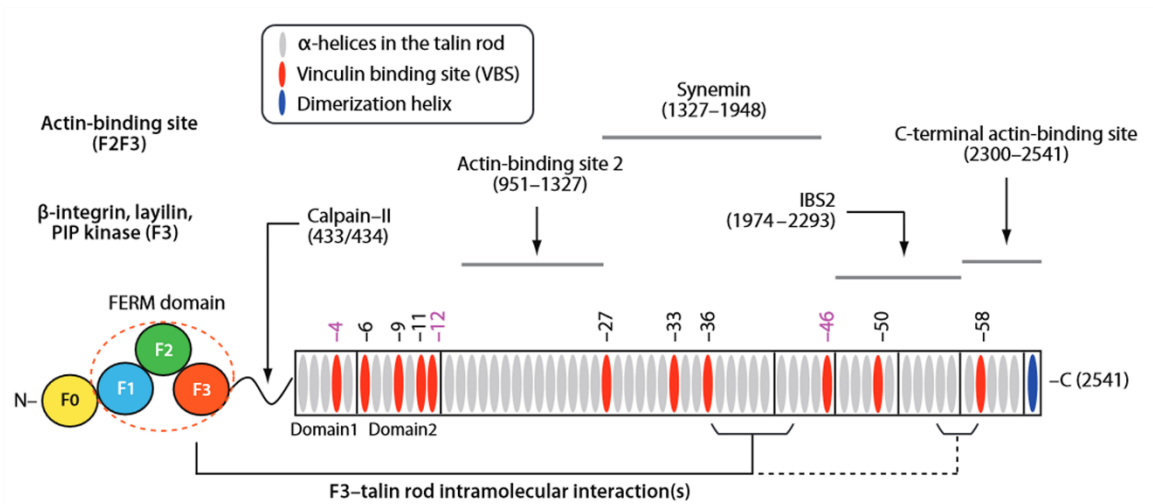


Figure 4.1. Talin domain map. Talin is a well-studied focal adhesion protein and plays a critical role in the regulation of binding to both vinculin and integrin, particularly in the F3-talin rod domains. Its 11 binding sites for focal adhesion structural protein vinculin are indicated in red. Modified from (Critchley 2009).

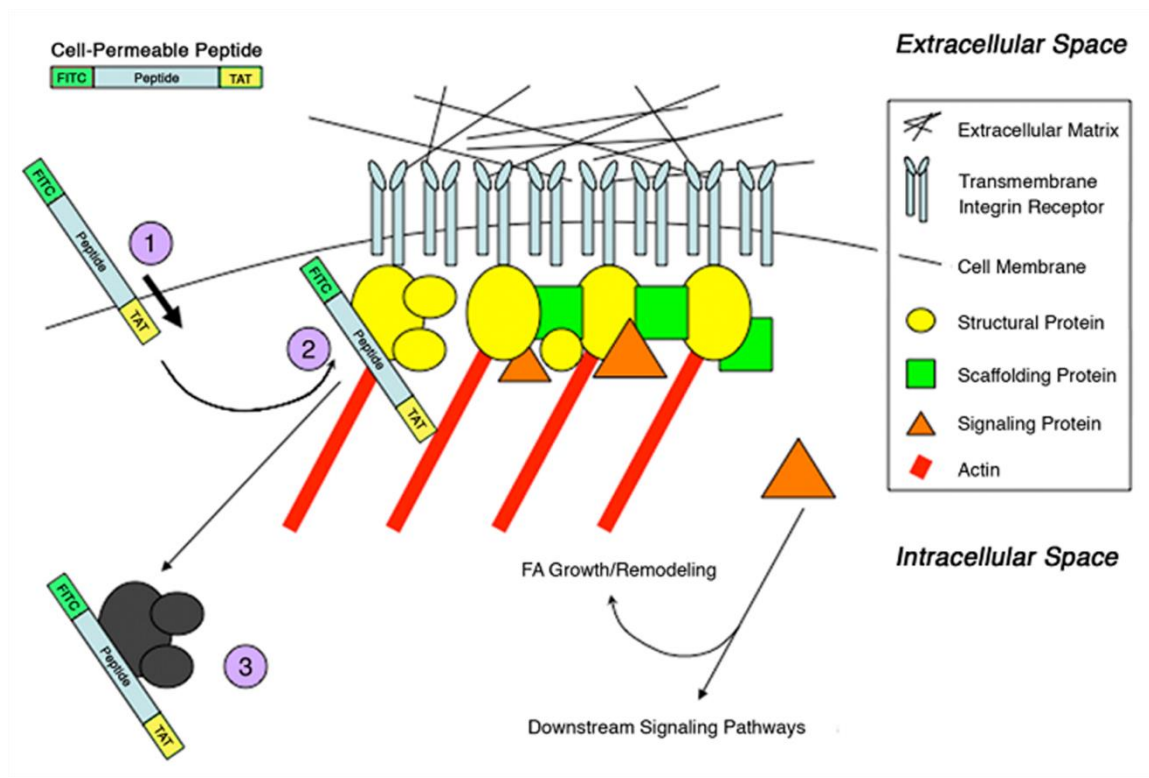


Figure 4.2. Conceptual diagram of cell-permeable decoy peptide mechanism targeting focal adhesion structural proteins (Saphirstein 2013). The TAT (transactivator of transcription) tag guides a fluorescently-labeled peptide across the smooth muscle cell membrane (1) and targets a focal adhesion structural protein within the cell (2) to disrupt its normal protein-protein interaction within the focal adhesion, weakening it to reduce vascular tissue stiffness (3). This mechanism of action can be generalized for the neuronal Wiskott-Aldrich syndrome protein (N-WASP) peptide, which seeks to inhibit actin polymerization.

4.3 Results

4.3.1 Talin-vinculin binding site cell-permeable peptide inhibits active aortic stiffness in young and old mice

From the aging study I conducted previously, I extracted a database of absolute values for baseline stiffness and agonist-induced stiffness increases without any inhibitory treatment in young and old mice. For this reason, I normalized the results from CPP experiments to express active stress and stiffness as percentages of the values obtained without any peptide. This streamlined the evaluation of the scrambled form of the peptide as an effective negative control for the active form. The experimental protocol adhered closely to the established high-frequency low-amplitude (HFLA) procedure, with the additional complexity of a treatment-loading step, designed to minimize drug usage while maintaining to the best of my ability all other conditions characterizing the original protocol. The details of this protocol have been described previously in Chapters 2.6.2 and 2.6.3.

My experiments revealed that the CPP TLN-VBS significantly inhibits increases in aortic steady-state stress and stiffness induced by both KCl depolarization and PE activation at the concentration of 100 μ M in both young (3-month) and old (29-month) male C57BL/6J mice, and that the scrambled form of TLN-VBS does not, thus serving as an effective negative control. There are two novel aspects to these findings, summarized in **Figure 4.3**, with respect to the previously presented aging study: first, that TLN-VBS is effective in reducing KCl-induced as well as PE-induced increases in stress and stiffness; and second, that it is also effective in old aortas. As shown in **Figure 4.3C–D**,

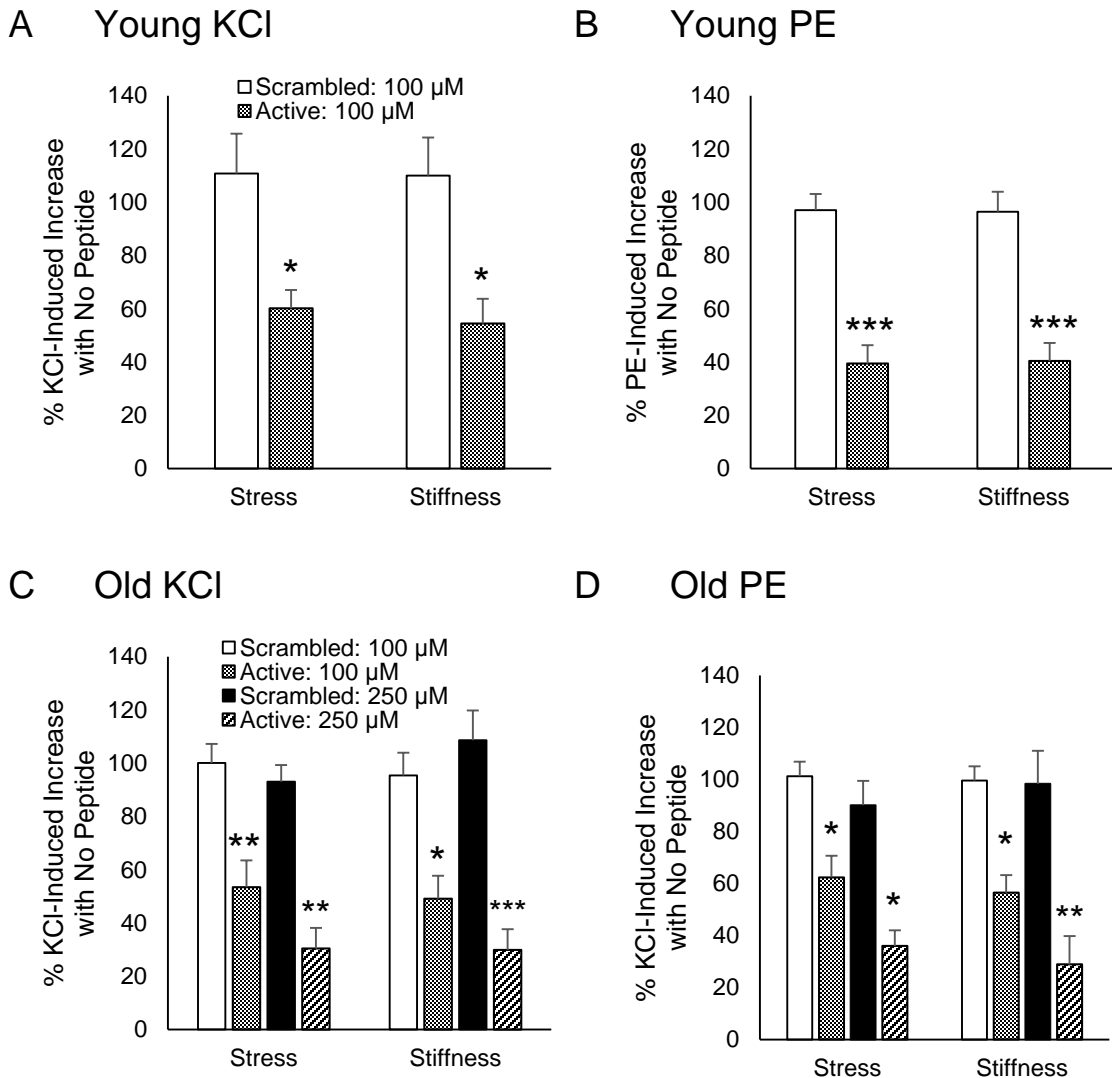


Figure 4.3. Talin-vinculin binding site (TLN-VBS) CPP inhibits active aortic stress and stiffness in young and old mice. Active-form TLN-VBS inhibits increases in aortic stress and stiffness due to smooth muscle activation by KCl as well as PE in young (A, B) and old (C, D) mice. Values are plotted as percentages of active stress and stiffness observed in tissue experiments without loaded peptide, showing that scrambled-form TLN-VBS suffices as a negative control. In old mice, there is no difference in potency between 100 and 250 μ M. $n = 5$ each for 100 μ M, 3 each for 250 μ M; */**/***, $p < 0.05/0.01/0.001$ by unpaired Student's t-test versus scrambled form of the same concentration.

there was evidence that the peptide did not inhibit active increases in old aortas as well as in young aortas (only ~40% inhibition versus ~60%), although there was no significant difference between the two effects. Still, this prompted the question of whether TLN-VBS had reached maximum potency in old mice at 100 μ M. Therefore, I followed with experiments using 250 μ M scrambled- and active-form peptide in old animals and found evidence for a stronger average effect (~65% inhibition of stress and ~70% inhibition of stiffness), although no statistically significant difference from 100- μ M inhibition was observed.

4.3.2 Neuronal Wiskott-Aldrich syndrome protein cell-permeable peptide inhibits active aortic stiffness in young mice

Repeating the procedure with the CPP N-WASP-CA, I amended the methodology slightly, producing a time course for active stress and stiffness, after the initial addition of agonist. The time course provides the ability to identify potentially phasic and tonic contractile phases, which are known to occur in smooth muscle in response to agonist stimulation (Thornbury 1997, Webb 2003), and also observed to a limited extent in other VSM studies performed by our group (Saphirstein et al. 2015).

As shown in **Figure 4.4**, the scrambled form of N-WASP-CA is a suitable negative control, and the active form, which inhibits actin polymerization, is able to inhibit active stress and stiffness induced by PE in young mouse aortas at the concentration of 250 μ M, chosen as presumed to be at or closer to maximal potency, following the results obtained with TLN-VBS. Here, the data were normalized to the

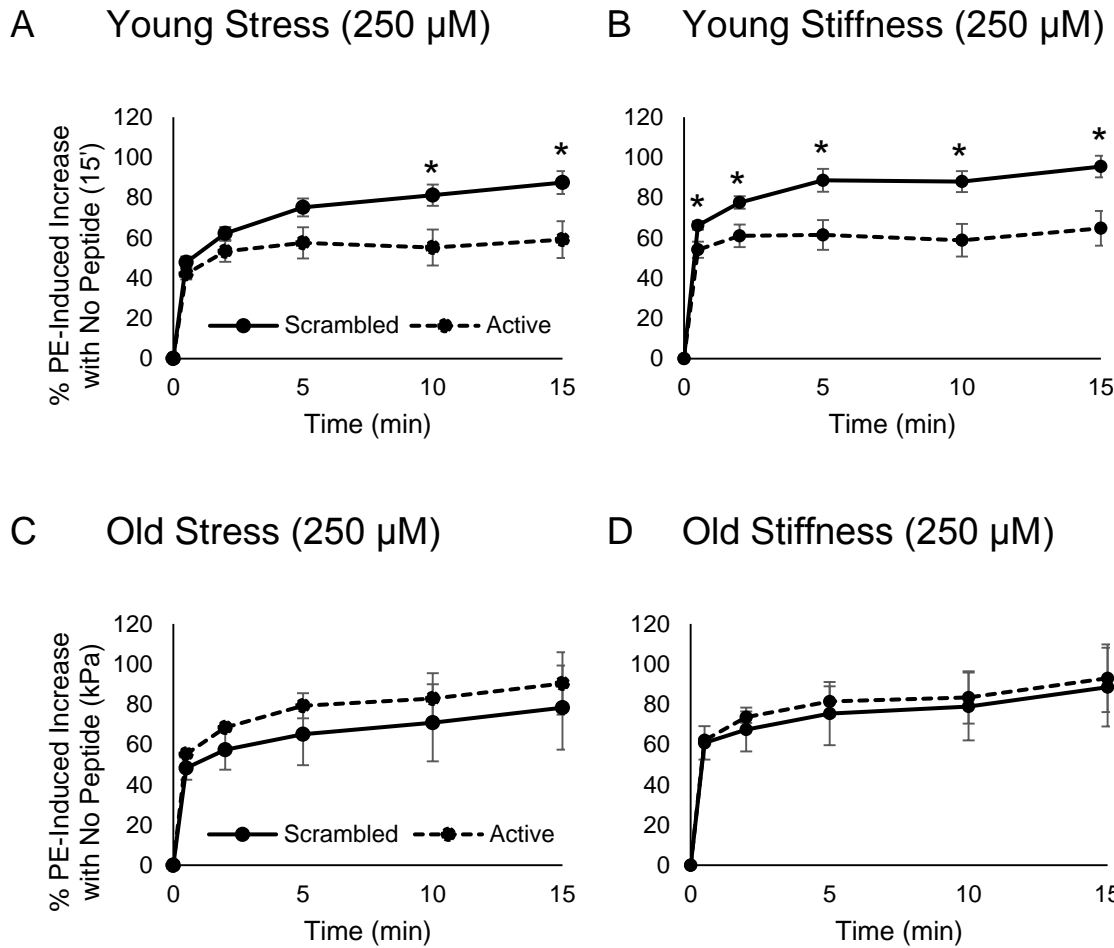


Figure 4.4. Neuronal Wiskott-Aldrich syndrome protein (N-WASP-CA) CPP inhibits active stiffness in young mice. Active-form N-WASP-CA (250 μ M) inhibits increases in aortic stress (A) and stiffness (B) due to smooth muscle activation by PE. Values are plotted along a time course as percentages of 15-minute steady-state active stress and stiffness observed in tissue experiments without any peptide loaded, demonstrating that scrambled-form N-WASP-CA also suffices as a negative control. Time points: 30 seconds, 2 minutes, 5 minutes, 10 minutes, 15 minutes. $n = 4-5$ each; *, $p < 0.05$ by unpaired Student's t-test.

equilibrated value of active stress and stiffness, observed with no peptide, 15 minutes after PE stimulation.

Further study is necessary to determine if this holds true in old aortas; there was no significant effect of this peptide in active form in old mice at the time of this writing, with low sample size and high variability providing inconclusive results. Additionally, a more robust potency study is necessary to ascertain whether the desired effects might be achievable with a lower peptide concentration.

4.4 Discussion

4.4.1 TLN-VBS inhibition of active stiffness in old mice demonstrates therapeutic potential and motivates further investigation of focal adhesion shock absorption

The initial success in using TLN-VBS and N-WASP-CA CPPs to reduce active stress and stiffness is encouraging of further exploration into cellular regulatory mechanisms of stiffness as well as the efficiency and efficacy of these decoy peptides.

My findings from the TLN-VBS loading experiments were especially promising. This peptide has not only emerged as an effective inhibitor of active stiffness in old aortas but also clarified certain aspects of aging-induced dysfunction of focal adhesion regulation. The ability to use TLN-VBS in order to regulate active stress and stiffness implies that focal adhesion dynamics, resulting from vinculin binding to talin linkages between actin and integrins, are “stuck” in a state disallowing normal aortic shock absorption in response to contractile stimuli. It remains to be seen if this is mechanistically linked to the defective Src pathway associated with aging, or if it is

indicative of altogether different of cellular processes. In other words, the question arises as to whether the targeting of TLN-VBS bypass defective signaling of Src, as well as phosphotyrosine levels further downstream. Regardless, this novel approach to regulate tissue stiffness may indeed form the basis for a therapeutic drug that compensates for the loss of normal smooth muscle mediation of increases in aortic stiffness.

To reinforce the biological rationale for usage of TLN-VBS, our group plans to confirm the hypothesis of its action. Using magnetic-microneedle technology (MT), we will probe the cortical cytoskeleton of differentiated vascular smooth muscle cells (dVSMCs) to assess whether TLN-VBS affects cortical stiffness. To test the molecular mechanism, we will use proximity ligation assays (PLA) at a resolution of 200 nm to determine if the distance between talin and vinculin within dVSMCs has increased, as well as immunoprecipitation (IP) to determine if talin-vinculin binding decreases, in the presence of the TLN-VBS CPP. Our group has previously published usage of the MT, PLA, and IP techniques in dVSMCs (Poythress et al. 2013, Saphirstein et al. 2013, Vetterkind et al. 2013) and we expect positive results from these assays.

In the previous aging study, I did not examine the effect of PP2 on effects of KCl depolarization of VSM, which was performed on strictly to confirm viability before pre-treatment with PP2 in order to assess its effect on PE-induced increases in stress and stiffness. Conversely, it was necessary to perform the peptide-loading protocol before any viability contraction with KCl (Chapter 2.7.3). As a result, I obtained KCl-induced contractility and stiffening data in the presence of active-form CPPs and found that TLN-VBS also effectively inhibits this type of active stiffness. This strongly implicates a role

for focal adhesions in mediating stiffness increases consequent upon cross bridge cycling and also that the model we established in our study of ferret portal vein (Chapter 3.5.3), which establishes the ERK1/2 pathway downstream from Src as the conduit for this regulation, is valid in mouse aorta. Therefore, another avenue of inquiry is to confirm this hypothesis in future subcellular studies.

4.4.2 Future studies are required for confirmation of N-WASP-CA efficacy and further pharmacological considerations

On the other hand, N-WASP-CA has not yet been confirmed to regulate aortic stiffness in old mice. Unlike with TLN-VBS, there were additional methodological factors in the usage of N-WASP-CA that rendered the peptide loading technique prone to significant human error. Specifically, I had to confront significant difficulties in preserving physiologic pH during the peptide loading procedure, which may have led to decreased drug potency or inconsistent smooth muscle viability across experiments with both active and scrambled forms of peptide. There are three distinct contexts in which this challenge presents itself: the dissolution of the peptide during preparation of the loading solution; the actual loading technique, in which the tissue is transferred into the temporarily deoxygenated loading solution; and, after loading, the maintenance of oxygenation for the experimental apparatus itself. Measuring the pH of the small loading volume in real time is difficult and is currently only practical before and after loading, which does not account for changes that may take place during the procedure. Therefore, the design of a more accessible apparatus may be necessary in order to enable persistent

supervision of pH within the loading volume.

Upon establishment of cellular targets and effective peptides, a more thorough pharmacological analysis should be conducted to address important considerations in developing a clinical product. For example, although I found that 100 μM was not the maximal dosage for TLN-VBS, it may also not be the minimal concentration at which it is effective in regulating aortic stiffness in old aortas. To elucidate the potency of TLN-VBS, a dose response curve for should be constructed after additional data collection. Furthermore, I also cannot assume that either peptide used in these studies is effective at early-middle or late-middle age. Complementary to the preliminary results of middle-aged mice presented in Chapter 3.4.10, future studies should also incorporate aortas from mice at 14 and 24 months of age. Finally, consideration of drug specificity, with respect to both the actual target as well as mechanism of action, should warrant the investigation of alternative supply methods into the smooth muscle cells, either through synthesis of other peptide configurations, or different delivery methods altogether.

In summary, many additional *ex vivo* trials may be needed, but a thorough experimental regimen will enable a more complete portrayal of aging-induced changes of cellular mechanisms, as well as how decoy peptides might counter any corresponding defects in the capacity of smooth muscle to regulate aortic stiffness.

Chapter 5: Assessment of Applied Biomechanical Methods in Evaluation of *Ex Vivo* Aortic Stiffness

5.1 Summary

Before concluding this dissertation with recommendations for prospective research endeavors, it is necessary to turn a more critical eye to the biomechanical methods employed in these studies of *ex vivo* aortic stiffness. Here, I review existing quantitative models for arterial stiffness and identify the ones most consistent with the new findings I presented in the previous two chapters. Subsequently, I provide a thorough analysis of the ability to evaluate aortic stiffness precisely with my experimental apparatus and techniques, as well as how one might address inherent methodological limitations. Finally, I discuss possible reconciliation of discrepancies between clinical interpretations of functional stiffness and *ex vivo* material stiffness as I have studied in this dissertation. In conducting this analysis, I hope to establish guidelines and context for future studies of vascular smooth muscle contributions to aortic biomechanical properties.

5.2 Quantitative Modeling of Vascular Smooth Muscle Contributions to Total Aortic Stiffness

5.2.1 Concurrence with Presented Discoveries

A relatively small proportion of the literature detailing mechanical properties of vascular tissue accounts for any activation of smooth muscle cells (Holzapfel and Ogden 2010), but even extensive quantitative models focusing primarily on extracellular matrix

acknowledge that mechanotransductive responses of VSMCs to blood flow and pressure, as well as external phenomena affecting vessel growth, are integral to understanding fully the complex dynamics of aortic biomechanical properties. In fact, damage to the VSMCs inflicted by cardiovascular disease may be the primary trigger for deterioration of normal structure and function in maintenance of the aortic wall (Wagenseil and Mecham 2009).

It is beyond the scope of this dissertation to develop a rigorous and comprehensive model encapsulating all components of the aortic wall, as my studies have focused primarily on emphasizing significant contributions to total aortic stiffness from VSM under physiologic conditions, rather than establishing a broad spectrum of the interplay between VSMCs and other wall components. Indeed, previous studies concede that aortic stiffness, in the form of incremental elastic modulus, has no singular representative value due to the nonlinearity of stress-strain or pressure-strain responses; this nonlinearity is reflected in geometric, compositional, and environmental conditions that render opaque the exact dimensional and structural state of the aorta at any given moment (Barra et al. 1993, McVeigh et al. 2007) Instead, I sought out two models developed from previous research with an explicit focus on VSMCs that are most likely compatible with my *ex vivo* measurements of aortic stiffness in young and old mice.

5.2.2 Vascular Smooth Muscle Cells as Protective Dampers in a Modified Maxwell Model of Total Aortic Stiffness

One study led by Barra and Armentano proposed a modified Maxwell model of the incremental elastic modulus of descending thoracic aorta in dogs, consisting of

passive springs comprising elastin and collagen (multiple springs progressively recruited as strain increases), both in parallel with an active VSMC component, featuring an underdamped spring as an elastic element and viscous force-generating contractile element in series (Barra et al. 1993). This model was initially developed by Dobrin and Canfield in dog carotid artery (Dobrin and Canfield 1977). Barra, Armentano, and their collaborators found via an isobaric pressure-diameter study that the majority component of total aortic stiffness shifts from elastic to smooth muscle cells as pressure increases (Barra et al. 1993). During their *in vivo* study, they observed decreases in total stiffness with PE stimulation under isobaric conditions and recommended isometric analysis—such as that applied to the stiffness measurements I made at sustained physiologic strain—as a more accurate reflection of agonist-induced stress and stiffness increases. Interestingly, they also concluded that their model fit the data well and that at very high levels of constant pressure, agonist-induced decreases in stiffness reflected a compensatory mechanism endowed by the VSM. Therefore, this simple modified Maxwell model stands out as one worthy of emulation when integrating physiologic stiffness measurements featuring activated VSM.

5.2.3 Vascular Smooth Muscle Recruitment of Collagen

In a series of publications by Alan J. Bank, based upon studies of brachial arteries in humans, a similar model of aortic stiffness is established. This variant of the modified Maxwell model couples the VSM to collagen in load-bearing duties. Arterial compliance was evaluated *in vivo* by relating pressure to arterial cross-sectional area as measured by

ultrasound catheter under conditions of baseline, as well as vasodilation and vasoconstriction through administration of norepinephrine and nitroglycerin respectively, then converted to incremental elastic modulus (Bank et al. 1999, Bank et al. 1995).

Bank and his collaborators concluded by fitting their data that the underdamped spring featured in the Barra-Armentano model is actually a collagen element in series with the contractile element of VSMCs, and that, similar to the parallel collagen element, is progressively recruited as arterial strain increases (Bank et al. 1996, McVeigh et al. 2007). Contrary to the findings in the Barra-Armentano study, Bank et al. found that elastin accounted for the same percentage of total stiffness regardless of pressure, while the majority of total stiffness is borne by parallel collagen at low pressures and almost overwhelmingly by VSM and series collagen at high pressures. Most strikingly, they measured a 15-fold increase in stiffness due to VSMC activity under isometric conditions, and that only 6% of total collagen fibers were recruited to bear wall stress at an average pressure of 100 mm Hg (Bank et al. 1996). Their designation of strong activation-induced increases in stiffness as due to recruitment of collagen may be consistent with my findings on focal adhesion regulation and encourages exploration of this model in the aorta.

5.2.4 Model Applicability to Aortic Stiffness

Bank's modified Maxwell model of wall stress (Bank et al. 1996), consisting of a contractile element in series with collagen, warrants an evaluation of compatibility with my own findings, depicted in **Figure 5.1** and quantified as:

$$\sigma_T = \sigma_e + \sigma_{c(p)} + \sigma_{SM-c(s)}$$

Equation 5.1

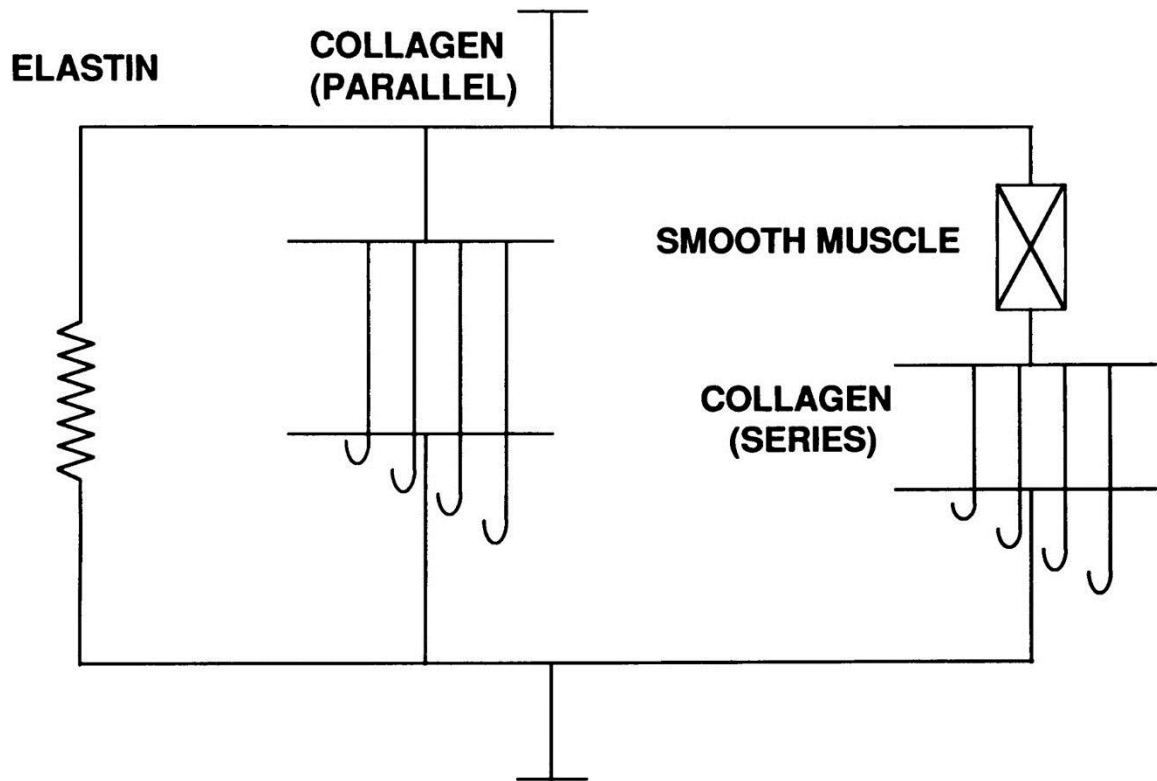


Figure 5.1. Modified Maxwell model for total wall stress in the brachial artery (Bank et al. 1996). The passive parallel elastic component consists of extracellular matrix proteins: elastin and collagen. The active component consists of smooth muscle in series with additional collagen. Collagen behaves analogously to stiff springs that are progressively recruited as the vessel undergoes large strains (parallel) or as the smooth muscle contracts (series). The elastic behavior of the collagen fibers is proportional to the fraction of fibers recruited.

where the individual terms of the total T assigned to elastin e , parallel collagen $c(p)$, and smooth muscle/collagen series $SM-c(s)$ are quantifiable by isolating them under certain conditions. For example, the elastin component could be isolated from stiffness measurements at very low levels of strain, where elastin is known to dominate, and the inverse of this directive would apply in the case of collagen. While it is possible to interpret some of these values from my quasi-static stress-strain experiments, there is no way to compare these data to my database of VSM contributions to aortic stiffness derived from HFLA measurements.

Therefore, more HFLA experiments would be necessary to maintain consistency and comparability in this regard. Additional parametric adjustments will likely be necessary to reconcile the expected discrepancies during the adaptation of this model, which should run parallel to implementation of improvements to the *ex vivo* stiffness protocol.

5.3 Methodological Advantages in Reductionism and Physiological Relevance of High-Frequency Low-Amplitude Stiffness Measurements

The traditional engineering approach of large-scale stress-strain analysis, prevalent in mechanical analysis of materials, typically uses a high-amplitude ramp input that produces a stress-strain curve through loading and unloading a tissue sample with large stretches from the unloaded state, otherwise known as slack length or 0% strain. Stiffness in this protocol is defined as the incremental slope (stress-strain ratio) at a particular strain level. In my aging study, I used stress-strain curves to contextualize my

observations of aortic stiffness with aging at specific strain levels (Chapter 3.4.5). At high strain levels, old aortas have higher passive material stiffness consistent with greater collagen content and recruitment (Wagenseil and Mecham 2012). On the other hand, I confirmed the lack of a stiffness increase in old aortas at physiologic strain levels, which I ascertained with the HFLA protocol.

While stress-strain curves define a large pool of stiffness data across a wide range of strain values, the high-amplitude protocol used to collect these data has several disadvantages. The large stretches disrupt actomyosin cross bridges, decreasing contractile responses in the VSM and removing a major source of cellular stiffness. In addition, VSMC force output depends critically on the level of stretch it experiences (Peiper et al. 1974). Therefore, large-amplitude stretches disturb the system whose properties I am trying to measure. Furthermore, the stress-strain curve protocol stipulates the slack or unloaded state as the equilibration point before and after stretch; this prohibits the acquisition of steady-state stress data at any physiologically relevant aortic strain or during the response to a contractile agonist, factors more relevant to the *in vivo* environment of the aorta.

In contrast, the HFLA protocol uses low-amplitude stretches and ample equilibration time after perturbations and treatments, in correspondence with traditional isometric studies of SMC contractility, cause minimal perturbation of the system (Brozovich and Morgan 1989, Kawai and Brandt 1980). Additionally, I am interested specifically in the mechanical properties of the aorta under physiologic conditions. HFLA allowed us in the present study to determine both steady-state stress and local stiffness

via incremental stress-strain measurements at optimal length that upholds SMC activity.

Although intended to minimize perturbation of smooth muscle dynamics, HFLA stretch at 40 Hz with small positive offset does have noticeable effects as interpretable from the force response. Typically, there is a slight drop in the average force reading. This was seen before and after stimulation with PE but was much more pronounced post-activation. Especially notable is the contractile response, which corrects itself upon cessation of the oscillatory stimulus. **Figure 5.2** offers a sample depiction of these observations. It is possible that this initial drop reflects a pre-conditioning process of the tissue to uniaxial cyclic stretch described in previous studies as “stress softening” (Holzapfel et al. 2000). Stress softening may be compatible with the Barra-Armentano view that vascular smooth muscle cells are mechanically equivalent to “smart viscoelastic spring-dampers,” offering protective effects through remodeling in response to pulsatile pressures of blood flow, adjusting energy dissipation due to high-frequency vibrations that would otherwise induce wall damage (Armentano et al. 2007). This is essentially complementary to my proposed model of aortic shock absorption discussed in Chapter 3.5.3.

To assess whether the HFLA protocol successfully minimizes viscous damping in force response to stretch, I conducted simple phase lag analysis of individual force-length response traces as summarized in **Figure 5.3**. Chart software can resolve length, force, and time to the nearest 0.5 μm , 0.5 mg and 0.001 seconds respectively, and at these scale factors, there was no significant phase difference in peak-to-peak intervals between length input (dL) and force output (dF), even after smooth muscle activation by PE

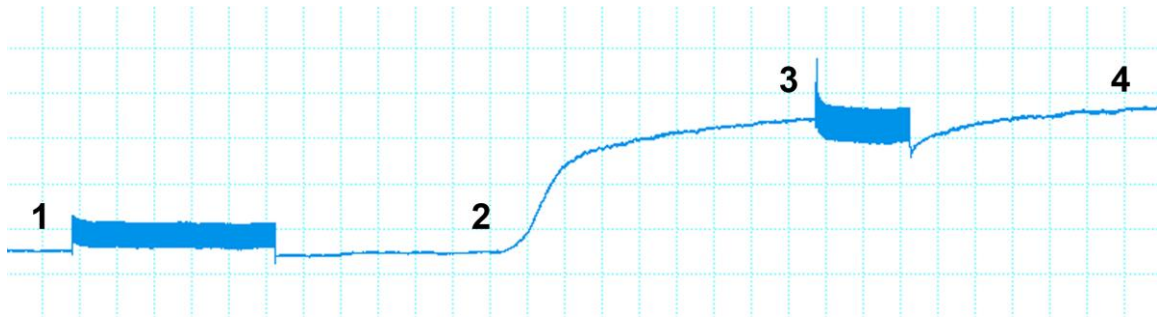


Figure 5.2. HFLA stretch *ex vivo* induces stress softening and indicates possible protective effect from vascular smooth muscle. Typical force trace of response to HFLA stretch before and after agonist-induced contractility in young mouse aorta is shown. (1) At 40 Hz, sinusoidal oscillatory input with small positive offset produces slight damping in average force response near the beginning of stimulus duration. (2) Smooth muscle cells are activated with alpha agonist phenylephrine. (3) Stress softening is greater upon post-activation HFLA stretch. (4) Contractility is restored post-stretch.

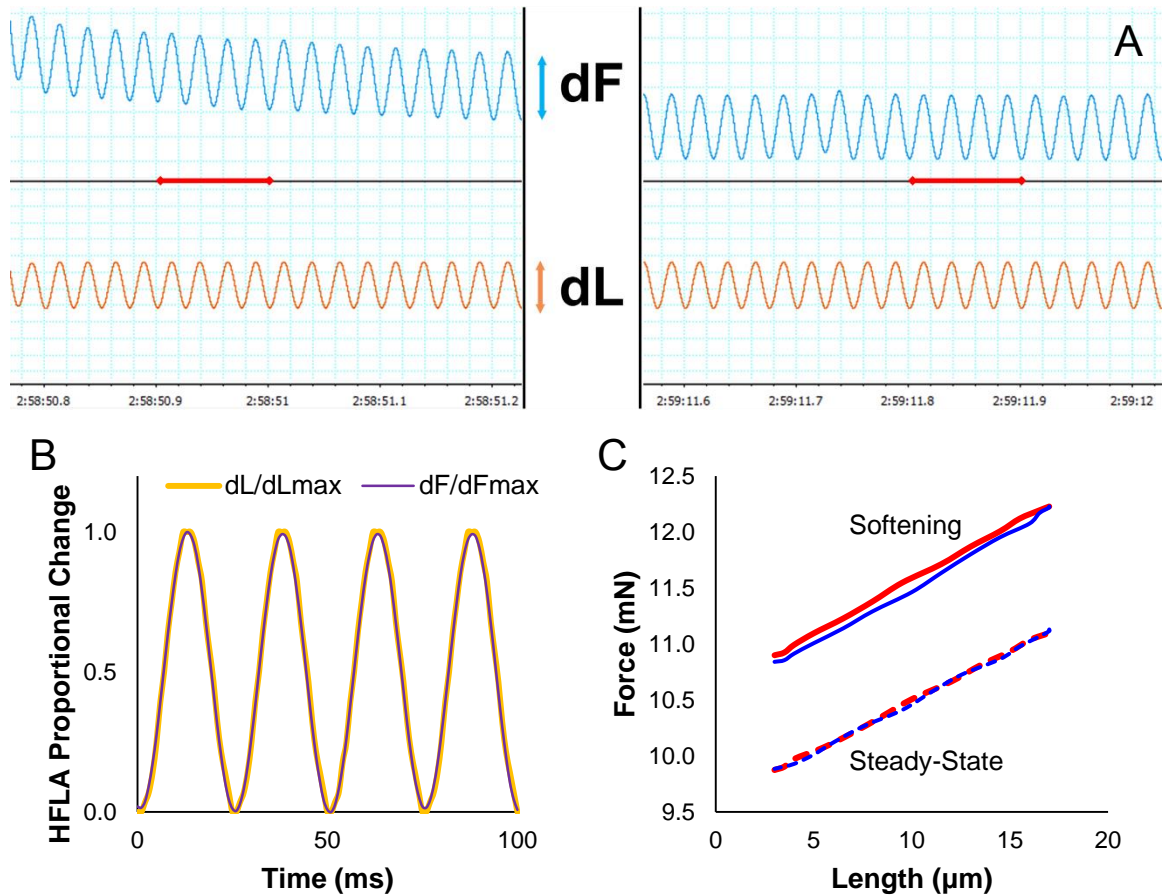


Figure 5.3. HFLA stiffness measurements minimize viscoelastic response from aortic tissue. (A) Over the course of ~ 20 seconds, four oscillatory periods consistently occur within the same one-tenth of a second (red) for both length input (dL) and force output (dF), irrespective of stress softening (left) that results in an overall decrease in the average force measurement to steady-state (right). (B) Superimposition of length and force changes during four cycles of typical HFLA stretch normalized to their oscillatory peaks. The phase lag for these traces was 1.47 degrees. (C) Typical hysteresis for one oscillatory cycle during softening (solid-line)) and steady-state (dashed) phases. Energy dissipation (bounded area) between loading (red) and unloading (blue) curves: 2.99 nJ softening, 1.92 nJ steady-state.

resulted in a drop in the force reading, as visualized in **Figure 5.3A**. Normalizing time courses for dL and dF to their maximal values, as shown in **Figure 5.3B**, rendered them comparable to complex vectors, enabling usage of the dot product to calculate a very small phase angle between them. Finally, energy dissipation was calculable by directly plotting the loading and unloading curves in the force-length plane, as is seen in **Figure 5.3C**, and determining the area inside the enclosure. In short, hysteresis was observable during stress softening, but was comparatively negligible at steady-state.

The lack of a significant viscoelastic effect in the current protocol may signify closer emulation of *in vivo* conditions, consistent with previous studies that have found a three-fold decrease in viscosity for *in vivo* aorta relative to *ex vivo* samples, and that smooth muscle tone is likely not responsible for viscous effects observed *ex vivo* (Boutouyrie et al. 1998). A stronger interpretation may be that the fleeting damping effect observable during stress softening is due to recruitment of collagen by the VSMCs.

These analytical results solidify the rationale for a transient HFLA stimulus. Superficially, it might seem far more appropriate to prescribe a level of stretch that is closer to that which is experienced during physiological blood flow, or what would essentially be a “physiologic stress-strain” protocol. One may easily intuit that a superimposed oscillatory input imposed upon optimal length should reflect the systolic pulse wave, and that the frequency and amplitude of the stimulus should correspond to typical heart rate and aortic distension experienced during systole, determined to be 8–10 Hz and ~10% strain from previous *in vivo* C57BL/6J mouse studies (Doevendans et al. 1998, Trachet et al. 2015). On the other hand, it may be presumptive to prioritize

parametric conditions over biological ones. I have already established critical differences between *in vivo* and *ex vivo* observations related to aortic stiffness in the context of smooth muscle viability. While I do not dismiss the basis behind a proposed physiologic stress-strain protocol, I believe that it may be more immediately valuable to seek minor corrective options while maintaining current parameters, rather than major changes to the overall methodological philosophy and a subsequent overhaul in experimental design.

5.4 Motivating Factors for Future Improvements in Measurements of *Ex Vivo* Aortic Geometry

Although the current method for *ex vivo* aortic stiffness measurements can satisfactorily maintain viable VSMCs, a number of minor but important changes could be made to the experimental apparatus to account for various geometric factors that would enhance the accuracy of subsequently collected data.

5.4.1 Initial Length

The measurement most prone to human error during the *ex vivo* aortic stiffness protocol is the resolution of the initial, or slack, length of a tissue sample. After mounting the tissue, initial length defined as the point beyond which any circumferential applied results in a positive change in the electronic force reading of the apparatus, which may not always be immediately detectable, given the inherent variability in readings due to the highly sensitive force transducer. Calibration of the equipment using this method is consistent, but also largely a heuristic process, refined with practice over hundreds of

independent experiments and supplemented with visual inspection of the mounted tissue. In theory, small adjustments of the lever arm, with the tissue initialized to an unloaded state, in order to determine slack length as close to the true value as possible, should have a minimal effect on the viability of the tissue. Also, despite the susceptibility to human error, this discrepancy is likely to be quite small in magnitude. Still, it may be desirable to develop a method enabling the determination of initial length more definitively.

5.4.2 Axial Strain and Axial Shortening

The experimental setup I used to produce *ex vivo* stiffness measurements imposed only uniaxial stretch in the circumferential direction in aortic samples. While this approach is fundamentally substantiated by the known circumferential orientation of the lamellar networks within the aortic wall (Holzapfel et al. 2000), it does not account for non-negligible axial stress and strain experienced by blood vessels *in vivo* due to normal biological organization and associated hemodynamics (Humphrey et al. 2009). There is no axial strain on the tissue sample in the current protocol, though it has been shown that physiologic axial strain is 10–20% in the proximal thoracic aorta (Doevendans et al. 1998). One indirect consequence was that during stress-strain experiments as detailed in Chapter 3.4.5, visible shortening in the axial direction was observed beyond 250% strain. Aside from the increased tendency for tissue to rupture above this level of stretch, this was the major factor limiting the range of analysis to a maximum of 250% strain.

Applying axial strain to the tissue in the current setup, possibly by fixing the ends of the tissue sample once it is mounted onto the triangular clasps, may prove

counterproductive to VSMC viability, extend experimental duration significantly, and increase the complexity of data interpretation. To maintain the current paradigm of reductionism, I propose that the issue of axial strain be revisited at a later iteration of this protocol, or evolve into a separate study. Alternatively, axial shortening could be measurable via high-resolution image analysis, even with the usage of a simple camera installation separate from the apparatus, though one would have to accommodate any refraction within the solution-filled organ bath. The most relevant consideration in this regard is whether or not any potential correction would differ with aging, as this has not been studied to my knowledge.

5.4.3 Wall Thickness

The thickness of the aortic wall will change upon stretching a tissue sample. Presently, there is no way to monitor thickness in real time after mounting the aorta on the apparatus. Instead, thickness is only ascertainable from separately imaging small rings cut from the ends of the segment to be stretched. Naturally, these small rings are not under physiologic strain and subsequent evaluation of thickness is not equivalent to that of the experimental sample under stretch. Again, this discrepancy could differ with aging, adding another variable to the final measurement that is not worrisome on its own, but contributes to cumulative geometric inaccuracy. Unfortunately, it is impossible to measure thickness of the stretched tissue without completely altering the current apparatus. The most appropriate remedy would be to address axial shortening, then apply a correction factor under the assumption that conservation of volume applies to the tissue.

5.4.4 Cross-Sectional Area and True Circumferential Strain

In my analysis, I stipulated that uniaxial stretch equates to circumferential strain incurred by the tissue sample at the midpoint in the direction of stretch, where the geometry can be approximated as a rectangular prism, thus simplifying the relevant cross-sectional area A to $A = 2hl$, where h is the wall thickness and l is the axial length. While it may seem that this calculation of cross-sectional area—critical to normalizing force responses to stress and stiffness—is subject to the same discrepant factors relevant to axial shortening and wall thickness, there is an additional variable in the final determination of area: the triangular wire clasps.

To obtain the stress-strain curves detailed in Chapter 3.4.5, it was necessary to use 0.01-inch wire, which was twice the diameter of that which was used for physiologic strain stiffness experiments. This is equivalent to 254 μm . I have previously established in Chapter 3.4.2 that average unloaded wall thickness of a young mouse aorta is under 60 μm , while average lumen diameter is 641 μm . Therefore, this thicker triangular wire has a non-negligible diameter that is greater than one-third the lumen size. Even the thinner 0.005-inch wire has a diameter greater than twice the wall thickness of a young aorta.

As a result, when we examine the actual geometric configuration of a stretched aorta, it resembles the schematic shown in **Figure 5.4**. These considerations give rise to a correction factor for true circumferential strain ϵ_{actual} , taken as the ratio between the actual stretched circumference, C_{actual} , calculated as shown in **Equation 5.2**, and its unloaded value at rest, which is simply π multiplied by the measured unloaded outer diameter d .

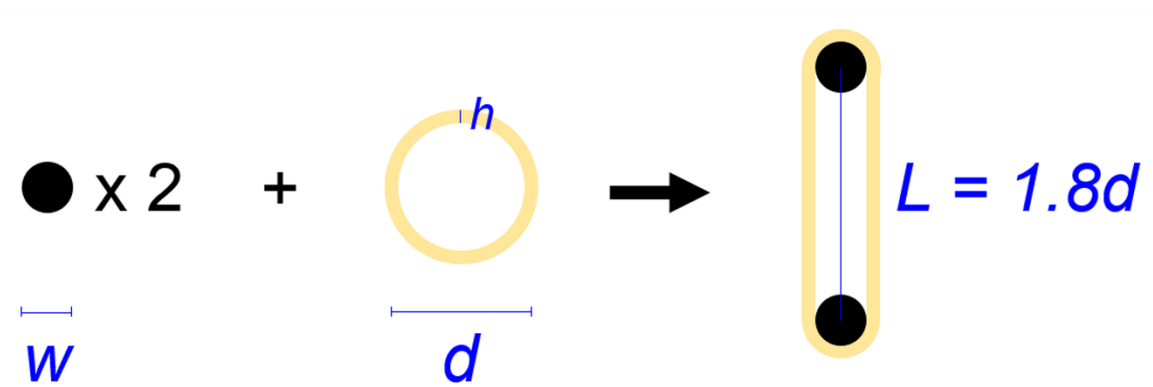


Figure 5.4. Deriving a correction factor for true circumferential strain in uniaxial stretch of aortic tissue. Schematic cross-sectional view of two wires of diameter w , an aortic ring segment with measured unloaded outer diameter d and wall thickness h , and the visual approximation of using the two wires to stretch the tissue uniaxially to desired length L , defined here as 1.8 times d . With the assumption that the most accurate definition of L , corresponding to the movement of the lever arm in the HFLA apparatus, is the distance between the centers of the wires, the actual circumference can be calculated as $2 L$ (the sections parallel to the direction of stretch) + $\pi (w + 2 h_2)$ (the sections wrapped around the wires).

$$C_{\text{actual}} = 2L + \pi(w + 2h_2)$$

Equation 5.2a

$$\varepsilon_{\text{actual}} = C_{\text{actual}} / \pi d$$

Equation 5.2b

Thus, I can determine the actual outer circumference of the wall for a desired strain level L (in this case 80% strain, or 1.8 times the resting outer diameter as depicted in **Figure 5.4**), the size of the wire w , and the altered wall thickness h_2 , which we can correct by applying conservation of volume to observed axial shortening to obtain a quadratic equation for h_2 with coefficients a , b , and c in terms of unloaded vessel outer diameter d , unloaded thickness h_1 , unloaded axial length l_1 , and shortened axial length l_2 : $a = 1$, $b = -d$, and $c = l_1/l_2 (h_1^2 - dh_1)$. Through this method, I could calculate h_2 after measuring l_2 to ascertain more precise values for cross-sectional area and true circumferential strain.

The ability to use this correction factor to its fullest extent is limited, as I have previously established that the experimental setup does not accommodate procedural measurements of axial shortening and thickness changes. Furthermore, it follows that the tissue may not truly be experiencing physiologic optimal length, and that, given the range of maximal contractility established in Chapter 3.4.1, I could implement strain correction in order to determine more accurately the amount of stretch required to reach 80% strain. Unfortunately, adding this step would require unloaded thickness measurements before the initial stretch, as well as real-time determination of axial shortening. Currently, the former is impractical as it would lengthen the experiment significantly, which is problematic for sustained viability of freshly dissected aortic samples if they are not immediately used, while the latter is not possible. If attempts to resolve these issues

methodologically are unsuccessful or impractical, a heuristic estimate for the average shortening and thickness changes experienced by samples of specific age and geometry may be an appropriate compromise in this regard.

Finally, it is prudent to return briefly to the discussion of wire size used for uniaxial stretch. Wire diameter is already incorporated into the equation for area and strain correction factors, so it is more important to consider the biological implications, rather than the mathematical ones, of using a certain wire size over another. It is much easier to mount the tissue with smaller wires, which occupy less of the lumen. This reduces the chance that the wires will cross and necessitate correction; repeated adjustments are likely to subject the tissue to unmeasurable and possibly harmful pre-stretch, leading to damage in SMCs and especially the endothelium, the latter of which can drastically affect stiffness measurements post-VSMC-activation, as I have previously detailed when discussing the inhibition of NOS. On the other hand, larger wires are effectively mandatory when applying extremely high-amplitude stretches to the tissue. In addition to axial shortening, visible deformation of the smaller wires corresponded to stretches beyond 250% strain during initial test experiments in pursuit of the stress-strain curve data presented in Chapter 3.4.5. Larger wires would mostly counter the risk that deformation might occur even at lower strains, albeit microscopically. Based upon these considerations, I believe that it is correct to default to smaller wires in order to uphold viable VSM.

Here, the progressive evaluation of every aspect of my methods to measure aortic stiffness *ex vivo* has reinforced many design choices I made, but also acknowledges

various shortcomings that should be addressed in order to improve the quality of these procedures. Nevertheless, the novelty of the knowledge presented in this dissertation owes to the research interests of me and our group to focus on the role that vascular smooth muscle plays in aortic stiffness. Efforts to amend protocol should retain thematic constancy and optimize the assessment of parameters without sacrificing any features that are currently integral to the preservation of smooth muscle viability.

5.5 Interpretation of *Ex Vivo* Results for *In Vivo* Predictions

Despite limiting characteristics of an *ex vivo* environment, I attempted to mimic *in vivo* conditions as closely as possible in my aging study. At physiologic mean strain and optimal length, in oxygenated salt solutions containing extracellular calcium, maintaining body temperature, and with fully viable VSMCs, I measured in this study material stiffness of young and old mouse aorta with high reproducibility.

The *ex vivo* measurements of aortic mechanical properties presented in this dissertation motivate the reconsideration of what “stiffness” means in a clinical (functional) context versus a scientific (material) one. On the clinical side, pulse wave velocity has great epidemiological value, but the extent to which it is truly a direct correlate of aortic stiffness is unclear, especially when interpreting observed increases with aging. Meanwhile, direct stiffness measurements from tissue samples enable the most reductive evaluation of biomechanical properties, but do not account for variable environmental conditions *in vivo*. According to the Moens-Korteweg equation, PWV is proportional to the square root of stiffness, but the actual relationship between these two

values is far less straightforward. The question arises as to how one might bridge the gap between the utility of PWV as a prognosticator and the robustness of *ex vivo* material stiffness as a biomechanical standard.

In this section, I briefly discuss a non-exhaustive list of several investigative possibilities to address this issue, stemming from discussion points presented throughout this dissertation.

- *Animal models.* The research presented in this dissertation was almost entirely performed in mice. As noted in Chapter 2.3, mice are not as physiologically comparable to humans as other animal models, such as ferret.
- *Wall thickness and vessel diameter.* As noted in Chapter 3.4.2, both wall thickness and outer diameter increased with aging in mouse aorta. These parameters are both relevant in the Moens-Korteweg relation. Thickness increased ~35% with aging, while outer diameter increased ~24%. This results in an expected increase of only ~4% in PWV, so these geometric considerations are insufficient. I have previously mentioned the difficulties in measuring changes in geometry during *ex vivo* stiffness experiments, but there are also challenges *in vivo*, as mice are generally anesthetized for PWV measurements, thus limiting the equivalence to true *in vivo* conditions during normal physiological activity.
- *Axial strain.* The current protocol applies only circumferential strain and does not account for the axial strain experienced by aorta *in vivo* (Humphrey et al. 2009). Accommodating axial stiffness is beyond the scope of this dissertation, but axial

strain may also raise basic geometric considerations for potential differences with aging in axial length that factor into the calculation of cross-sectional area.

- *Operating strain.* An operating strain of 80%, evaluated in Chapter 3.4.1 and approximate of the strain experienced *in vivo* during normal blood flow, was applied in both young and old mouse aortas. This enabled optimally comparable values of material stiffness, but to the best of my knowledge, in old mice there is no definitive physiologic strain range. Therefore, differences with aging in functional stiffness could well be attributable to non-identical operating strains.
- *Physiologic stress-strain perturbations.* HFLA stretch is designed to minimize perturbations to cross bridges, but *in vivo* aortas undergo significantly larger deformation during the cardiac cycle, which may in itself alter cross bridge formation. One can alter the parameters of sinusoidal oscillations to match expected frequency and amplitude, corresponding to heart rate and systolic circumferential distension experienced *in vivo*, as previously discussed at the end of Chapter 5.3.
- *Viscoelasticity.* While HFLA stretch, coupled with smooth muscle activation, does minimize viscoelasticity in aortic stiffness measurements, a more physiologic stretch protocol at lower frequencies and higher amplitudes would almost certainly give rise to more pronounced viscosity in the response of the aortic wall. Additionally, any discrepancy in parameters that characterize an accurate “physiologic” stimulus for young versus old aortas would further highlight a difference in their respective viscoelastic properties. Results from previous *in vivo* arterial studies in dogs (Gamero et al. 2001) and sheep (Gamero et al. 2002), including those shown in **Figure 5.5**,

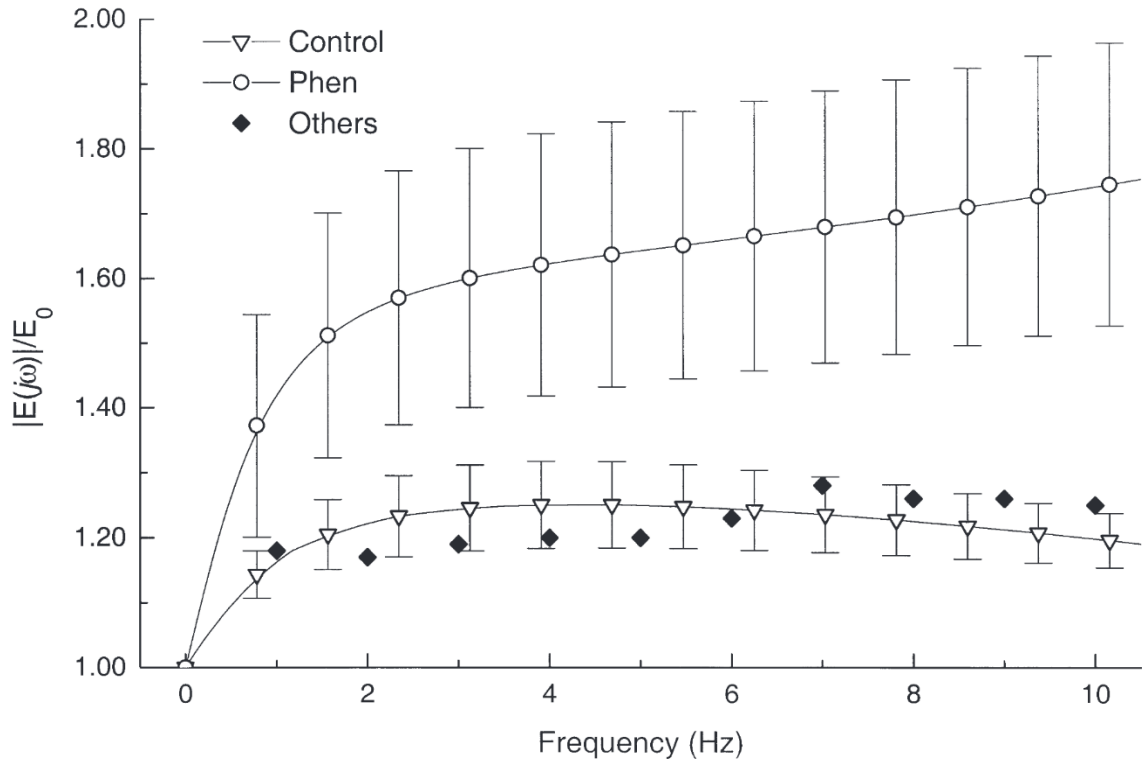


Figure 5.5. Frequency dependence of the magnitude of normalized dynamic elastic modulus during control and active (Phen) states in dogs (Gamero et al. 2001). Mean values cited from past studies (Others) are also shown.

have shown interdependence between factors such as smooth muscle activation, heart rate or stimulus frequency, and vessel diameter—all previously discussed in this work—in measurements of viscoelasticity. Although these relations may not hold exactly in the context of mouse aorta or even in humans, they provide strong evidence that there are multiple variables that could all contribute cumulatively to differences in vessel stiffness with aging.

- *In vivo regulators of smooth muscle activation.* Following these points, another element missing from an *ex vivo* environment is the presence of multiple ill-defined neuro-humoral mediators, the absence of which would mainly affect the smooth muscle cells (Armentano et al. 2007). A comprehensive database of these mediators is lacking and the manner in which they might adjust smooth muscle activation levels is currently not well-known. The *ex vivo* results in this dissertation, specifically through usage of phenylephrine and L-NAME, define the maximal activation states in aortic smooth muscle and quantify them as components of total stiffness. Therefore, the details of *in vivo* activation states, and whether they differ with aging, are left to future studies.
- *Endothelial response to shear stress.* It is appropriate and necessary to understand the aging of the endothelium in concert with that of aortic smooth muscle. Nitric oxide is a critical regulator of vascular smooth muscle contributions to aortic stiffness. Here I have shown the capacity of NO to dramatically modify the biomechanical properties of the aorta. Levels of NO activity have especially wide-reaching implications in the context of shear stress, which is experienced *in vivo* but not taken into account in my

ex vivo experiments. In fact, the endothelium produces NO to alleviate shear stress resulting from blood flow in a Src-dependent manner, transiently by increasing transcription for nitric oxide synthase, which leads to long-term stability of endothelial NOS (Davis et al. 2001). Unfortunately, determination of NO released at any point in time *in vivo* by blood shear forces is technically challenging (Irace et al. 2012, Soucy et al. 2006), but this connection to my finding in Chapter 3.4.9 that Src availability decreases with aging hints at the critical and possibly aging-deficient role that Src might play in reducing aortic stiffness through the endothelium.

The results of the aging study detailed in Chapter 3 are an important first step in fully understanding the mechanisms of changes in aortic stiffness with aging, with a spotlight cast on Src-dependent regulation in vascular smooth muscle. In Chapter 4, potential molecular targets for the prevention or reversal of aging-induced aortic stiffness were probed. This chapter began with my proposal for integration of aortic stiffness data obtained here with existing quantitative models based upon previous literature. Then, I conducted a more detailed methodological review of how these data might be acquired more robustly moving forward. Finally, I outlined the current uncertainties in using *ex vivo* aortic stiffness to frame the understanding of its *in vivo* representations, most significantly in the form of pulse wave velocity, in encouragement of future elaboration upon the body of work featured in this dissertation.

Chapter 6: Conclusions

To this point in modern biomedical research, the notion of smooth muscle as the likely lynchpin for structural and functional integrity within blood vessels and its translation into scientific strategy have not been adequately appreciated. Although this work has attempted to confer convincing evidence for aortic smooth muscle cells as important sites of biochemical and biomechanical regulation, it is still limited in scope and serves sufficiently only as an underpinning for future inquiries, both rational and empirical.

Overarching principles of hemodynamics have supported the assertion that increased pulse wave velocity with aging incident and observable *in vivo* reflects higher aortic stiffness, an outcome interpretable in and correlative to cardiovascular pathologies. Therefore, aortic stiffness has emerged within the clinical repertoire as a vitally important prognosticative tool for cardiovascular disease. It is desirable to seek a greater understanding of the biological processes that manifest and explain this relationship, thus strengthening the biomechanical basis of this diagnostic method and motivating the conception and development of possible therapeutic treatments.

Most mechanical studies of the vasculature have emphasized the extracellular matrix proteins elastin and collagen and put forth the conjecture that these are the primary constituents of aortic material stiffness. Such an emphasis on these extracellular components of the aortic wall may be attributable to the relative ease with which one may study them *ex vivo*. In contrast, this dissertation offers new and novel insights into

biological principles underlying the quantification of significant contributions from smooth muscle cells in the regulation of total aortic stiffness, especially in the context of aging-induced dysfunction in relevant cellular mechanisms. *Ex vivo* stiffness measurements were demonstrated to be separable into distinct quantities corresponding to specific components of the aortic wall. This led to the definition of active stiffness, the proportion of total stiffness that is discernible only upon activation of aortic smooth muscle cells. Under physiologic conditions, the active component constitutes roughly half of maximal total stiffness. Defective smooth muscle regulation of stiffness, specifically with respect to signaling pathways characterizing protective and compensatory mechanisms within focal adhesions and the non-muscle cytoskeleton tied to the regulatory kinase Src, accounts for aging-induced increases in stiffness.

These findings may spur efficient, specific, and safe therapeutics to treat increased aortic stiffness. Preliminary studies presented here used prototype drugs, in the form of cell-permeable peptides, to probe potential cellular targets. Successful inhibition of active stiffness in young aortas was achieved by peptides directed to compete with two specific protein-protein interactions regulating focal adhesion dynamics and actin polymerization. Moreover, aging-induced increases in active stiffness were tempered by targeting a specific interface between talin and vinculin that plays an important structural role in focal adhesions. Despite these promising beginnings, much remains to be done en route to developing a viable option for the treatment of aging-induced aortic stiffness. Further studies are required to expand or establish more concretely a catalog of potential therapeutic targets and also to address important pharmacological considerations of drug

efficacy, potency, specificity, and delivery.

The distinct procedures employed to acquire the quantitative results presented here warranted a critical methodological review in anticipation of future studies. This analysis concluded that there is a strong potential compatibility between these findings and existing mathematical models in other arteries that propose a significant role for vascular smooth muscle in the determination of vessel stiffness. Suggested improvements to the experimental design would serve only to enhance the precision of *ex vivo* stiffness measurements. These would serve to develop more a robust representation of aortic biomechanics and strengthen the link between clinical assessment and scientific knowledge.

Biomedical engineering is a discipline that aspires to combine strong biological evidence with sound engineering principles in order to devise new technologies and medicines to improve human health. It is the hope of the author that this offered work has adhered faithfully to this philosophy and contributed, however incrementally, toward overall progress in confronting the clinical challenges of cardiovascular disease.

Bibliography

1. Armentano RL, Barra JG, Pessana FM, Craiem DO, Graf S, Santana DB, and Sanchez RA. Smart Smooth Muscle Spring-Dampers. *IEEE Engineering in Medicine and Biology Magazine*. 2007; 26(1): 62–70.
2. Aronson D. Cross-linking of glycated collagen in the pathogenesis of arterial and myocardial stiffening of aging and diabetes. *Journal of Hypertension*. 2003; 21(1): 3–12.
3. Avolio A, Butlin M, Liu Y-Y, Viegas K, Avadhanam B, and Lindsay G. Regulation of arterial stiffness: Cellular, molecular and neurogenic mechanisms. *Artery Research*. 2011; 5: 122–7.
4. Bank AJ, and Kaiser DR. Smooth Muscle Relaxation: Effects on Arterial Compliance, Distensibility, Elastic Modulus, and Pulse Wave Velocity. *Hypertension*. 1998; 32: 356–9.
5. Bank AJ, Kaiser DR, Rajala S, and Cheng A. In Vivo Human Brachial Artery Elastic Mechanics: Effects of Smooth Muscle Relaxation. *Circulation*. 1999; 100: 41–7.
6. Bank AJ, Wang H, Holte JE, Mullen K, Shammass R, and Kubo SH. Contributions of Collagen, Elastin, and Smooth Muscle to In Vivo Human Brachial Artery Wall Stress and Elastic Modulus. *Circulation*. 1996; 94(12): 3263–70.
7. Bank AJ, Wilson RF, Kubo SH, Holte JE, Dresing TJ, and Wang H. Direct Effects of Smooth Muscle Relaxation and Contraction on In Vivo Human Brachial Artery Elastic Properties. *Circulation Research*. 1995; 77: 1008–16.
8. Barra JG, Armentano RL, Levenson J, Fischer EI, Pichel RH, and Simon A. Assessment of smooth muscle contribution to descending thoracic aorta elastic mechanics in conscious dogs. *Circulation Research*. 1993; 73: 1040–50.
9. Barton M, Haudenschild CC, D'Uscio LV, Shaw S, Münter K, and Lüscher TF. Endothelin ETA receptor blockade restores NO-mediated endothelial function and inhibits atherosclerosis in apolipoprotein E-deficient mice. *Proceedings of the National Academy of Sciences of the United States of America*. 1998; 95: 14367–72.
10. Beenakker J-WM, Ashcroft BA, Lindeman JHN, and Oosterkamp TH. Mechanical Properties of Extracellular Matrix Studied by Enzymatic Treatments. *Biophysical Journal*. 2012; 102: 1731–37.

11. Ben-Shlomo Y, Spears M, Boustred C, May M, Anderson SG, Benjamin EJ, Boutouyrie P, Cameron J, Chen C-H, Cruickshank JK, Hwang S-J, Lakatta EG, Laurent S, Maldonado J, Mitchell GF, Najjar SS, Newman AB, Ohishi M, Pannier B, Pereira T, Vasani RS, Shokawa T, Sutton-Tyrell K, Verbeke F, Zoungas S, McEniery CM, Cockcroft JR, and Wilkinson IB. Aortic pulse wave velocity improves cardiovascular event prediction: an individual participant meta-analysis of prospective observational data from 17,635 subjects. *Journal of the American College of Cardiology*. 2013; 63(7): 636–46.
12. Berry CL, Greenwald SE, and Rivett JF. Static mechanical properties of the developing and mature rat aorta. *Cardiovascular Research*. 1975; 9: 669–78.
13. Blacher J, Guerin AP, Pannier B, Marchais SJ, Safar ME, and London GM. Impact of aortic stiffness on survival in end-stage renal disease. *Circulation*. 1999; 99: 2434–39.
14. Blaustein MP, Kao JPY, and Matteson DR. Dynamics of smooth muscle contraction differ markedly from those of skeletal and cardiac muscle. *Cellular Physiology and Neurophysiology*. 2nd ed: Elsevier; 2012.
15. Boutouyrie P, Boumaza S, Challande P, Lacolley P, and Laurent S. Smooth Muscle Tone and Arterial Wall Viscosity: An In Vivo/In Vitro Study. *Hypertension*. 1998; 32: 360–4.
16. Brandes RP, Fleming I, and Busse R. Endothelial aging. *Cardiovascular Research*. 2005; 66(2): 286–94.
17. Brooke BS, Karnik SK, and Li DY. Extracellular matrix in vascular morphogenesis and disease: structure versus signal. *Trends in Cell Biology*. 2003; 13(1): 51–6.
18. Brozovich FV, and Morgan KG. Stimulus-specific changes in mechanical properties of vascular smooth muscle. *American Journal of Physiology – Heart and Circulatory Physiology*. 1989; 257: H1573–80.
19. Campbell G, and Campbell J. Development of the vessel wall: overview. *The Vascular Smooth Muscle Cell*: Academic Press; 1995. p. 1–15.
20. Cannon III RO. Role of nitric oxide in cardiovascular disease: focus on the endothelium. *Clinical Chemistry*. 1998; 44(8): 1809–19.
21. Cattell M, Anderson J, and Hasleton P. Age-related changes in amounts and concentrations of collagen and elastin in normotensive human thoracic aorta. *Clinica Chimica Acta*. 1996; 245(1): 73.

22. Cavagna P, Menotti A, and Stanyon R. Genomic homology of the domestic ferret with cats and humans. *Mammalian Genome*. 2000; 11(10): 866–70.
23. Chen CS, Alonso JL, Ostuni E, Whitesides GM, and Ingber DE. Cell shape provides global control of focal adhesion assembly. *Biochemical and Biophysical Research Communications*. 2003; 307: 355–61.
24. Cipolla MJ, and Osol G. Pressure-induced actin polymerization in vascular smooth muscle as a mechanism underlying myogenic behavior. *FASEB Journal*. 2002; 16: 72–6.
25. Clark JM, and Glagov S. Transmural organization of the arteria media. The lamellar unit revisited. *Arteriosclerosis, Thrombosis, and Vascular Biology*. 1985; 5: 19–34.
26. Critchley DR. Biochemical and Structural Properties of the Integrin-Associated Cytoskeletal Protein Talin. *Annual Review of Biophysics*. 2009; 38: 235–54.
27. Cruickshank K, Rise L, Anderson SG, Wright JS, Dunn G, and Gosling RG. Aortic pulse-wave velocity and its relationship to mortality in diabetes and glucose intolerance: an integrated index of vascular function? *Circulation*. 2002; 106: 2085–90.
28. Davis ME, Cai H, Drummond GR, and Harrison DG. Shear stress regulates endothelial nitric oxide synthase expression through c-Src by divergent signaling pathways. *Circulation Research*. 2001; 89(11): 1073–80.
29. Dobrin P, and Canfield T. Identification of smooth muscle series elastic component in intact carotid artery. *American Journal of Physiology – Heart and Circulatory Physiology*. 1977; 232(2): H122–30.
30. Dobrin PB. Mechanical properties of arteries. *Physiological Reviews*. 1978; 58(2): 397–460.
31. Doevendans PA, Daemen MJ, de Muinck ED, and Smits JF. Cardiovascular phenotyping in mice. *Cardiovascular Research*. 1998; 39(1): 34–49.
32. Draeger A, Amos WB, Ikebe M, and Small JV. The cytoskeletal and contractile apparatus of smooth muscle: contractile bands and segmentation of the contractile elements. *Journal of Cell Science*. 1990; 111: 2463–73.
33. Dustan HP, Roccella EJ, and Garrison HH. Controlling hypertension - a research success story. *Archives of Internal Medicine*. 1996; 156(17): 1926–35.

34. Flavahan NA, Bailey SR, Flavahan WA, Mitra S, and Flavahan S. Image remodeling of the actin cytoskeleton in vascular smooth muscle cells after mechanosensitive arteriolar restriction. *American Journal of Physiology – Heart and Circulatory Physiology*. 2005; 288: H660–H9.
35. Fleenor BS, Eng JS, Sindler AL, Pham BT, Kloor JD, and Seals DR. Superoxide signaling in perivascular adipose tissue promotes age-related artery stiffness. *Aging Cell*. 2014; 13: 576–8.
36. Fleenor BS, Marshall KD, Durrant JR, Lesniewski LA, and Seals DR. Arterial stiffening with ageing is associated with transforming growth factor- β 1-related changes in adventitial collagen: reversal by aerobic exercise. *Journal of Physiology*. 2010; 588(20): 3971–82.
37. Fleenor BS, Sindler AL, Eng JS, Nair DP, Dodson RB, and Seals DR. Sodium nitrite de-stiffening of large elastic arteries with aging: role of normalization of advanced glycation end-products. *Experimental Gerontology*. 2012; 47(8): 588–94.
38. Flurkey K, Curren JM, and Harrison DE. Mouse Models in Aging Research. In: Fox JG, Davisson MT, Quimby FW, Barthold SW, Newcomer CE, Smith AL, editors. *The Mouse in Biomedical Research*. 2nd Edition ed2007. p. 637–72.
39. Fry JL, Shiraishi Y, Turcotte R, Yu X, Gao YZ, Akiki R, Bachschmid M, Zhang Y, Morgan KG, Cohen RA, and Seta F. Vascular Smooth Muscle Sirtuin-1 Protects Against Aortic Dissection During Angiotensin II-induced Hypertension. *Journal of the American Heart Association*. 2015.
40. Galbraith CG, Yamada KM, and Sheetz MP. The relationship between force and focal complex development. *Journal of Cell Biology*. 2002; 159(4): 695–705.
41. Gamble G, Zorn J, Sanders G, MacMahon S, and Sharpe N. Estimation of arterial stiffness, compliance, and distensibility from M-mode ultrasode measurements of the common carotid artery. *Stroke*. 1994; 25: 11–6.
42. Gamero LG, Armentano RL, Barra JG, Simon A, and Levenson J. Identification of arterial wall dynamics in conscious dogs. *Experimental Physiology*. 2001; 86(4): 519–28.
43. Gamero LG, Armentano RL, and Levenson J. Arterial wall diameter and viscoelasticity variability. *Computers in Cardiology*. 2002: 513–6.
44. Gao YZ, Saphirstein RJ, Yamin RY, Suki B, and Morgan KG. Aging Impairs Smooth Muscle Mediated Regulation of Aortic Stiffness: A Defect in Shock

- Absorption Function? *American Journal of Physiology – Heart and Circulatory Physiology*. 2014; 307(8):H1252-61. doi: 10.1152/ajpheart.00392.2014.
45. Geiger B, Spatz JP, and Bershadsky AD. Environmental sensing through focal adhesions. *Nature Reviews. Molecular Cell Biology*. 2009; 10(1): 21–33.
 46. Gerthoffer WT, and Gunst SJ. Invited review: focal adhesion and small heat shock proteins in the regulation of actin remodeling and contractility in smooth muscle. *Journal of Applied Physiology*. 2001; 91: 963–72.
 47. Glagov S, Zarins CK, Masawa N, Xu CP, Bassiouny H, and Giddens DP. Mechanical functional role of non-atherosclerotic intimal thickening. *Frontiers of Medical & Biological Engineering*. 1993; 5(1): 37–43.
 48. Gleason RL, Dye WW, Wilson E, and Humphrey JD. Quantification of the mechanical behavior of carotid arteries from wild-type, dystrophin-deficient, and sarcoglycan- δ knockout mice. *Journal of Biomechanics*. 2008; 41: 3213–8.
 49. Gorenne I, Kumar S, Gray K, Figg N, Yu H, Mercer J, and Bennett M. Vascular smooth muscle cell sirtuin 1 protects against DNA damage and inhibits atherosclerosis. *Circulation*. 2013; 127(3): 386–96.
 50. Gosling RG, and Budge MM. Terminology for describing the elastic behavior of arteries. *Hypertension*. 2003; 41(6): 1180–2.
 51. Greenwald S. Ageing of the conduit arteries. *Journal of Pathology*. 2007; 211: 157–72.
 52. Guerin AP, Blacher J, Pannier B, Marchais SJ, Safar ME, and London GM. Impact of aortic stiffness attenuation on survival of patients in end-stage renal failure. *Circulation*. 2001; 103: 987–92.
 53. Gunst SJ, and Zhang W. Actin cytoskeletal dynamics in smooth muscle: a new paradigm for the regulation of smooth muscle contraction. *American Journal of Physiology – Cell Physiology*. 2008; 295: C576–87.
 54. Gupta B, Levchenko TS, and Torchilin VP. Intracellular delivery of large molecules and small particles by cell-penetrating proteins and peptides. *Advanced Drug Delivery Reviews*. 2005; 57(4): 637–51.
 55. Haigis MC, and Sinclair DA. Mammalian sirtuins: biological insights and disease relevance. *Annual Review of Pathology Mechanisms of Disease*. 2010; 5: 254–95.

56. Heitz F, Morris MC, and Divita G. Twenty years of cell-penetrating peptides: from molecular mechanisms to therapeutics. *British Journal of Pharmacology*. 2009; 157(2): 195–206.
57. Holzapfel GA, Gasser TC, and Ogden RW. A new constitutive framework for arterial wall mechanics and a comparative study of material models. *Journal of Elasticity and the Physical Science of Solids*. 2000; 61(1-3): 1–48.
58. Holzapfel GA, and Ogden RW. Constitutive modelling of arteries. *Proceedings of the Royal Society*. 2010; 466: 1551–97.
59. Huang R, and Wang C-LA. A caldesmon peptide activates smooth muscle via a mechanism similar to ERK-mediated phosphorylation. *FEBS Letters*. 2006; 580(1): 63–6.
60. Humphrey JD, Eberth JF, Dye WW, and Gleason RL. Fundamental Role of Axial Stress in Compensatory Adaptations by Arteries. *Journal of Biomechanics*. 2009; 42(1): 1–8.
61. Humphrey JD, and Holzapfel GA. Mechanics, mechanobiology, and modeling of human abdominal aorta and aneurysms. *Journal of Biomechanics*. 2011; 45: 805–14.
62. Hynes RO. Integrins: bidirectional, allosteric signaling machines. *Cell*. 2002; 110: 673–87.
63. Ingber DE. Cellular mechanotransduction: putting all the pieces together again. *FASEB Journal*. 2006; 20(7): 811–27.
64. Ingber DE. Mechanobiology and diseases of mechanotransduction. *Annals of Medicine*. 2003; 35(8): 564–77.
65. Intengan HD, and Schiffrin EL. Structure and mechanical properties of resistance arteries in hypertension: role of adhesion molecules and extracellular matrix determinants. *Hypertension*. 2000; 36: 312–8.
66. Irace C, Carallo C, De Franceschi MS, Scicchitano F, Milano M, Tripolino C, Scavelli F, and Gnasso A. Human common carotid wall shear stress as a function of age and gender: a 12-year follow-up study. *Age*. 2012; 34(6): 1553–62.
67. Izaguirre G, Aguirre L, Hu YP, Lee HY, Schlaepfer DD, Aneskievich BJ, and Haimovich B. The cytoskeletal/non-muscle isoform of alpha-actinin is phosphorylated on its actin-binding domain by the focal adhesion kinase. *Journal of Biological Chemistry*. 2001; 276: 28676–85.

68. Joliot A, and Prochiantz A. Transduction peptides: from technology to physiology. *Nature Cell Biology*. 2004; 6(3): 189–96.
69. Juliano RL. Signal transduction by cell adhesion receptors and the cytoskeleton: functions of integrins, cadherins, selectins, and immunoglobulin-superfamily members. *Annual Review of Pharmacology and Toxicology*. 2002; 42: 283–323.
70. Kaess BM, Rong J, Larson MG, Hamburg NM, Vita JA, Levy D, Benjamin EJ, Vasan RS, and Mitchell GF. Aortic stiffness, blood pressure progression, and incident hypertension. *JAMA: The Journal of the American Medical Association*. 2012; 308(9): 875–81.
71. Kawai M, and Brandt PW. Sinusoidal analysis: a high resolution method for correlating biochemical reactions with physiological processes in activated skeletal muscles of rabbit, frog and crayfish. *Journal of Muscle Research and Cell Motility*. 1980; 1(3): 279–303.
72. Kawai Y, Garduno L, Theodore M, Yang J, and Arinze IJ. Acetylation-deacetylation of the transcription factor Nrf2 (nuclear factor erythroid 2-related factor 2) regulates its transcriptional activity and nucleocytoplasmic localization. *Journal of Biological Chemistry*. 2011; 286(9): 7629–40.
73. Kim HR, Appel S, Vetterkind S, Gangopadhyay S, and Morgan KG. Smooth muscle signalling pathways in health and disease. *Journal of Cellular and Molecular Medicine*. 2008; 12(6A): 2165–80.
74. Kim HR, Gallant C, Leavis PC, Gunst SJ, and Morgan KG. Cytoskeletal remodeling in differentiated vascular smooth muscle is actin isoform dependent and stimulus dependent. *American Journal of Physiology – Cell Physiology*. 2008; 295(3): C768–78.
75. Kim HR, Graceffa P, Ferron F, Gallant C, Boczkowska M, Dominguez R, and Morgan KG. Actin polymerization in differentiated vascular smooth muscle cells requires vasodilator-stimulated phosphoprotein. *American Journal of Physiology – Cell Physiology*. 2010; 298: C559–C71.
76. Kim HR, Leavis PC, Graceffa P, Gallant C, and Morgan KG. A new method for direct detection of the sites of actin polymerization in intact cells and its application to differentiated vascular smooth muscle. *American Journal of Physiology – Cell Physiology*. 2010; 299(5): C988–93.
77. Kohn JC, Lampi MC, and Reinhart-King CA. Age-related vascular stiffening: causes and consequences. *Frontiers in Genetics*. 2015; 6(112).

78. Konova E, Baydanoff S, Atanasova M, and Velkova A. Age-related changes in the glycation of human aortic elastin. *Experimental Gerontology*. 2004; 39(2): 249–54.
79. Korteweg DJ. Über die Fortpflanzungsgeschwindigkeit des Schalles in Elastischen Röhren. *Annalen der Physik*. 1878; 241(12): 525–42.
80. Kuo J-C, Han X, Hsiao C-T, Yates III JR, and Waterman CR. Analysis of the myosinII-responsive focal adhesion proteome reveals a role for β -Pix in negative regulation of focal adhesion maturation. *Nature Cell Biology*. 2011; 13(4): 383–93.
81. Lakatta EG. Arterial and Cardiac Aging: Major Shareholders in Cardiovascular Disease Enterprises: Part III: Cellular and Molecular Clues to Heart and Arterial Aging. *Circulation*. 2003; 107: 490–7.
82. Laurent S, and Boutouyrie P. Recent advances in arterial stiffness and wave reflection in human hypertension. *Hypertension*. 2007; 49(6): 1202–6.
83. Laurent S, Boutouyrie P, Asmar R, Gautier I, Laloux B, Guize L, Ducimetiere P, and Benetos A. Aortic stiffness is an independent predictor of all-cause and cardiovascular mortality in hypertensive patients. *Hypertension*. 2001; 37: 1236–41.
84. Lee YH, Gallant C, Guo H, Li Y, Wang CA, and Morgan KG. Regulation of vascular smooth muscle tone by N-terminal region of caldesmon. Possible role of tethering actin to myosin. *Journal of Biological Chemistry*. 2000; 275(5): 3213–20.
85. Leikina E, Merts MV, Kuznetsova N, and Leikin S. Type I collagen is thermally unstable at body temperature. *Proceedings of the National Academy of Sciences of the United States of America*. 2002; 99(3): 1314–8.
86. Li Y, Reznichenko M, Tribe RM, Hess PE, Taggart M, Kim H, DeGnore JP, Gangopadhyay S, and Morgan KG. Stretch activates human myometrium via ERK, caldesmon and focal adhesion signaling. *PLoS One*. 2009; 4(10): e7489.
87. Marganski WA, Gangopadhyay SS, Je HD, Gallant CM, and Morgan KG. Targeting of a Ca^{2+} /Calmodulin-Dependent Protein Kinase II Is Essential for Extracellular Signal-Regulated Kinase-Mediated Signaling in Differentiated Smooth Muscle Cells. *Circulation Research*. 2005; 97(6): 541–9.
88. Martinez-Lemus LA, Hill MA, and Meininger GA. The plastic nature of the vascular wall: a continuum of remodeling events contributing to control of arteriolar diameter and structure. *Physiology*. 2009; 24: 45–57.

89. Matsumoto T, and Nagayama K. Tensile properties of vascular smooth muscle cells: bridging vascular and cellular biomechanics. *Journal of Biomechanics*. 2011; 45(2012): 745–55.
90. Mattace-Raso FUS, van der Cammen TJM, Hofman A, van Popele NM, Bos ML, Schalekamp MADH, Asmar R, Reneman RS, Hoeks APG, Breteler MMB, and Witteman JCM. Arterial stiffness and risk of coronary heart disease and stroke: the Rotterdam study. *Circulation*. 2006; 113: 657–63.
91. McAllister DA, Maclay JD, Mills NL, Mair G, Miller J, Anderson D, Newby DE, Murchison JT, and MacNee W. Arterial stiffness is independently associated with emphysema severity in patients with chronic obstructive pulmonary disease. *American Journal of Respiratory and Critical Care Medicine*. 2007; 176: 1208–14.
92. McGill Jr. HC, McMahan A, and Gidding SS. Preventing heart disease in the 21st century: implications of the pathobiological determinants of atherosclerosis in youth (PDAY) study. *Circulation*. 2008; 117: 1216–27.
93. McVeigh GE, Bank AJ, and Cohn JN. Arterial Compliance. In: Willerson JT, Wellens HJJ, Cohn JN, Holmes DR, editors. *Cardiovascular Medicine*. Springer London; 2007. p. 1811–31.
94. Mendis S, Puska P, and Norrving B. *Global atlas on cardiovascular disease prevention and control*. Geneva: World Health Organization. 2011.
95. Mierke CT. The role of vinculin in the regulation of the mechanical properties of cells. *Cell Biochemistry and Biophysics*. 2009; 53(3): 115–26.
96. Min J, Reznichenko M, Poythress RH, Gallant CM, Vetterkind S, Li Y, and Morgan KG. Src modulates contractile vascular smooth muscle function via regulation of focal adhesions. *Journal of Cellular Physiology*. 2012; 227(11): 3585–92.
97. Mitchell GF. Clinical achievements of impedance analysis. *Medical & Biological Engineering & Computing*. 2009; 47(2): 153–63.
98. Mitchell GF. Effects of central aging on the structure and function of the peripheral vasculature: implications for end-organ damage. *Journal of Applied Physiology*. 2008; 105(5): 1652–60.
99. Mitchell GF, Guo CY, Benjamin EJ, Larson MG, Keyes MJ, Vita JA, Vasan RS, and Levy D. Cross-sectional correlates of increased aortic stiffness in the community: the Framingham Heart Study. *Circulation*. 2007; 115(20): 2628–36.

100. Mitchell GF, Pfeffer MA, Finn PV, and Pfeffer JM. Comparison of techniques for measuring pulse-wave velocity in the rat. *Journal of Applied Physiology*. 1997; 82(1): 203–10.
101. Mitra SK, Hanson DA, and Schlaepfer DD. Focal adhesion kinase: in command and control of cell motility. *Nature Reviews. Molecular Cell Biology*. 2005; 6: 56–68.
102. Mozaffarian D, Benjamin EJ, Go AS, Arnett DJ, Blaha MJ, Cushman M, de Ferranti S, Després J-P, Fullerton HJ, Howard VJ, Huffman MD, Judd SE, Kissela BM, Lackland DT, Lichtman JH, Lisabeth JD, Liu S, Mackey RH, Matchar DB, McGuire DK, Mohler ER, Moy CS, Muntner P, Mussolino ME, Nasir K, Neumar RW, Nichol G, Palaniappan L, Pandey DK, Reeves MJ, Rodriguez CJ, Sorlie PD, Stein J, Towfighi A, Turan TN, Virani SS, Willey JZ, Woo D, Yeh RW, and Turner MB. Heart Disease and Stroke Statistics–2015 Update: A Report From the American Heart Association. *Circulation*. 2015.
103. Murphy RA. Mechanics of Vascular Smooth Muscle. Supplement 7: Handbook of Physiology. The Cardiovascular System, Vascular Smooth Muscle 1980. p. 325–51.
104. Nemoto S, Fergusson MM, and Finkel T. SIRT1 functionally interacts with the metabolic regulator and transcriptional coactivator PGC-1 α . *Journal of Biological Chemistry*. 2005; 280(16): 16456–60.
105. O'Rourke M. Arterial stiffness, systolic blood pressure, and logical treatment of arterial hypertension. *Hypertension*. 1990; 15: 339–47.
106. Ogut O, and Brozovich FV. Regulation of force in vascular smooth muscle. *Journal of Molecular and Cellular Cardiology*. 2003; 35: 347–55.
107. Pawlowski J, and Morgan KG. Mechanisms of intrinsic tone in ferret vascular smooth muscle. *Journal of Physiology*. 1992; 448: 121–32.
108. Peiper U, Laven R, Regnat K, and Schmidt E. Mechanical response to stretch of depolarized vascular smooth muscle fibres. *Basic Research in Cardiology*. 1974; 69(1): 1–10.
109. Pezet M, Jacob M-P, Escoubet B, Gheduzzi D, Tillet E, Perret P, Huber P, Quaglino D, Vranckx R, Li DY, Starcher B, Boyle WA, Mecham RP, and Fauray G. Elastin Haploinsufficiency Induces Alternative Aging Processes in the Aorta. *Rejuvenation Research*. 2008; 11(1): 97–112.

110. Philibert C, Bouillot S, Huber P, and Faury G. Protocadherin-12 deficiency leads to modifications in the structure and function of arteries in mice. *Pathologie Biologie*. 2012; 60(1): 34–40.
111. Poythress RH, Gallant CM, Vetterkind S, and Morgan KG. Vasoconstrictor-induced endocytic recycling regulates focal adhesion protein localization and function in vascular smooth muscle. *American Journal of Physiology – Cell Physiology*. 2013; 305(2): C215–27.
112. Prado CM, and Rossi MA. Circumferential wall tension due to hypertension plays a pivotal role in aortic remodeling. *International Journal of Experimental Pathology*. 2006; 87: 425–36.
113. Qiu H, Zhu Y, Sun Z, Trzeciakowski JP, Gansner M, Depre C, Rusuello RRG, Natividad FF, Hunter WC, Genin GM, Elson EL, Vatner DE, Meininger GA, and Vatner SF. Vascular smooth muscle cell stiffness as a mechanism for increased aortic stiffness with aging. *Circulation Research*. 2010; 107(5): 615–9.
114. Rachev A, and Hayashi K. Theoretical Study of the Effects of Vascular Smooth Muscle Contraction on Strain and Stress Distributions in Arteries. *Annals of Biomedical Engineering*. 1999; 27: 459–68.
115. Reddy AK, Li Y-H, Pham TT, Ochoa LN, Treviño MT, Hartley CJ, Michael LH, Entman ML, and Taffet GE. Measurement of aortic input impedance in mice: effects of age on aortic stiffness. *American Journal of Physiology – Heart and Circulatory Physiology*. 2003; 285: H1464–H70.
116. Rees DD, Palmer RM, Schulz R, Hodson HF, and Moncada S. Characterization of three inhibitors of endothelial nitric oxide synthesis in vitro and in vivo. *British Journal of Pharmacology*. 1990; 101(3): 746–52.
117. Rembold CM, Tejani AD, Ripley ML, and Han S. Paxillin phosphorylation, actin polymerization, noise temperature, and the sustained phase of swine carotid artery contraction. *American Journal of Physiology – Cell Physiology*. 2007; 293: C993–C1002.
118. Rensen SSM, Doevendans PAFM, and van Eys GJJM. Regulation and characteristics of vascular smooth muscle cell phenotypic diversity. *Netherlands Heart Journal*. 2007; 15(3): 100–8.
119. Roach MR, and Burton AC. The reason for the shape of the distensibility curves of arteries. *Canadian Journal of Biochemistry*. 1957; 35: 681–90.

120. Rodgers JT, Lerin C, Haas W, Gygi SP, Spiegelman BM, and Puigserver P. Nutrient control of glucose homeostasis through a complex of PGC1- α and SIRT1. *Nature*. 2005; 434(7029): 113–8.
121. Romer LH, Birukov KG, and Garcia JGN. Focal Adhesions: Paradigm for a Signaling Nexus. *Circulation Research*. 2006; 98: 606–16.
122. Ross R. Atherosclerosis - an inflammatory disease. *New England Journal of Medicine*. 1999; 340(2): 115–26.
123. Ross R. The pathogenesis of atherosclerosis: a perspective for the 1990s. *Nature*. 1993; 362(6423): 801–9.
124. Russell A, and Watts S. Vascular Reactivity of Isolated Thoracic Aorta of C57BL/6J Mouse. *Journal of Pharmacology and Experimental Therapeutics*. 2000; 294(2): 598–604.
125. Saphirstein RJ. Regulation of Blood Vessel Stiffness by Focal Adhesions of Vascular Smooth Muscle. Doctoral Dissertation, Boston University; 2013.
126. Saphirstein RJ, Gao YZ, Jensen MH, Gallant CM, Vetterkind S, Moore JR, and Morgan KG. The Focal Adhesion: A Regulated Component of Aortic Stiffness. *PLoS One*. 2013; 8(4).
127. Saphirstein RJ, Gao YZ, Lin QQ, and Morgan KG. Cortical actin regulation modulates vascular contractility and compliance in veins. *Journal of Physiology*. 2015.
128. Saphirstein RJ, and Morgan KG. The contribution of vascular smooth muscle to aortic stiffness across length scales. *Microcirculation*. 2014; 21(3): 201–7.
129. Schlaepfer DD, Hauck CR, and Sieg DJ. Signaling through focal adhesion kinase. *Progress in Biophysics and Molecular Biology*. 1999; 71: 435–78.
130. Schlaepfer DD, Mitra SK, and Ilic D. Control of motile and invasive cell phenotypes by focal adhesion kinase. *Biochimica et Biophysica Acta*. 2004; 1692: 77–102.
131. Schulze-Bauer CA, Regitnig P, and Holzapfel GA. Mechanics of the human femoral adventitia including the high-pressure response. *American Journal of Physiology – Heart and Circulatory Physiology*. 2002; 282(6): H2427–H40.
132. Schwartz MA. Integrin signaling revisited. *Trends in Cell Biology*. 2001; 11: 466–70.

133. Shadwick RE. Mechanical design in arteries. *Journal of Experimental Biology*. 1999; 202: 3305–13.
134. Shaw L, Ahmed S, Austin C, and Taggart MJ. Inhibitors of actin filament polymerisation attenuate force but not global intracellular calcium in isolated pressurised resistance arteries. *Journal of Vascular Research*. 2003; 40: 1–10.
135. Small JV, and Gimona M. The cytoskeleton of the vertebrate smooth muscle cell. *Acta Physiologica Scandinavica*. 1998; 164(4): 341–8.
136. Soucy KG, Ryoo S, Benjo A, Lim HK, Gupta G, Sohi JS, Elser J, Aon MA, Nyhan D, Shoukas AA, and Berkowitz DE. Impaired shear stress-induced nitric oxide production through decreased NOS phosphorylation contributes to age-related vascular stiffness. *Journal of Applied Physiology*. 2006; 101(6): 1751–9.
137. Srinivasan R, Forman S, Quinlan RA, Ohanian J, and Ohanian V. Regulation of contractility by Hsp27 and Hic-5 in rat mesenteric small arteries. *American Journal of Physiology – Heart and Circulatory Physiology*. 2008; 294: H961–H9.
138. Taddei S, Virdis A, Ghiadoni L, Salvetti G, Bernini G, Magagna A, and Salvetti A. Age-related reduction of NO availability and oxidative stress in humans. *Hypertension*. 2001; 38(2): 247–79.
139. Tan JL, Tien J, Pirone DM, Gray DS, Bhadriraju K, and Chen CS. Cells lying on a bed of microneedles: an approach to isolate mechanical force. *Proceedings of the National Academy of Sciences of the United States of America*. 2002; 100: 1484–9.
140. Thornbury KD. Tonic and Phasic Activity in Smooth Muscle. *Irish Journal of Medical Science*. 1997; 168(3): 201–7.
141. Trachet B, Fraga-Silva RA, Londono FJ, Swillens A, Stergiopoulos N, and Segers P. Performance Comparison of Ultrasound-Based Methods to Assess Aortic Diameter and Stiffness in Normal and Aneurysmal Mice. *PLoS One*. 2015.
142. Tsamis A, Krawiec JT, and Vorp DA. Elastin and collagen fibre microstructure of the human aorta in ageing and disease: a review. *Journal of the Royal Society Interface*. 2013; 10(83).
143. Uehata M, Ishizaki T, Satoh H, Ono T, Kawahara T, Morishita T, Tamakawa H, Yamagami K, Inui J, Maekawa M, and Narumiya S. Calcium sensitization of smooth muscle mediated by a Rho-associated protein kinase in hypertension. *Nature*. 1997; 389(6654): 990–4.

144. Valentin A, Humphrey JD, and Holzapfel GA. A multi-layered computational model of coupled elastin degradation, vasoactive dysfunction, and collagenous stiffening in aortic aging. *Annals of Biomedical Engineering*. 2011; 39(7): 2027–45.
145. Vetterkind S, Poythress RH, Lin QQ, and Morgan KG. Hierarchical scaffolding of an erk1/2 activation pathway. *Cell Communication and Signaling*. 2013; 11(65).
146. Vyas M, Izzo Jr. JL, Lacourcière Y, Arnold JMO, Dunlap ME, Amato JL, Pfeffer MA, and Mitchell GF. Augmentation Index and Central Aortic Stiffness in Middle-Aged to Elderly Individuals. *American Journal of Hypertension*. 2007; 20(6): 642–7.
147. Wagenseil JE, and Mecham RP. Elastin in Large Artery Stiffness and Hypertension. *Journal of Cardiovascular Translational Research*. 2012; 5(3): 264–73.
148. Wagenseil JE, and Mecham RP. Vascular extracellular matrix and arterial mechanics. *Physiological Reviews*. 2009; 89(3): 957–89.
149. Wang M, Kahzan B, and Lakatta EG. Central Arterial Aging and Angiotensin II Signaling. *Current Hypertension Reviews*. 2010; 6(4): 266–81.
150. Wang N, Ostuni E, Whitesides GM, and Ingber DE. Micropatterning tractional forces in living cells. *Cell Motility and the Cytoskeleton*. 2002; 52: 97–106.
151. Wang ZL, Pavalko FM, and Gunst SJ. Tyrosine phosphorylation of dense plaque protein paxillin is regulated during smooth muscle contraction. *American Journal of Physiology – Cell Physiology*. 1996; 270: C1594–C602.
152. Webb RC. Smooth Muscle Contraction and Relaxation. *Advances in Physiology Education*. 2003; 27(4): 201–6.
153. Weisbrod RM, Shiang T, Al Sayah L, Fry JL, Bajpai S, Reinhart-King CA, Lob HE, Santhanam L, Mitchell GF, Cohen RA, and Seta F. Arterial stiffening precedes systolic hypertension in diet-induced obesity. *Hypertension*. 2013; 62: 1105–10.
154. Wheeler JB, Mukherjee R, Stroud RE, Jones JA, and Ikonomidis JS. Relation of Murine Thoracic Aortic Structural and Cellular Changes with Aging to Passive and Active Mechanical Properties. *Journal of the American Heart Association*. 2015; 2015(4).

155. Wilkinson IB, Fuchs SA, Jansen IM, Spratt JC, Murray GD, Cockcroft JR, and Webb DJ. Reproducibility of pulse wave velocity and augmentation index measured by pulse wave analysis. *Journal of Hypertension*. 1998; 16(12): 2079–84.
156. Wilkinson IB, MacCallum H, Flint L, Cockcroft JR, Newby DE, and Webb DJ. The influence of heart rate on augmentation index and central arterial pressure in humans. *Journal of Physiology*. 2000; 525(1): 263–70.
157. Willeum-Hansen T, Staessen JA, Torp-Pedersen C, Rasmussen S, Thijs L, Ibsen H, and Jeppesen J. Prognostic value of aortic pulse wave velocity as index of arterial stiffness in the general population. *Circulation*. 2006; 113(5): 664–70.
158. Winlove CP, Parker KH, Avery NC, and Bailey AJ. Interactions of elastin and aorta with sugars *in vitro* and their effects on biochemical and physical properties. *Diabetologia*. 1996; 39(10): 1131–9.
159. Wolfenson H, Bershadsky A, Henis YI, and Geiger B. Actomyosin-generated tension controls the molecular kinetics of focal adhesions. *Journal of Cell Science*. 2011; 124(9): 1425–32.
160. Wolfenson H, Henis YI, Geiger B, and Bershadsky AD. The heel and toe of the cell's foot: a multifaceted approach for understanding the structure and dynamics of focal adhesions. *Cell Motility and the Cytoskeleton*. 2009; 66: 1017–29.
161. Wolinsky H, and Glagov S. Structural basis for the static mechanical properties of the aortic media. *Circulation Research*. 1964; 14: 400–13.
162. Xie J, Zhou J, and Fung YC. Bending of blood vessel wall: stress-strain laws of the intima-media and adventitial layers. *Journal of Biomechanical Engineering*. 1995; 117(1): 136–45.
163. Yamin R, and Morgan KG. Deciphering actin cytoskeletal function in the vascular smooth muscle cell. *Journal of Physiology*. 2012; 590(Pt 17):4145-54. doi: 10.1113/jphysiol.2012.232306.
164. Yeung F, Hoberg JE, Ramsey CS, Keller MD, Jones DR, Frye RA, and Mayo MW. Modulation of NF- κ B-dependent transcription and cell survival by the SIRT1 deacetylase. *EMBO Journal*. 2004; 23(12): 2369–80.
165. Zaidel-Bar R, Itzkovitz S, Ma'ayan A, Iyengar R, and Geiger B. Functional atlas of the integrin adhesome. *Nature Cell Biology*. 2007; 9(8): 858–67.
166. Zamir E, and Geiger B. Molecular complexity and dynamics of cell-matrix adhesions. *Journal of Cell Science*. 2001; 114(20): 3583–90.

167. Zhang W, and Gunst SJ. Interactions of Airway Smooth Muscle Cells with Their Tissue Matrix. *Proceedings of the American Thoracic Society*. 2008; 5: 32–9.
168. Zhang W, Wu Y, Du L, Tang DD, and Gunst SJ. Activation of the Arp2/3 complex by N-WASp is required for actin polymerization and contraction in smooth muscle. *American Journal of Physiology – Cell Physiology*. 2005; 288(5): C1145–60.
169. Zhou S, Chen HZ, Wan YZ, Zhang QJ, Wei YS, Huang S, Liu JJ, Yu YB, Zhang ZQ, Yang RF, Zhang R, Cai H, Liu DP, and Liang CC. Repression of P66Shc expression by SIRT1 contributes to the prevention of hyperglycemia-induced endothelial dysfunction. *Circulation Research*. 2011; 109(6): 639–48.
170. Ziegler WH, Liddington RC, and Critchley DR. The structure and regulation of vinculin. *Trends in Cell Biology*. 2006; 16(9): 453–60.
171. Zorko M, and Lagnel U. Cell-penetrating peptides: mechanisms and kinetics of cargo delivery. *Advanced Drug Delivery Reviews*. 2005; 57(4): 529–45.
172. Zulliger MA, and Stergiopoulos N. Structural strain energy function applied to the ageing of the human aorta. *Journal of Biomechanics*. 2007; 40: 3061–9.

Curriculum Vitae

